A DETERMINATION OF THE PRIMARY AND SECONDARY IONIZATION COEFFICIENTS IN HYDROGEN, HELIUM AND NEON

being

a thesis presented for the

Degree of Doctor of Philosophy

at the University of Keele

by

J. Fletcher, B.A., Grad.Inst.P.

Department of Physics,
University of Keele,
Keele,
Staffordshire,
England.
September, 1963.

Fig 29 and fig 30 between p.36 to 37

Fig 31.a between p.37 to 38

NOT DIGITISED BY REQUEST OF THE UNIVERSITY

SYNOPSIS

The spatial growth of pre-breakdown ionization currents between parallel plate electrodes has been investigated in hydrogen, helium and neon. A pyrex glass experimental tube has been constructed containing gold evaporated film electrodes and having a variable electrode separation. Residual gas pressures of less than 10^{-9} mms. Hg. were obtained by means of ultra high vacuum techniques. The hydrogen used was obtained by the thermal decomposition of uranium hydride whilst both helium and neon have been purified by cataphoresis.

The Davies and Milne and the Haydon and Robertson analyses have been applied to the measurements of pre-breakdown ionization currents as a function of electrode separation, from which the first Townsend ionization coefficient has been determined as a function of E/p_o for the range $50 < E/p_o < 450$ volts/cm.mm.Hg. in hydrogen, $10 < E/p_o < 1000$ volts/cm.mm.Hg. in helium, and $30 < E/p_o < 1000$ volts/cm.mm.Hg. in neon. Values of α/p given by both analyses were found to agree over the full range of E/p investigated. Raising the residual gas pressure from 10^{-9} mm.Hg. to 10^{-5} mm.Hg. was found to cause a 20% increase in α/p at E/p = 400 volts/cm.mm.Hg in hydrogen. The final values of α/p in hydrogen agree with those of Myatt but fall below those of other determinations. α/p in helium and neon was also found to be lower than previous results, the percentage discrepancy increasing as E/p decreased. These discrepancies are attributed to the increased

purity of the present gas samples.

The variation of the generalised secondary coefficient, ω/α, with E/p was also determined from both pre-breakdown current data and from breakdown potential measurements. ω/α was found to be a monotonic function of E/p in hydrogen but peaks were noted in helium and neon due to the strong excitation and metastable states of these gases. Deviations from Paschen's law have been observed in all the gases investigated, V_s being found to be a function of $p_0 d_s$ and of electrode separation and of pressure seperately. This has been explained in terms of photon absorption in the gas, geometric photon loss from the discharge and the decrease in ionization as the mean free path increases with decreasing pressure.

ACKNOWLEDGEMENTS

I wish to express my thanks to

Dr. D. Elwyn Davies, for his guidance and helpful suggestions:

Professor D.J.E. Ingram, for the use of the laboratory and facilities:

My colleagues of the Physics Department for their many helpful discussions:

Messrs. W.J. Robinson and H. Birchall for their assistance with the photographic work:

Miss S. Lawson for typing and presentation of this thesis:

The Department of Scientific and Industrial Research for the award of a grant towards this work.

CONTENTS

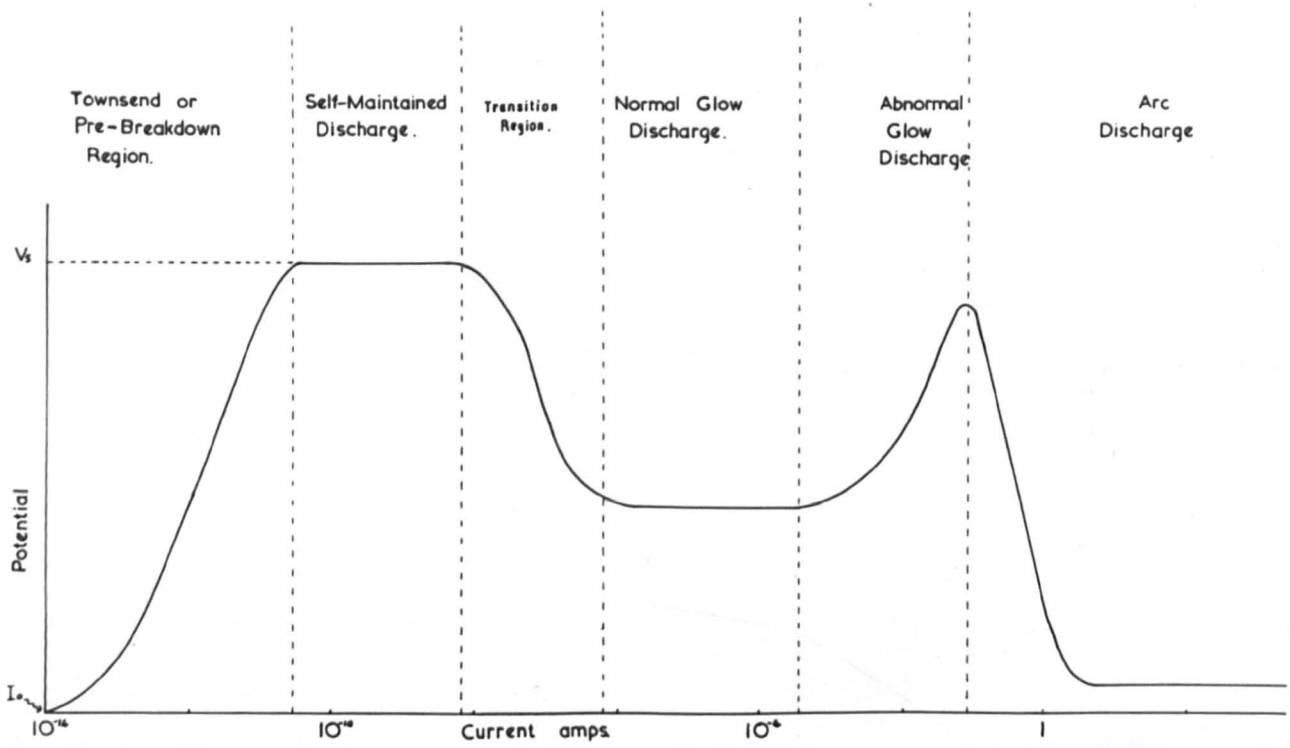

Inter-dependence of Potential and Current in a gas.

Figure 1.

CHAPTER I

THE BASIC PROCESSES

INTRODUCTION

All gases are good insulators so long as they are dry and only a small potential difference is applied across them. However, a gas that has been exposed to ultra-violet light, X-rays, or the radiations from radio-active material, possesses appreciable conductivity. So also do gases generated by electrolysis or drawn from the region around a flame. It is found that even the atmosphere possesses a slight conductivity due to cosmic radiation.

It was not possible to study in great detail the mechanisms by which a current passes through a gas until the electron was postulated by Stoney in 1891. Following this, much work was done on the subject by J.J. Thomson, J.S. Townsend, P. Langevin and many others in the Clarendon Laboratory at Oxford. In their work two approaches may be seen, the atomic approach of Thomson, (1), and the macroscopic approach of Townsend, (2, 3, 4) who studied the mechanism of the actual discharge. These two fields have come together again in the present day study of thermonuclear and plasma physics. Unfortunately the parameters associated with current growth in a gas are not all agreed upon and it was with two of these in mind that the work presented in this thesis was initiated.

The variation of current flowing in a gas, I, as a function of the applied potential difference between the electrodes, V, at constant pressure, p, and inter-electrode gap distance, d, is not a

simple one, as may be seen from Figure 1. At low values of V no current will flow unless some ionizing radiation is incident upon the gas or the cathode surface to produce an initial current I_0. If this is present the current will build up as V increases, but if the radiation is removed the current will collapse. At a definite value of V, termed the sparking potential, V_s, the current becomes self-maintained, that is, the radiation may be removed without the current collapsing. The value of this sparking potential is characteristic of the gas-electrode system and varies with both pressure and the inter-electrode gap distance, d. It is in this region below the sparking potential that the theory evolved by Townsend, and given in this chapter, is obeyed.

Once the sparking potential has been reached and a self-maintained discharge occurs, the current flow is dependent only upon the external circuit. A higher current flow in the gap may be achieved by reducing the external resistance of the circuit and, if this resistance is lowered sufficiently, the applied potential may also be reduced as the current increases. When the current reaches a high enough value, about 10^{-3} amps, the normal glow discharge occurs, which starts as a narrow discharge and increases in size as the current increases until it covers the whole electrode surface. Throughout this normal glow discharge region the current density is constant but, once the glow has filled the gap it becomes stable and further current increase can only be obtained by increasing the current density. This can be achieved by further decreasing

the external impedance of the circuit and increasing the applied potential once more. The current then builds up into the abnormal glow discharge, when currents in the order of 10^{-1} amps flow, and eventually an arc passes between the elctrodes and currents as high as several hundred amps may pass.

The work presented in this thesis was carried out entirely in the Townsend region.

1.1. Excitation and Ionization

An atom is said to be excited when an electron is raised from a lower to a higher potential energy. It may be caused by the atom colliding with an electron or an ion and the kinetic energy of the high energy particle being converted to the necessary potential energy, or it may be caused by the absorption of a quantum of radiation of the correct frequency. In the case of excitation by electrons, the angular momentum of the atom-electron system with respect to the common centre of mass must be conserved. Hence

$$\Delta p = p_1 - p_2$$

where p_1 is the angular momentum of the system before impact, p_2 is the angular momentum of the system after impact and Δp is the change in the angular momentum of the atom. As Δp is quantized its values can only be integers of $h/2\pi$. Hence

$$\Delta p = \Delta J \ (h/2\pi)$$

where ΔJ is the change in the inner quantum number. This means that the probability of excitation will be zero until the incident electron has a kinetic energy equal to the excitation energy and for

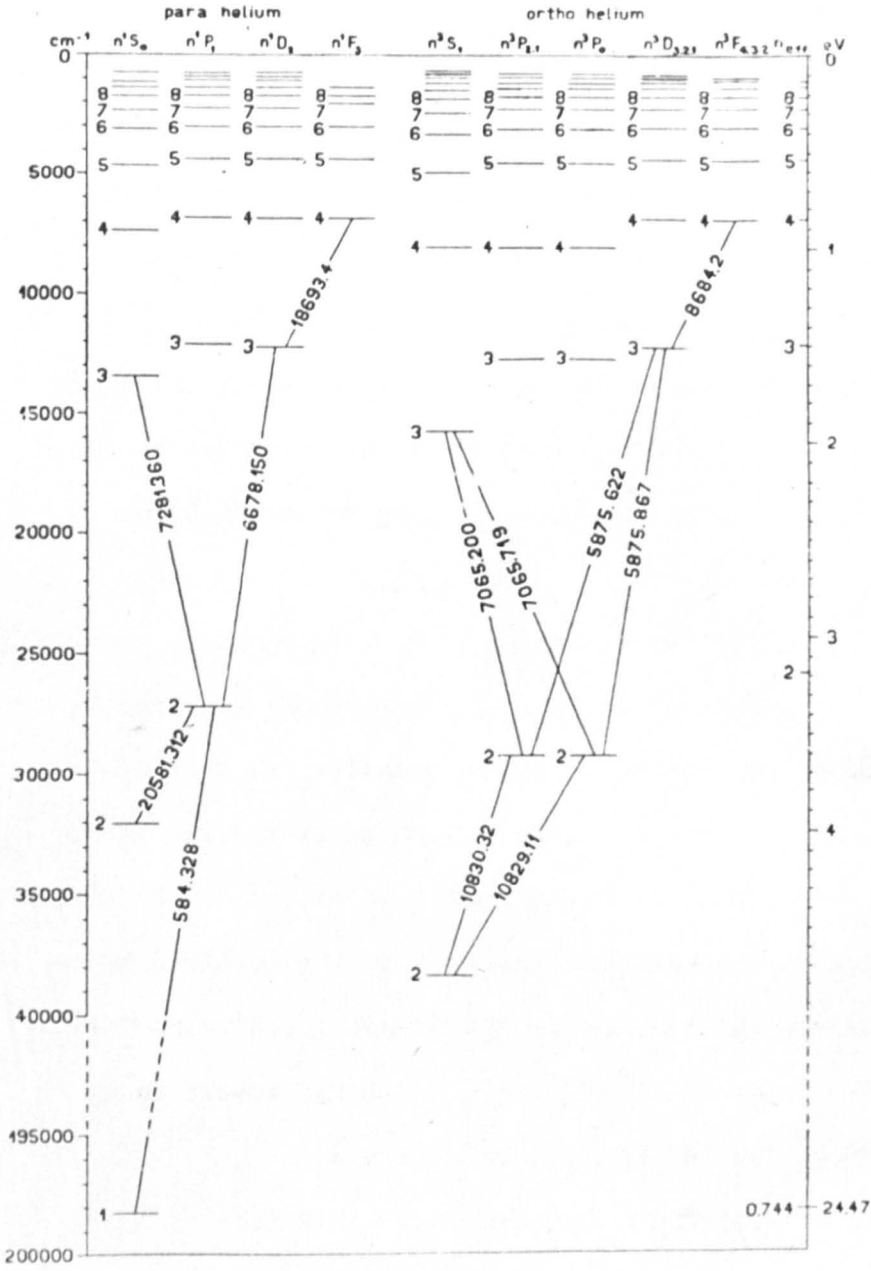

Level diagram of *He*

Figure 2.

electron energies higher than this the electron can balance the angular momentum and carry away the excess energy.

The time during which the atom is excited is about 10^{-8} seconds after which it decays back to the ground state in one or several jumps. The electron may be excited to a state from which it cannot decay spontaneaously, that is, a metastable state. Metastable atoms are destroyed by impact with another particle. If the probability that the excited atom will emit a photon on decaying is high and conversly, the probability of an atom being excited to that state by the absorption of radiant energy is large, the state is known as a resonance state and the radiation termed resonance radiation.

Since quite a high energy is needed for excitation very few atoms or ions will be able to excite by collision since they are relatively slow moving. The much smaller electron however has a much higher velocity and hence most excitation is due to electron-atom collisons. The probability of excitation defined as "the number of electron collisions leading to the required transition, divided by the total number of collisions per electron" is given for helium in Figure 1 and the various energy levels to which the atom may be excited is given in Figure 2.

Ionization may be regarded as an excitation in which the electron is removed to infinity. The probability of ionization as a function of incident electron energy closely resembles the case of excitation to a singlet level, Figure 3.

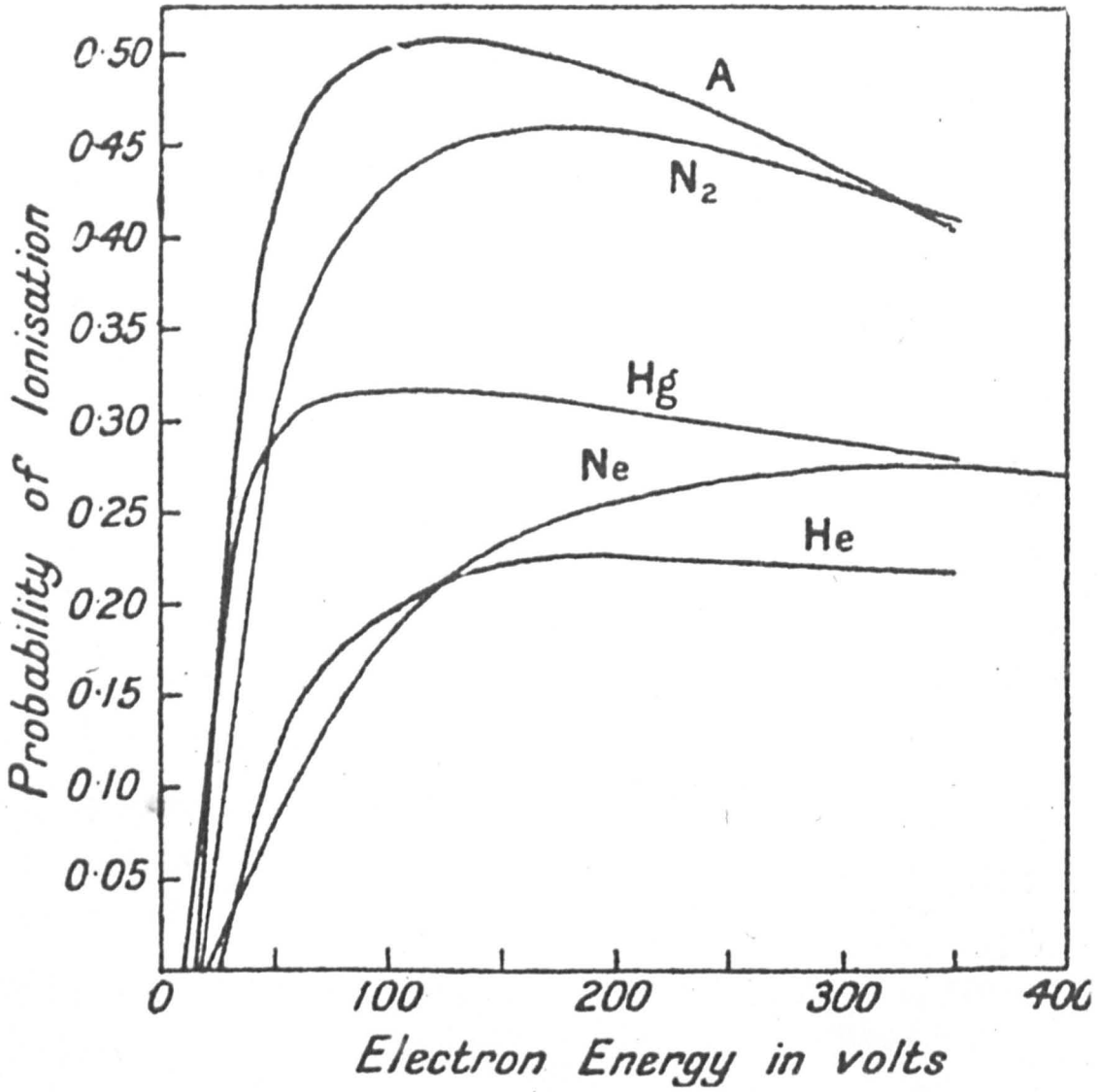

Figure 3.

Curves showing the probability of ionization at a collision as a function of impacting electron energy in volts.

1.2. The First Townsend Ionization Coefficient

The interpretation of the spatial growth of the pre-breakdown currents flowing between parallel plate electrodes in a uniform electric field was evolved by Townsend in 1900 (2, 3, 4). He found that the current flowing, I, was directly proportional to the initial photo-electric current, I_o, and increased exponentially with the inter-electrode gap distance, d. Hence

$$I = I_o \, e^{\alpha d} \qquad 1.1.$$

where α is the proportionality constant termed the Townsend first ionization coefficient and is defined as the average number of ionizing collisions made by one electron advancing 1 cm. in the direction of the applied electric field, E. This expression only holds if the ratio of the electric field to the gas pressure, E/p which is a measure of the mean electron energy, is kept constant.

Townsend found empirically (4) that α/p is a function of E/p and that the relationship is of the form

$$\alpha/p = A \exp. - \frac{(BV_i p)}{E} \qquad 1.2.$$

where A and B are constants characteristic of the gas used and V_i is the ionization potential of the gas. The form of this expression, although involving several important approximations which will be discussed in Chapter 3, nevertheless gives good agreement with experimental results over limited ranges of E/p. It is significant to note that this was the first time that the concept of an ionization potential had ever been used.

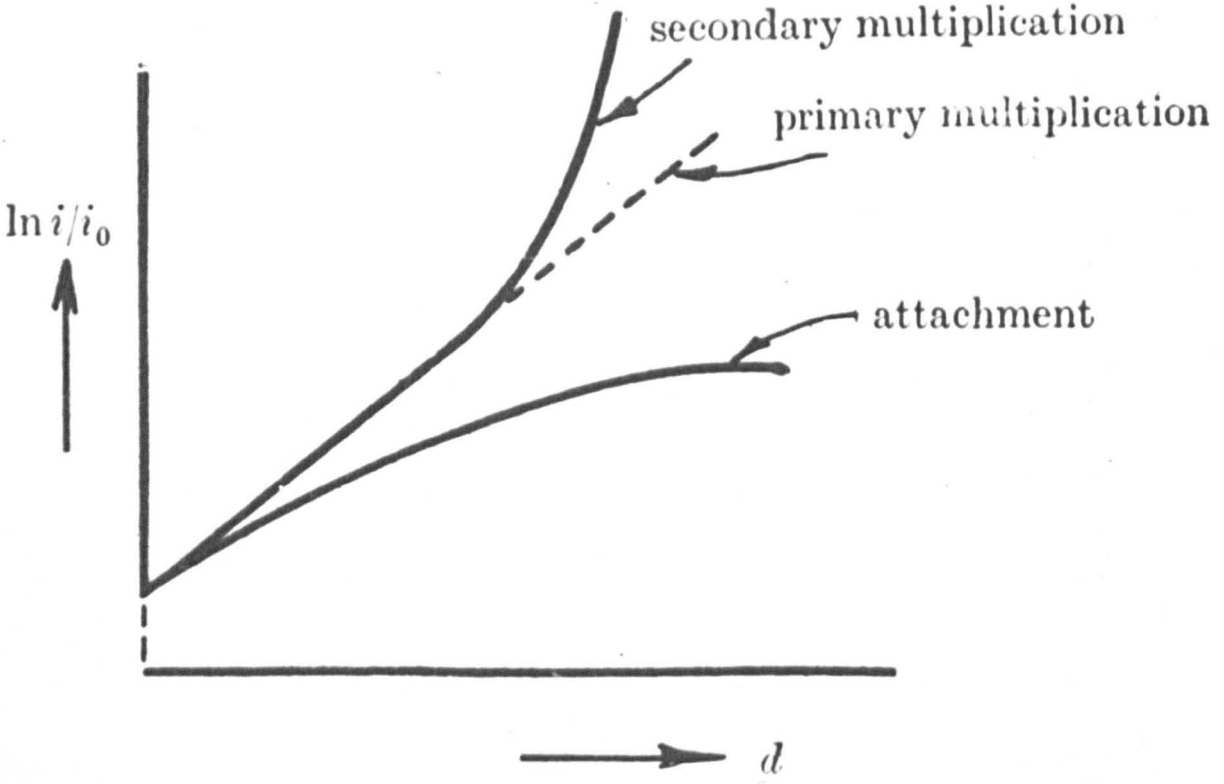

Typical Current Growth Curve.

Figure 4.

A more useful approach to the Townsend first ionization coefficient is to consider it as the number of ionizing collisions an electron undergoes whilst falling through a potential difference of 1 volt. The coefficient termed η, has the advantage of being a function of E/p itself and it connected to α by the expression

$$\eta = \alpha/E \qquad 1.3.$$

Since α is the number of electrons produced on collision of the primary electron travelling 1 cm. in the direction of the field

$$\alpha = \nu_i/\bar{v}_d$$

where ν_i is the frequency of ionization on collision and $\bar{v}_d$ is the mean drift velocity of the electron in the field. Since $\bar{v}_d = \mu E$, where μ is the electron mobility coefficient

$$\alpha = \nu_i/\mu E \quad \text{or} \quad \eta = \nu_i/\mu E^2 \qquad 1.4.$$

From a consideration of equation 1.1. it is evident that a graph of $\log_e$ i.v.d. should be a straight line of gradient α. As may be seen from Figure 4 this is observed at low values of d, but at higher values the current tends to rise faster than if it were a simple exponential function of d, until, at a definite gap distance, d_s, the current increases very rapidly and becomes theoretically infinite. When this occurs the current flow in the gap is said to be self-maintained, that is, the current continues to flow even though the photo-electric current, I_o, is reduced to zero.

1.3. The Second Townsend Ionization Coefficient

The extra ionization observed as d approaches d_s, indicated by the upcurving of the current growth curves, was attributed by Townsend to ionization of the gas molecules by positive ions formed in the primary ionizing collisions, (5, 6). This was a logical conclusion at the time since, at this early date, Townsend thought that the primary ionizing collisions were caused by negative ions, not electrons, and hence it was natural to assume that the positive ions also could ionize. He therefore postulated a new current growth equation which fitted both the linear part of the curve and the upcurving

$$I = \frac{I_0(\alpha-\beta)\exp.(\alpha-\beta)d}{\alpha-\beta\exp.(\alpha-\beta)d} \qquad 1.5.$$

where β is the mean number of ionizing collisions made by each positive ion per centimeter of path in the field direction.

In 1923, however, Holst and Oosterhuis (7), found that the sparking potential, which depends upon the secondary coefficient, varies with cathode material as well as with the gas used. This seemed to indicate that ionization of the gas atoms by positive ion collisions was not the predominant process, but a cathode dependence is explained if electron emission by positive ion bombardment of the cathode is the chief operative mechanism. A current growth equation was derived for this process which is of the same form as that postulated by Townsend for the β process,

$$I = \frac{I_0\exp.(\alpha d)}{1-\gamma[\exp.(\alpha d)-1]} \qquad 1.6.$$

where γ is the coefficient for this mechanism and is defined as the number of electrons emitted from the cathode per positive ion produced in the gas.

It is now known that there are six possible secondary mechanism which can contribute electrons to the discharge, so causing an upcurving in the current growth curve as d approaches d_s. Three of these processes are due to bombardment of the cathode and three are due to collisions in the gas.

Cathode Processes

1. Electron liberation by positive ion bombardment of the cathode:
2. Electron liberation by excited or metastable atom bombardment of the cathode:
3. Electron liberation by photon bombardment of the cathode.

Gaseous Processes

1. Ionization by positive ion collision with gas atoms:
2. Ionization by excited or metastable atom collision with gas atoms:
3. Ionization by photon collision with gas atoms.

Unfortunately the variation of I as a function of d is of the same form for each mechanism and hence it is not possible to separate them by a theoretical analysis of the current growth curves. For this reason, all the secondary coefficients are combined as the generalised secondary coefficient, which, to a first

approximation, has been shown by Druyvesteyn and Penning to be the arithmetic sum of all the individual secondary coefficients, (8). Equation 1.4. thus becomes

$$I = \frac{I_0 \exp.(\alpha d)}{1-\omega/\alpha[\exp.(\alpha d)-1]} \qquad 1.7.$$

Since all the above possible mechanisms do not apply to the conditions under which the work presented in this thesis were carried out, it is necessary to consider these processes individually and to decide which of these will contribute to the value of ω/α obtained from the present work.

1.3.1. Electron Liberation by Positive Ion Bombardment of the Cathode

A positive ion, incident upon a metal surface may be reflected, either with or without loss of energy; it may also cause sputtering of the surface, (9, 10, 11), or it may cause an electron to be emitted.

The emission of electrons from a cathode surface due to the incidence of high energy positive ions is thought to be a thermionic effect due to intense local heating of the cathode at the point of impact, (12). This is supported by the fact that the energy distribution of the ejected electrons is that which would be expected from thermionic emission, (13).

For slow positive ions, the process of electron liberation can occur in two stages. When the ion is very close to the surface of the metal it may be neutralized by an electron from the filled energy band of the metal entering a level of equal energy in the

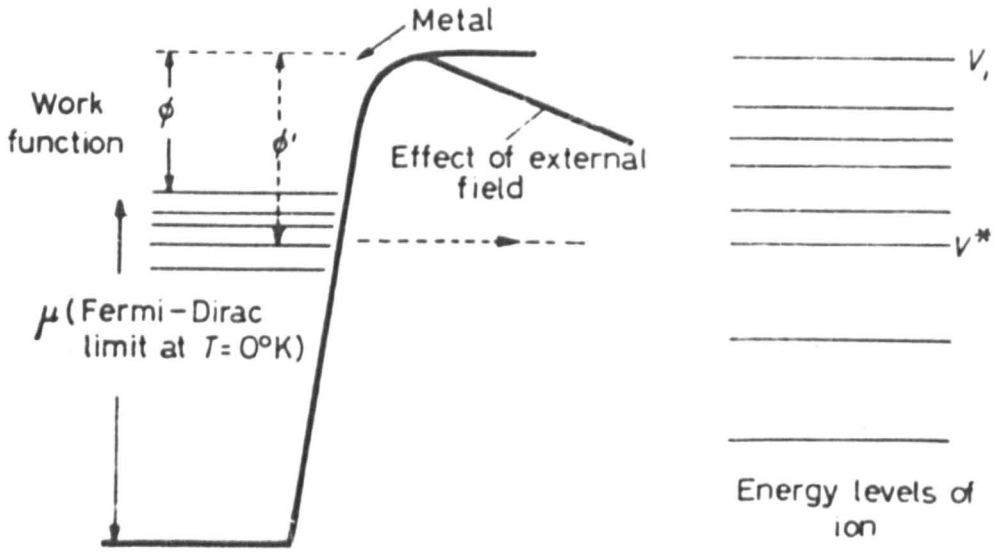

Figure 5. *Energy level diagram of a positive ion close to the surface of a metal. Here the external field is due to the charge on the ion*

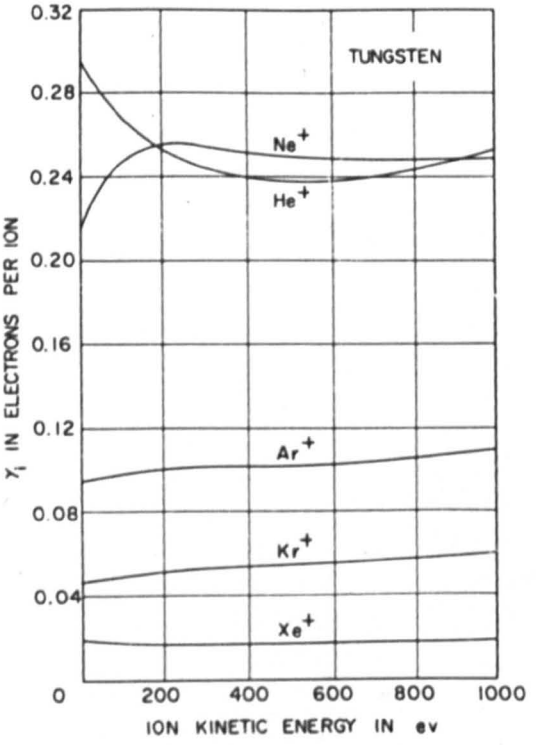

Figure 6. Total electron yield for singly charged ions of Ne, He, A, Kr, Xe on atomically clean tungsten.

ion so long as such a level is empty or half-empty, Figure 5. An excited atom is thus formed having an excitation energy E_e. Most of these excited atoms are formed less than 10^{-7} cms. from the cathode and, since the positive ion drift velocity, $\bar{V}$, is of the order of 10^5cms/sec. the ion is only excited for 10^{-12} secs. before striking the cathode. In this short time the ion is unable to fall to the ground state and emit a photon in the conventional manner, and hence a radiationless transition of energy from the ion to the cathode occurs which can eject another electron from the metal.

The initial neutralization is most likely to occur when

$$\phi = E_i - E_e$$

where ϕ = work function of the metal

E_i = ionization energy of the gas atom.

Therefore $E_e = (E_i - \phi)$

But if E is the energy of the final ejected electron

$$E = E_e - \phi$$

$$\therefore \quad E = E_i - 2\phi$$

Hence if $E_i > 2\phi$ and $E_e > \phi$ an electron may be emitted by this mechanism.

An alternative one stage process is also possible if the positive ion can penetrate the potential barrier before capturing an electron. In this process two electrons are involved at the same time, one being captured into the ground state of the ion and the other being emitted.

Hagstrom has determined the effect of bombarding an atomically clean metal with positive ions of the rare gases (15, 16, 17, 18, 19), Figure 6, and has shown that the "one-step" process is the main one (20).

1.3.2. Electron Liberation by Excited and Metastable Atom Bombardment of the Cathode

Von Engel (21) has shown that metastable atoms incident upon a cathode surface cause secondary electron emission due to their possessing potential energy. 10^{-2} electrons per incident metastable atom are recorded in mercury (22) and still greater yields in the rare gases, (23).

Metastable bombardment of the cathode is not of great importance in hydrogen since the metastable state is so weak that it is easily destroyed at low pressures by a moderate electric field. In the rare gases, e.g. helium, the effect of metastable bombardment is not negligable. In helium the $2S^3$ and the $2S^1$ states can both cause electron liberation. Hagstrom (2), has claimed that a two-stage electron ejection process similar to the two-stage positive ion process given above, is probable for metastable atoms incident upon the cathode. The incident metastable atom is first resonance ionized provided

$$\phi > E_i - E_m$$

where E_m is the energy of the metastable state, and the ion so formed is then neutralized by an Auger process.

Since the metastable atom is uncharged and hence not

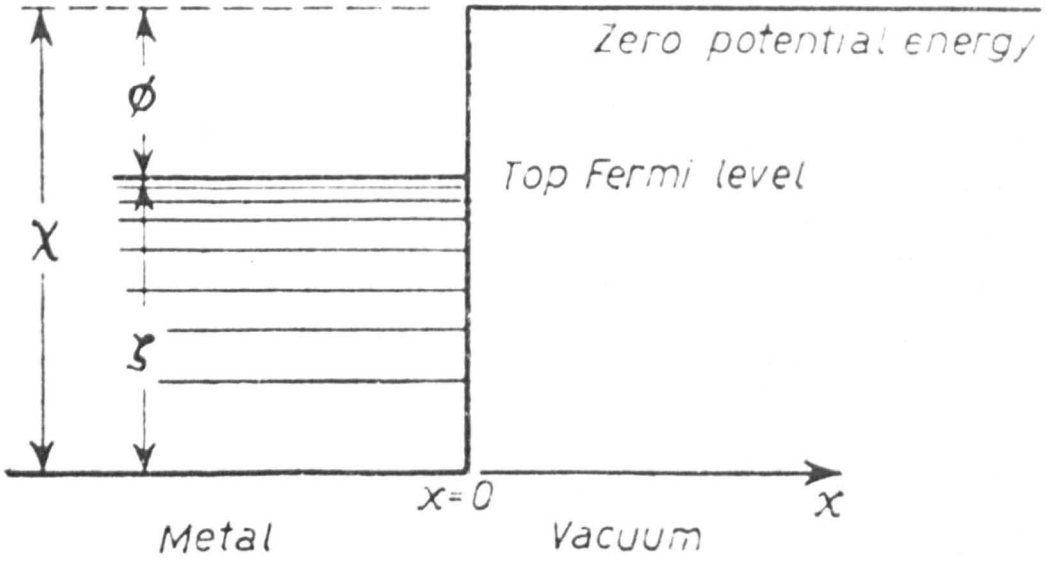

Energy diagram of electrons in a metal

Figure 7.

influenced by the electric field it is unlikely that more than about 20% of those formed in the gap will be incident upon the cathode even at small gap distances. Despite this, however, Dorrestein, (23), found that when helium atoms were bombarded by 22 e.v. electrons, so producing both metastable atoms and excited atoms which gave photons, the metastable atoms were four times more effective in liberating secondary electrons from a platinum cathode than were the photons.

Since excited atoms have a life of only about 10^{-8} secs. they have little chance of reaching the cathode and hence it appears that, in hydrogen, neither of these processes will contribute to ω/α, whereas in the rare gases the effect of metastable atoms can be considerable.

1.3.3. Electron Liberation by Photon Bombardment of the Cathode

When an excited atom decays to the ground state it loses energy. This energy is usually emitted as a photon, which, if incident upon the cathode, can cause secondary electron emission from the cathode. From a consideration of Figure 7, it may be seen that the least energy required for an electron to escape from the metal is $e\phi$, therefore

$$h\nu_0 = e\phi$$

where h = Planck's constant

ν_0 = threshold frequency

For photons of higher frequency

$$\nu h = e\phi + \tfrac{1}{2} mv^2 \qquad 1.8.$$

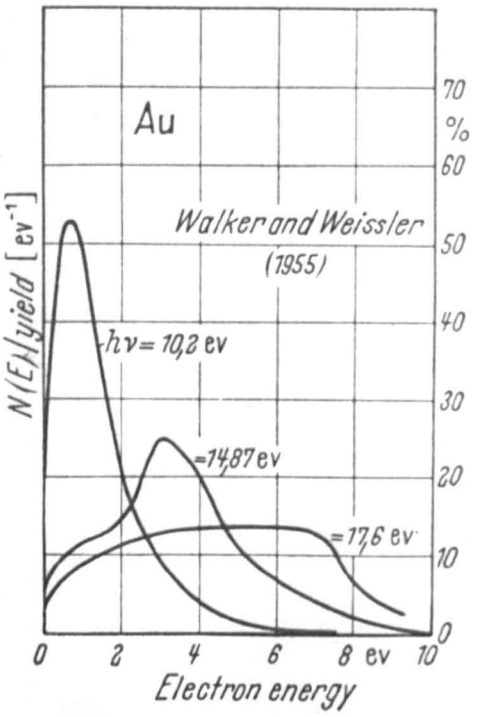

Figure 8.

Energy distributions of photoelectrons from Au with radiation of the extreme ultraviolet.

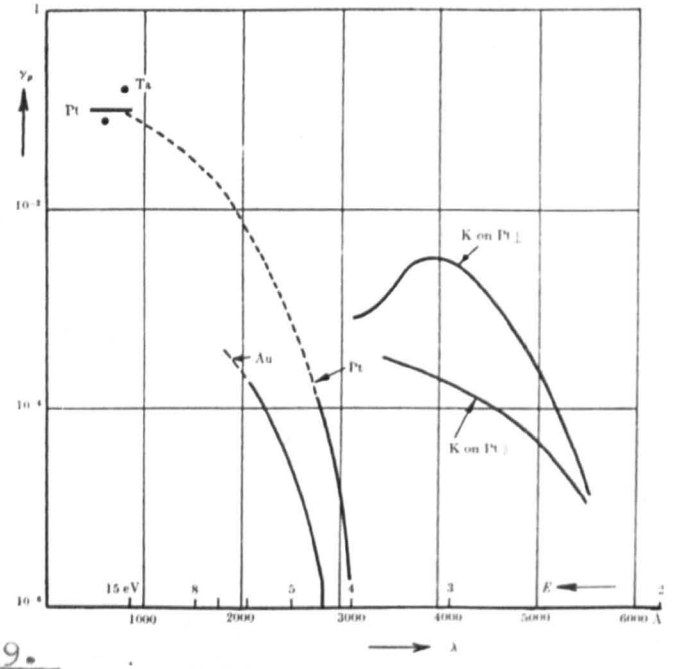

Figure 9.

Photo-electric yield γ_p as a function of the wavelength λ of the incident light (energy E of quantum) for various substances

From these considerations it may be seen that to release an electron from a gold surface for which ϕ = 4.7 e.v., a photon must have a wavelength of less than 2630 Å, i.e. the radiation must be in the ultra-violet region.

Since the electrons emitted come from different depths in the conduction band of the metal an energy distribution of photo-electrons is obtained. Such a distribution of electrons from a gold surface is shown in Figure 8.

Each incident quantum of sufficient energy is capable of ejecting an electron. Only a small percentage are actually emitted, however. The number of electrons emitted per incident quantum is termed the photo-electric yield and is a function of the wavelength of the radiation, Figure 9.

The effect of this mechanism on the spatial growth of ionization in a gap has been studied by Bowles (24), Hale (25, 26, 27) and by Druyvesteyn and Penning (8). The latter have published curves showing the percentage electron energy lost in various processes which indicates that a marked excitation peak is present in hydrogen at values of E/p_o < 100 volts/cm.mm.Hg. In practice however this peak is not observed.

1.3.4. Ionization by Positive Ion Collisions with Gas Atoms

Two types of positive ion-atom collisions are possible, elastic collisions in which no change of internal energy is experienced and inelastic collisions during which the internal energy of the particles is altered. For an elastic collision

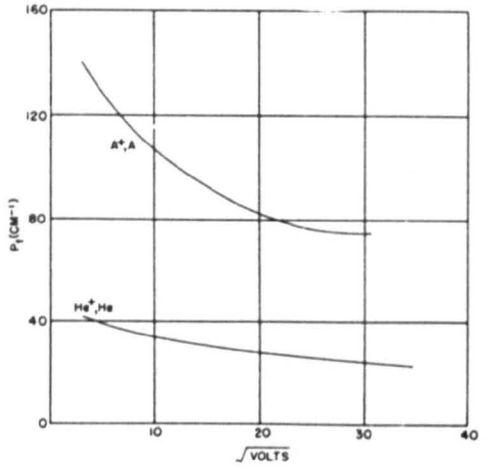

Figure 10. Charge-transfer cross sections of A^+ in A and He^+ in He as a function of energy.

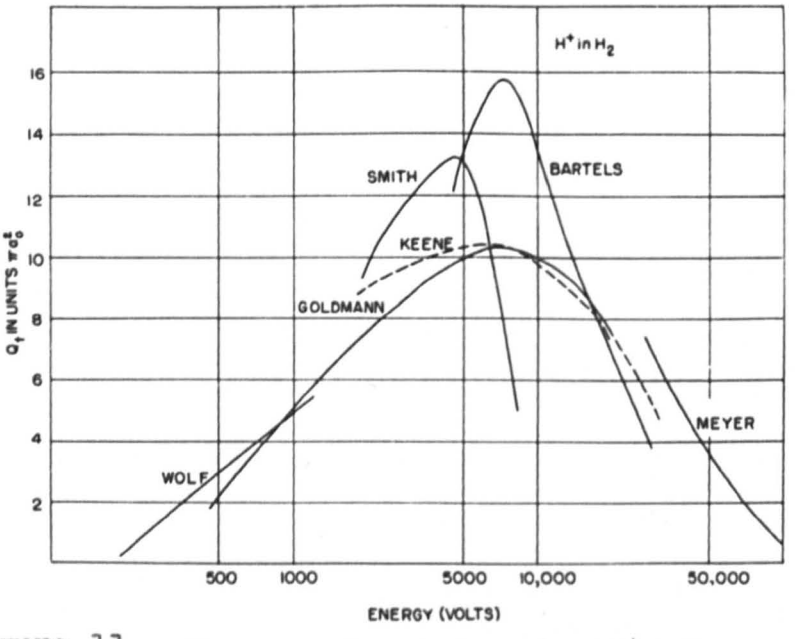

Figure 11. Charge-transfer cross section of H^+ in H_2.

$$\Delta E_i = \frac{2mM}{(m+M)^2} E_i$$

where ΔE_i is the energy loss of the positive ion, m is the mass of the positive ion, and M is the mass of the gas atom. Since the two masses are about equal

$$\Delta E_i = \frac{2m^2 E_i}{4m^2}$$

Therefore $$\Delta E_i = \tfrac{1}{2} E_i \qquad 1.9.$$

From this expression it is seen that a positive ion loses half its energy at each collision and since many collisions occur at all but very low pressures (< 1mm.Hg.), few positive ions will ever give enough energy to undergo inelastic collisions. When an elastic collision does occur three phenomena are possible, firstly the atom may become excited and reverting to the ground state emit a photon, secondly, charge transfer may result, and, thirdly, ionization may be caused. Charge transfer results in the formation of slow ions and atoms having energies in the order of the initial ion. An ion which has sufficient energy to engage in charge transfer becomes a neutral atom retaining most of its velocity whilst the atom which has given up an electron and becomes a positive ion, starts with zero velocity, is accelerated in the field and eventually may undergo a further reaction. The probability of charge transfer decreases as the positive ion energy increases in helium whereas in hydrogen a maximum probability occurs at an ion energy of about 5000 volts, Figures 10, 11. For any of these processes, the reaction must take place in a time equal to or less than the period of internal

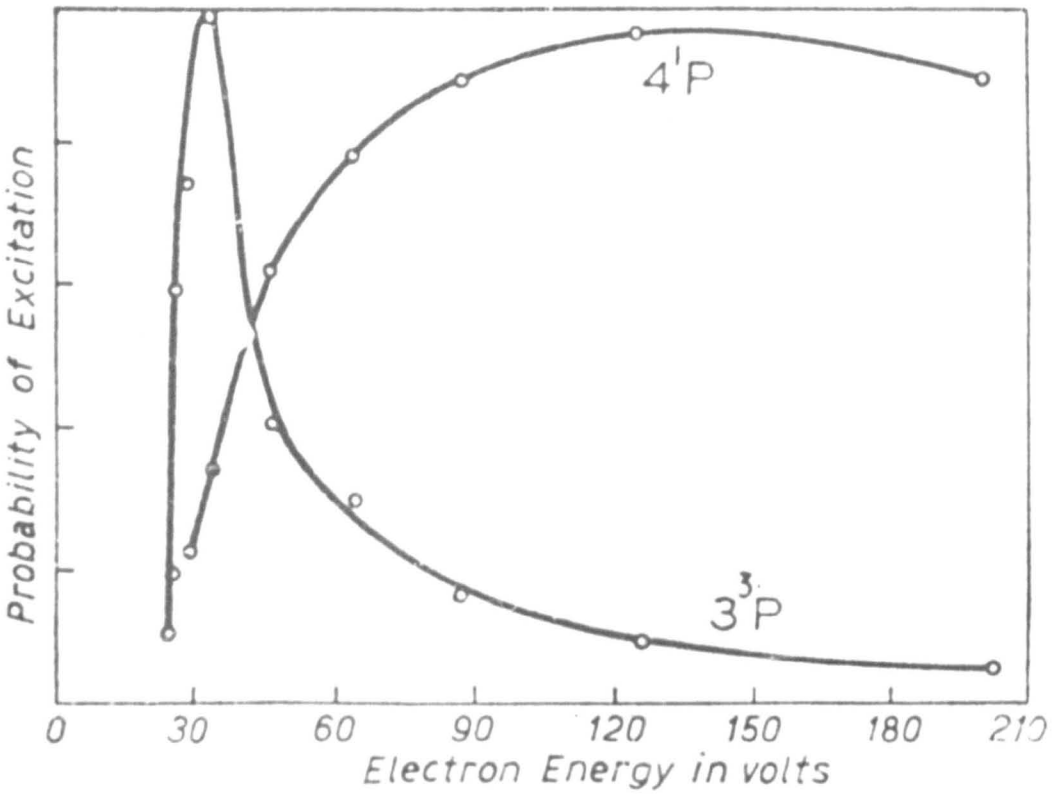

Excitation function for the 4^1P and 3^3P levels of helium

Figure 12.

vibration of the system, since otherwise the electrons would have time to rearrange themselves whilst momentum is being transferred. Since ions need at least 300 e.v. (25, 26, 27), to ionize an atom by collision in hydrogen, and even more in helium, it seems unlikely that this process is of importance in the range of E/p discussed in this thesis.

1.3.5. Ionization by Metastable and Excited Atom Collisions with Gas Atoms

An excited atom, on falling to the ground state, emits a photon, the energy of which is equal to the excitation energy of the excited atom. Since the excitation energy, and hence the photon energy, must be below the ionization energy, this photon cannot ionize other unexcited atoms of the same gas. In gas mixtures, however, where the ionization energy of one gas is below the excitation energy of the other gas, this process can be important (28, 29). Indeed it is the basis of the process known as cataphoresis which is discussed in detail in Chapter IV. If in a pure gas the photon from the decay of an excited atom is incident upon a further excited or metastable atom, this second atom may be ionized. Since the probability of this is very small due to the short life time of the excited atom, this process will only be significant at high gas pressures.

Although metastable atoms suffer many collisions during their life time the probability of ionization is negligable since the metastable energy level must be below the ionization energy level and the collision of two metastable atoms or a metastable atom and an excited atom, which could produce an electron, will be very

rare.

1.3.6. Ionization by Photon Collisions with Gas Atoms

For a photon to ionize an atom in the ground state the condition

$$h\nu > eV_i$$

must apply, where h is Planck's constant. Most absorption occurs when

$$h\nu \approx eV_i$$

Since the only radiation present in the discharge is that from the decay of excited atoms discussed above, this process may be neglected in a pure gas at low pressures.

1.4. Recombination

When positive ions and electrons are present together in a gas there is a finite probability that they will react to form a neutral atom. The excess potential energy may then be evolved as kinetic energy of the atom or as a photon. If the latter is the case the frequency of the photon will be given by

$$h\nu = eV_i + K$$

where K is the kinetic energy of the incident electron and V_i is the ionization potential of the atom.

Since the Townsend first ionization coefficient is determined by measuring the actual spatial growth of ionization, the value obtained will appear to be lower than the true value if recombination is present. To allow for this equation, 1.6. must be written

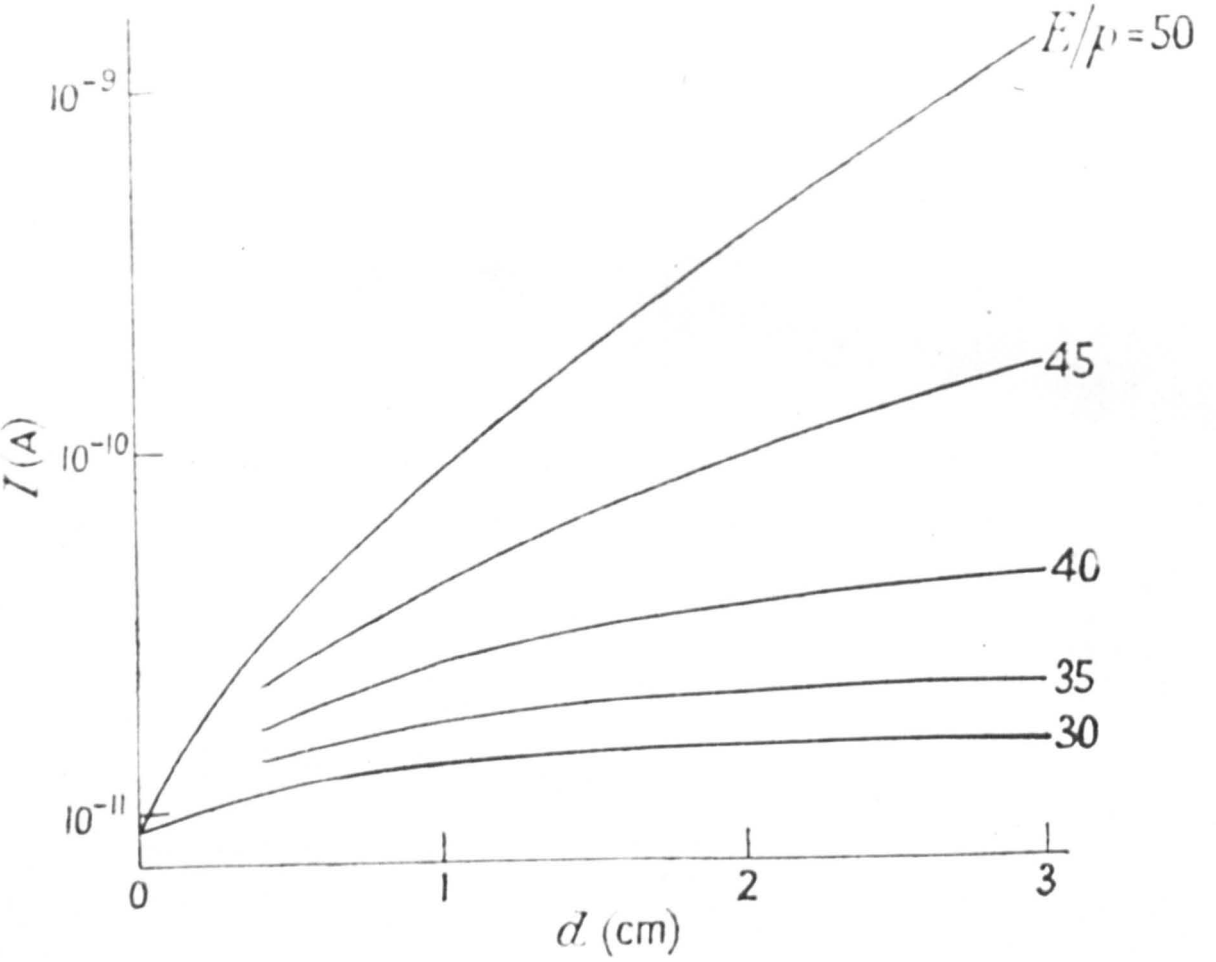

Current Growth Curves in Water Vapour.

Figure 13.

$$I/I_o = \frac{(\frac{\alpha}{\alpha-a})[\exp.(\alpha-a)d-(\frac{a}{\alpha-a})]}{1-\frac{\omega}{\alpha}[(\frac{\alpha}{\alpha-a})[\exp.(\alpha-a)d-1]]} \qquad 1.10.$$

where a is the recombination coefficient. The probability of recombination will decrease as the relative velocity of the electron and ion increases, since the time during which the particles are near to each other and can attach is decreased. The probability will increase as the effective diameter of the ion increases, that is it will be larger for excited ions than for normal ions. Since the electron velocity is a function of E/p, the effect of recombination should be noticed at low values of E/p. This is indeed observed, Figure 13.

In the helium discharge the molecular ion He_2^+ is the principal ion at low values of E/p (< 10 volts/cm.mm.Hg.), since 70% of the ions are He_2^+ (30) and its mobility is almost twice that of the atomic ion He^+, (31). This molecular ion can undergo dissociative recombination so:-

$$He_2^+ + e \dashrightarrow He^* + He$$

where He* represents an excited helium atom.

It would, therefore, be expected that some indication of this would be apparent at low values of E/p.

1.5. Breakdown Criterion

For a discharge in the absence of any recombination or electron loss processes, it may be seen from equation 1.7. that the current flowing, I, is dependent upon I_o. For the current to have

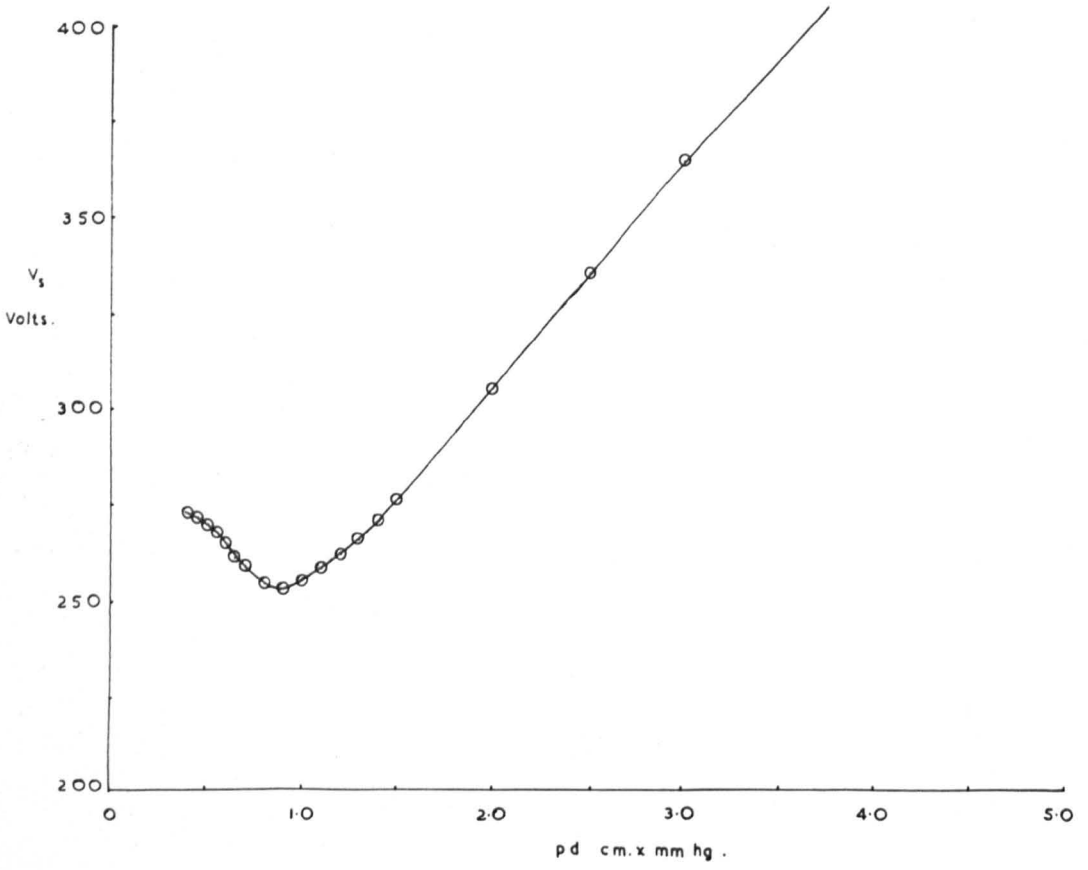

Typical Paschen Curve.

Figure 14.

a finite value when I_0 is zero, as happens when breakdown occurs, the denominator of this expression must be zero, that is

$$1 - {}^{\omega}/_{\alpha}\,[\exp.(\alpha d_s)-1] = 0 \qquad 1.11.$$

This is taken as the criterion of a self-maintained discharge and indicates that the sparking distance, d_s, is dependent upon the generalised secondary coefficient, ${}^{\omega}/_{\alpha}$, which in turn depends upon the cathode surface. If d is kept constant and the potential difference of the electrodesis increased the potential difference at which the above expression is satisfied is termed the sparking potential, V_s. V_s is defined as the lowest potential difference at which a current will flow through the gas without the aid of any electron producing radiation. Since V_s is dependent upon ${}^{\omega}/_{\alpha}$ the sparking potential may be used to determine values of the secondary coefficient as a function of ${}^{E}/_{p_0}$ so long as values of ${}^{\alpha}/_{p_0}$ as a function of ${}^{E}/_{p_0}$ are also known.

If equation 1.11. is rearranged and ${}^{\omega}/_{\alpha}$ and ${}^{\alpha}/_{p_0}$ are functions of ${}^{E}/_{p_0}$ only it is seen that

$$V_s = f(p_0 d_s) \qquad 1.12.$$

This was found empirically by De la Rue and Muller (32) and by Paschen (33) who gave his name to the law. This function is seen to have a minimum value which should correspond to the value of ${}^{E}/_{p_0}$ at which the ionization efficiency is a maximum, Figure 14.

For the case in which recombination processes are operative equation 1.11 becomes

$$1 - {}^{\omega}/\alpha \left(\frac{\alpha}{\alpha-a}\right)[\exp.(\alpha-a)\,d-1] = 0 \qquad 1.13.$$

where a is the recombination coefficient analogous to α and is defined as the number of electrons which recombine per cm. of path at 0°C and 1 mm.Hg pressure. By applying equations 1.10 and 1.13. to the observed $\log_e$ i.v.d. curves, the values of α, a and ${}^{\omega}/\alpha$ can be obtained by a process of curve fitting.

Conclusion

In this chapter the relevant theory of pre-breakdown currents and of breakdown itself have been considered together with the various mechanisms which can contribute to the generalised secondary coefficient. The theory has been shown to apply to the range of pressures considered in the present work.

To understand the need for the present determinations it is first necessary to consider the previous work in this field which will be given in Chapter II.

CHAPTER II

REVIEW OF PREVIOUS EXPERIMENTAL DETERMINATIONS

2.1. D.C. Measurements in Hydrogen

Many of the early experimental investigations of the spatial growth of ionization were hampered by limitations in the techniques involved. Early attempts at measuring the primary and secondary ionization coefficients were affected by the presence in the gas studied of impurities of the residual gas left after the experimental tube had been evacuated. Very little outgassing of the experimental apparatus was employed and although mercury diffusion pumps were used, liquid air trapping of the mercury vapour was not. Against this background, therefore, it is creditable that the results obtained from the original work of Townsend (4, 5, 6) and the early work of Ayres, (34), are so close to modern values, particularly as Bowls, (11), later showed, that mercury contamination could increase the value of α/p by as much as 50%.

Despite the inevitable doubt as to the absolute values obtained from these determinations, many valuable trends were observed. Using slightly better equipment than Townsend or Ayres, Holst and Oosterhius (7) and Penning, (35), observed that the secondary ionization coefficient was cathode dependent, so showing that secondary electron emission must be predominantly a cathode mechanism not a gaseous process as postulated by Townsend. That this variation had not been observed before has been attributed to the fact that both these groups used liquid air trapping between

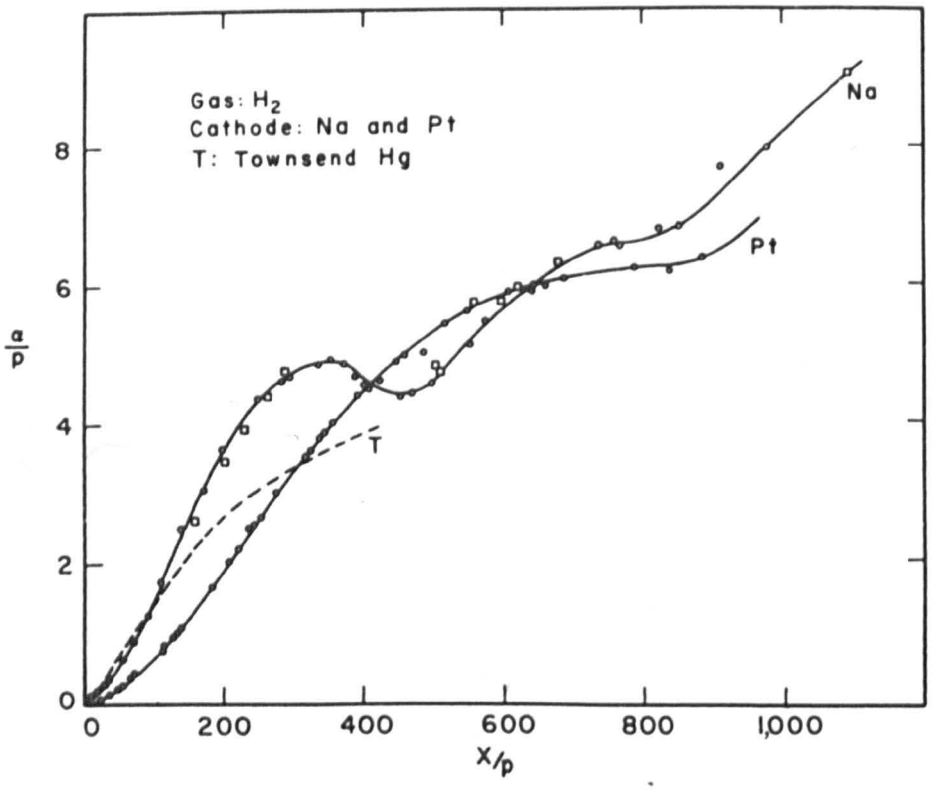

Hale's curves for α/p as a $f(X/p)$ in pure H_2.

Figure 15

their mercury diffusion pumps and experimental tubes so obtaining mercury free surfaces, whereas earlier workers had mercury contaminated cathodes which resulted in all cathode materials having the same surface. This hypothesis, which was put forward by Loeb, was investigated by Bowls (11) who obtained values of α/p and ω/α as functions of E/p_o in pure mercury free nitrogen. It was found that different cathode materials gave totally different curves of ω/α v. E/p and that when the cathode was contaminated with mercury agreement was reached with Townsend's results thus supporting Loeb's theory.

Hale (36, 37, 38) using the same apparatus as Bowls, redetermined the ionization coefficients in hydrogen. Tank hydrogen was purified over a purification train and the experimental tube was baked at 425°C for several hours. Liquid air trapping was extensivly used. Since α/p is the measure of a gaseous process it is not surprising that similar values of α/p as a function of E/p were obtained with cathodes of nickel, aluminium on nickel and platinum. When sodium hydride on nickel was used as the cathode, however, values of α/p obtained were 100% higher at low values of E/p than those from the other cathodes. This was attributed to the presence of a stable volatile compound of sodium which had a low ionization potential and which was being ionized by the excited states of the hydrogen. The occurrance of excited hydrogen atoms in the discharge was supported by Hales' values of ω/α calculated from the upcurving of the spatial growth curves at low pressures.

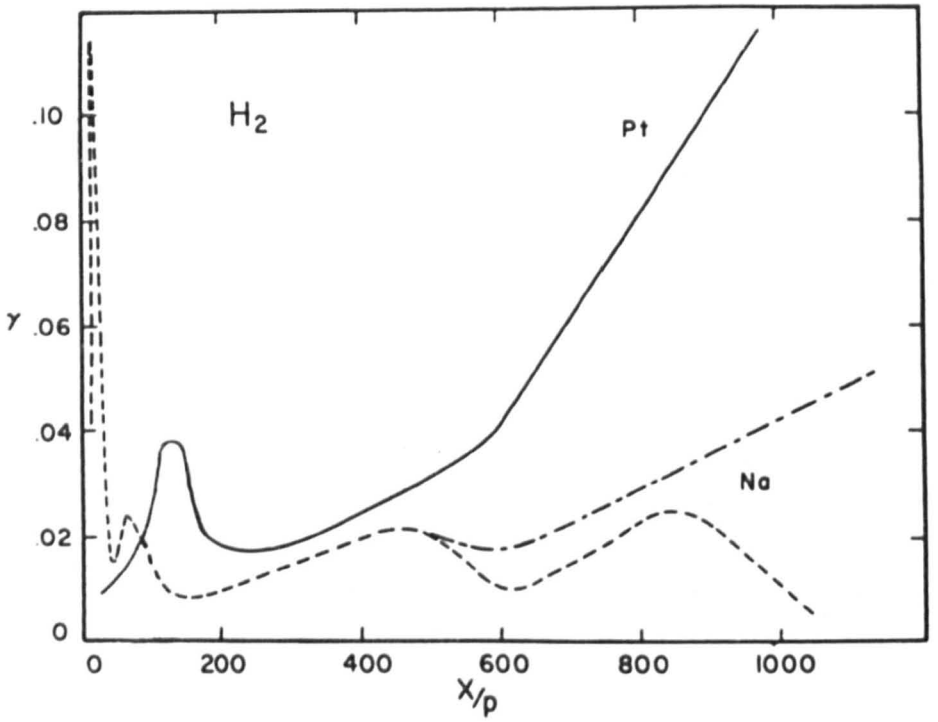

Hale's curves for γ_c as a function of X/p for pure H_2, calculated from the same data as in figure 9.21. Note the very marked photo peaks with pure Pt and Na-coated Pt.

Figure 16.

These results gave a sharp peak in the ω/α v. E/p curve at an E/p of 131 volts/cm.mm.Hg. for the aluminium and the nickel cathodes and at E/p = 120 volts/cm.mm.Hg for the platinum cathode. The peaks were assumed to be due to photo-electric emission from the cathode by photons emitted by the decay of excited hydrogen atoms, whilst the variation in the value of E/p at which it occured was attributed to the aluminium and nickel cathodes having been cleaned in a glow discharge whilst the platinum had not. From the values of ω/α obtained from current growth data, Hale calculated the sparking potential, V_s. This was found to show some discrepancies with observed values of V_s in which case the calculated values were always higher than the observed values. The explanation of this was that the cathode surface was non-homogeneous which resulted in the observed sparking potential relating only to the region of lowest work function and highest ω/α whereas the values calculated from pre-breakdown measurements would be an average value over the whole surface.

The results obtained by Hale are given in Figures 15 and 16 and are compared with other determinations in Figure 17. It may be seen that his results do not agree with Ayres values or with later determinations. Contamination of the gas or of the electrode surfaces or a systematic error in the measuring instruments cannot be entirely ruled out but more recent work with the same type of apparatus, (39), has failed to repeat Hale's values.

At high pressures Hale found no upcurving in the $\log_e I$.v.d.

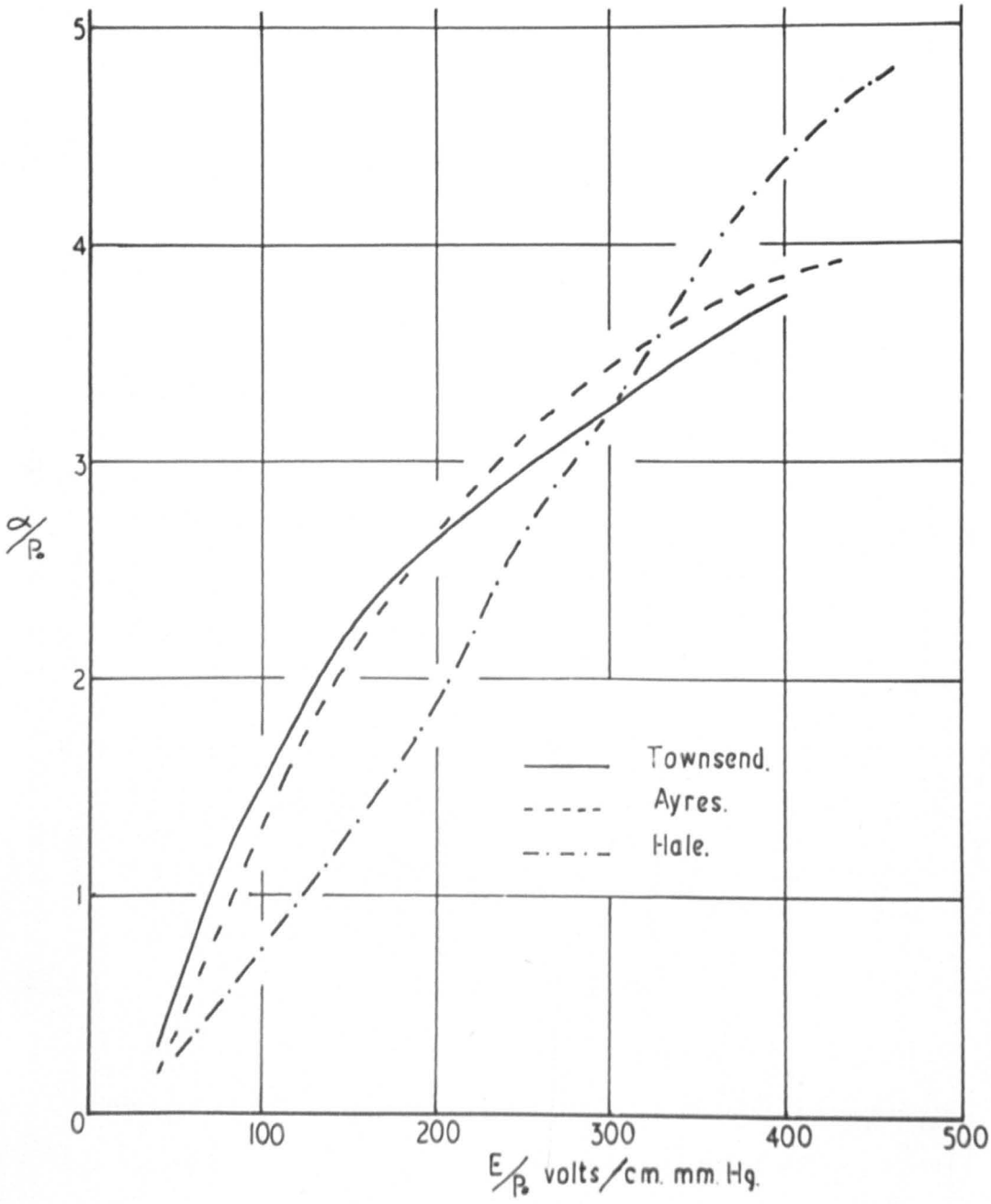

Figure 17.

Comparison of early determinations of /p as a function of E/p.

curves, an effect which had previously been noticed by Sanders, (40), but, whereas in Sanders' work the equipment had been suspect, this did not apply to Hale. On the basis of this Loeb and Meek, (41), put forward the streamer theory of breakdown to try to explain the mechanism whereby a discharge can become self-maintained with no apparent secondary processes. More recent work, however, (42, 43), has shown that even at high pressures upcurving does occur and that Townsend theory is applicable even at pressures of several hundred millimetres of mercury.

In recent years techniques have improved to a very great extent. Residual gas pressures have been lowered to less than 10^{-9} mm.Hg. by means of ultra-high vacuum techniques and the extension of the outgassing process, gas purity has been improved and a much higher standard of instrumentation has been achieved. Despite all these advances, however, perhaps the most important advance in modern determinations is the realisation that secondary effects are present at even low values of inter-electrode gap distance and that this will give a falsely high value to the gradient of the linear portion of the current growth curve. This must hence be allowed for by a mathematical analysis of the current growth data in order to obtain true values of both α/p and ω/α as functions of E/p. It is surprising that until the present investigations no one determination has incorporated all these facilities.

In 1950 Llewellyn-Jones and Davies, (44), carried out

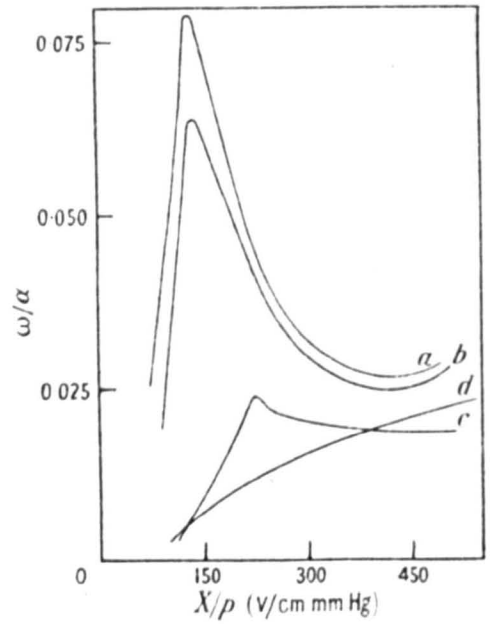

Figure 18. The effect on ω/α of deposition of a copper film on nickel : curve *a*, thin copper film; curve *b*, film outgassed; curves *c* and *d*, increase of film thickness and outgassing.

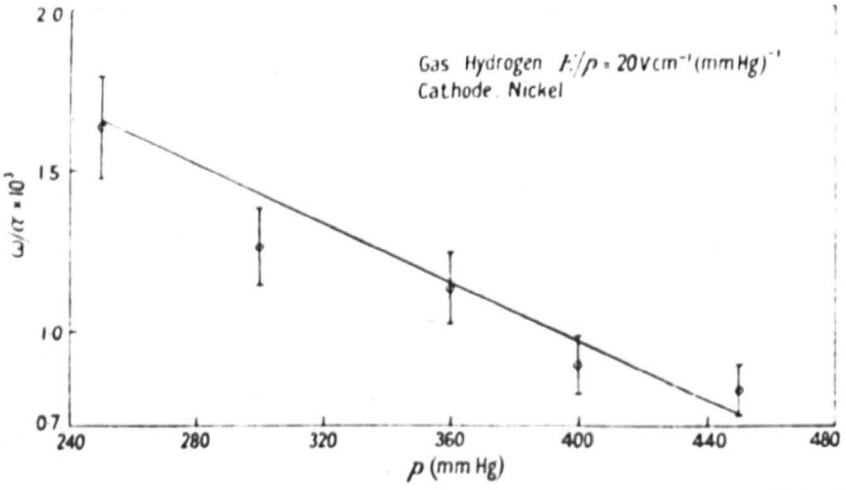

Calculated curve and experimental values of ω/α as a function of gas pressure in hydrogen at a value of $E/p = 20$ v cm $^{-1}$ (mm Hg) $^{-1}$. The calculated curve was obtained using equation (5) and the values of the atomic constants given in the text.

Figure 19.

experimental determinations of breakdown in hydrogen in an attempt to investigate how the ω/α v. E/p curve varied with the thickness of an evapourated film cathode. Unfortunately the α/p v. E/p values obtained by Hale were used as they were accepted as the most accurate until 1956. Photo-electric peaks were found which decreased as the cleanliness of the cathode increased, Figure 18.

In 1956 both Hopwood, Peacock and Wilkes, (43), and Rose (39), redetermined the ionization coefficients in hydrogen. The work of the former was aimed essentially at determining over what range of pd the Townsend theory was applicable. To this end the spatial growth of ionization was followed to within a few percent of breakdown at pressures of up to 700 mms.Hg. In all cases breakdown was preceded by upcurving of the $\log_e$ I.v.d. curve so substantiating the Townsend theory up to a value of pd = 2800 mm.Hg.cms. at least. The vacuum techniques for this work were not very rigorous. A residual gas pressure of 10^{-5} mm.Hg. was used along with commercial grade hydrogen, purified only by being passed through liquid air traps. The values of α/p published were obtained straight from the slope of the linear section of the current growth curves, no analysis being applied. They agreed at $E/p > 30$ volts/cm.mm.Hg. with Ayres results, but not with Hale's. Indeed this was only one of several indications that Hale's results were not as accurate as they had previously been considered.

In order to check these results fully Rose, (39), undertook to determine α/p as a function of E/p over a range of E/p from 20

to 1000 volts/cm.mm.Hg. A rigorous baking procedure was adhered to and a residual gas pressure of 10^{-9} mm.Hg. was achieved. Just before each run the cathode surface was bombarded by a high current pulsed discharge in pure hydrogen during which the cathode temperature rose to about 800°C. Extensive liquid air trapping was employed and the hydrogen used was obtained from the decomposition of uranium hydride. Hence every care was taken to ensure that the results obtained would be for pure hydrogen and not a contaminated gas. Unfortunately three criticisms can be levelled against this work, firstly, the cathode was of bulk metal which experience indicates will outgas even after cleaning in a glow discharge, secondly, the cathode was in the form of a Rogowski profile, (45), which, although it would reduce field distortions would not eliminate them as would a guard ring assembly (46), and thirdly, no analysis was used to compensate α/p for the effect of ω/α at low values of d. The results obtained agreed with Ayres values, except at low values of E/p, and with the results of Hopwood, Peacock and Wilkes in the range in which they overlapped. Agreement could not be reached with Hale even when a system the same as Hale's was used, Figure 20.

The first mathematical analysis of spatial current growth measurements was carried out in 1957 by Crompton, Dutton and Haydon, (42), Only a limited range of E/p was used, ($20<E/p<25$ volts/cm.mm.Hg.), but within this range α/p. fell below the corresponding values of Ayres and of Rose but agreed quite well

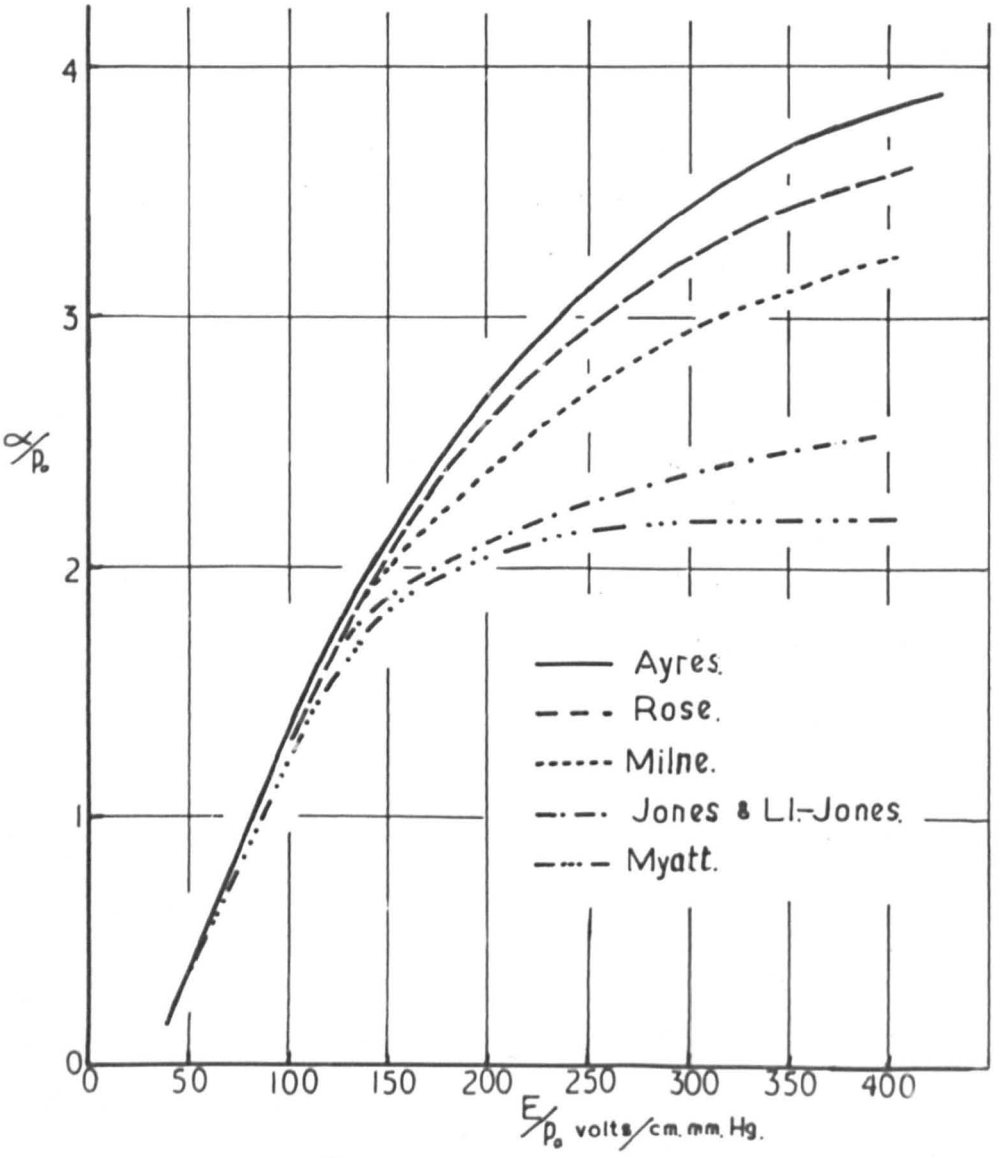

α/p_o v. E/p_o from previous determinations

Figure 20.

with more recent values. Values of α/p and ω/α for both a silver and a nickel cathode were measured before and after a glow discharge was passed. It was found that the primary coefficient remained unchanged whereas the secondary coefficient was considerably reduced by this cathode clean-up. This work also showed that the mechanism of breakdown in hydrogen is the same at a pd of 1000mm.Hg.cms. as it is at 50 mm.Hg.cms..

In 1958 the research group at Swansea published the results of two important pieces of work. The first by Jones and Llewellyn-Jones, (47), used a glass experimental tube containing bulk metal electrodes of 3 cms. diameter. The hydrogen was obtained by the electrolysis of barium hydroxide and dried by standing over phosphorus pentoxide. It was then passed through hot palladium thimbles to a tube containing reactor grade uranium turnings which had previously been baked at 450°C in vacuum. In this way the hydride of uranium was formed which when heated to 300°C would give off pure hydrogen. However, it was believed by Rose and experience in these laboratories indicate that a temperature of 800°C - 1000°C is required. Measurements were taken over a range of $40 < E/p < 350$ volts/cm.mm.Hg. and the maximum error estimated at $\pm 5\%$. The results obtained by taking α from the linear section of the current growth curves agree well with those of Rose, but after correcting for secondary effects by the Crompton, Dutton and Haydon method the final values of α/p were lower than previous determinations, particularly at high E/p, Figure 20.

The work of Davies, Dutton and Llewellyn-Jones, (48), was carried out at pressures between 250 and 450 mm.Hg.. ω/α was calculated from the upcurving of the $\log_e$ I.v.d. curve and, as in previous determinations, it was found that ω/α was dependent upon the cathode material. Unlike previous measurements, however, Davies et al found a pressure dependence as well with ω/α decreasing as p increased. From this it was initially postulated that back-diffusion of electrons to the cathode was the predominant process but this had been shown to be a function of E/p only, (1, 49, 50). However, if photo-excitation of the gas is considered a possible process presents itself. Any photons in the gap must have come predominantly from the anode region and hence must cross most of the gap before striking the cathode. If these photons interact with gas molecules the molecules will be raised to excited states. As stated in Chapter I, at low gas pressures these interactions are negligable but at higher gas pressures they become appreciable and will be dependent upon the pressure alone. If the excited molecule falls to the ground states with the emission of a photon the only net effect will be that the direction of propagation of the photon has been changed and the overall effect will be a dispersion of the photons which will have a negligable effect on ω/α. If, however, the molecule loses its excess energy on collision by dissociating, the photon will not be re-emitted and its energy will be lost to the discharge. On the assumption that at this low value of E/p 80% of all secondary electrons were produced by

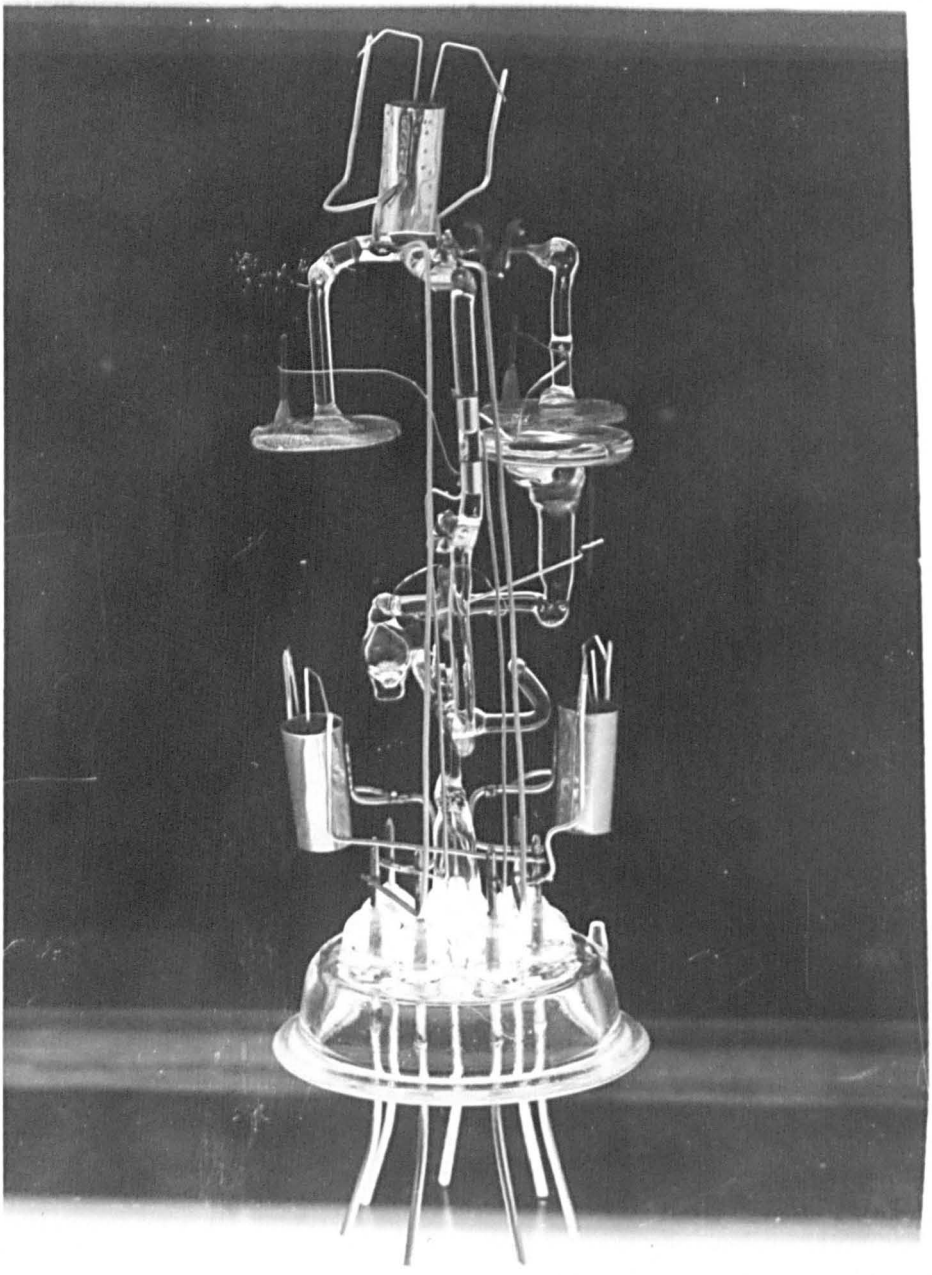

Figure 21

Milne's Experimental Tube.

photo-electric emission from the cathode, the variation of ω/α with p_o was calculated theoretically and was found to give good agreement with the observed points, Figure 19.

The work in these laboratories was initiated by D.E. Davies and the first determinations were published by Davies and Milne in 1959, (51). Values of η were obtained in the range $40 < E/p < 500$ volts/cm.mm.Hg. to an accuracy of $\pm$ 2%. The original experimental tube used incorporated bulk metal electrodes, the inter-electrode distance, d, being changed by means of a large screw assembly. A residual gas pressure of less than 10^{-5} mm.Hg. was not possible with the tube and the large amount of bulk metal meant that a high impurity content was inevitable and that rigorous outgassing was not feasible. Because of this a new experimental tube, made almost entirely of pyrex glass, was constructed containing evapourated metal film electrodes on a glass substrate. As may be seen from Figure 21, three electrodes were used, one of the upper electrodes being the anode and the lower electrode the cathode. Both of these were of copper evapourated on to glass at a gas pressure of less than 10^{-8} mm.Hg. The other upper electrode, on to which a gold reference surface was evapourated, was attached to the glass support by means of crossed tungsten strips which enabled it to vibrate when the tube was tapped. Using this electrode the work function of the copper cathode could be measured by the Kelvin contact potential difference method. All metal within the system was rigorously outgassed by eddy current heating and the glass was

Evaporated Film Tube With variable Separation.

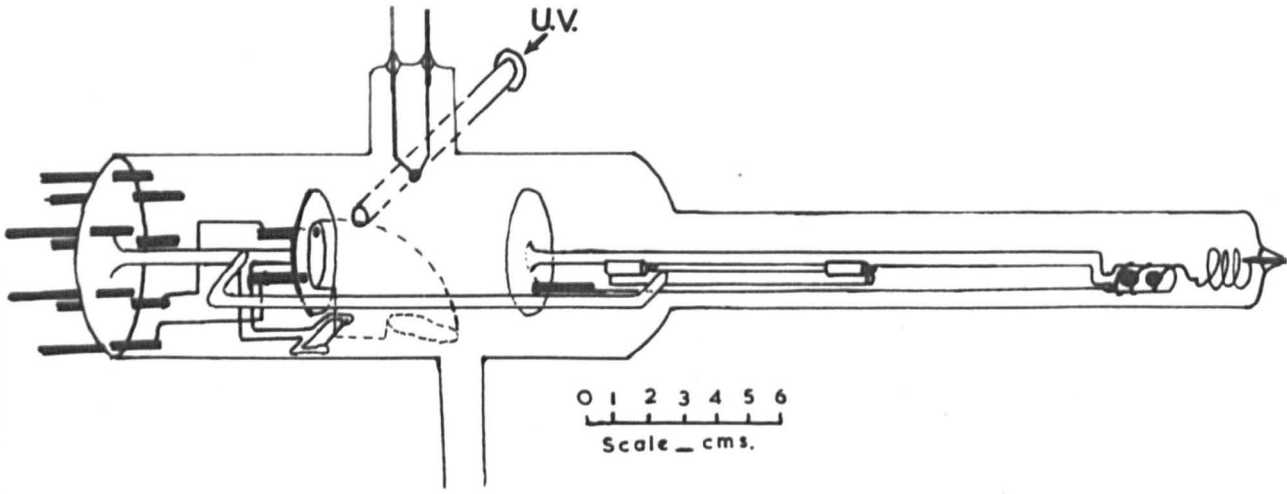

Figure 22.

Myatt's Experimental Tube. Note the nickel ring which could be pivoted across the anode-guard ring substrate to throw an anular shadow on to it. In this way both anode and guard ring were deposited on the same disc.

baked at 420°C for many hours. With such extensive outgassing possible, ultra-high vacuum techniques enabled residual gas pressures of less than 10^{-8} mm.Hg. to be obtained. The main disadvantage of this arrangement was that the inter-electrode distance was fixed which meant that the current growth had to be studied as a function of applied potential, changing the pressure so as to keep the value of E/p constant. This procedure necessarily takes longer than varying d with the result that I_0 may change during the run.

An analysis was developed to be applied to the data obtained which gave true values of η and ω/α. The values of α/p as a function of E/p obtained from the analysis, lay well below those obtained from the linear section of the current growth curve. The uncorrected values of α/p agreed with those of Rose and of Ayres but the corrected values fell above the determination of Jones and Llewellyn-Jones, Figure 20, This disturbing feature led Davies and Myatt, (52, 53), to develop a new tube with variable gap distance. This type of experimental tube which was similar to those used in the present determinations, is shown in Figure 22. It was made almost entirely of glass with gold film electrodes evapourated on to a glass substrate. The anode was supported by a glass rod running in a horizontal V groove. At the end of the rod was a soft iron slug enclosed in glass so that the whole anode assembly could be moved from outside the tube by means of a solenoid. Field distortion was eliminated by including a nickel guard ring around the cathode. The experimental tube and the ultra-high vacuum system were baked for

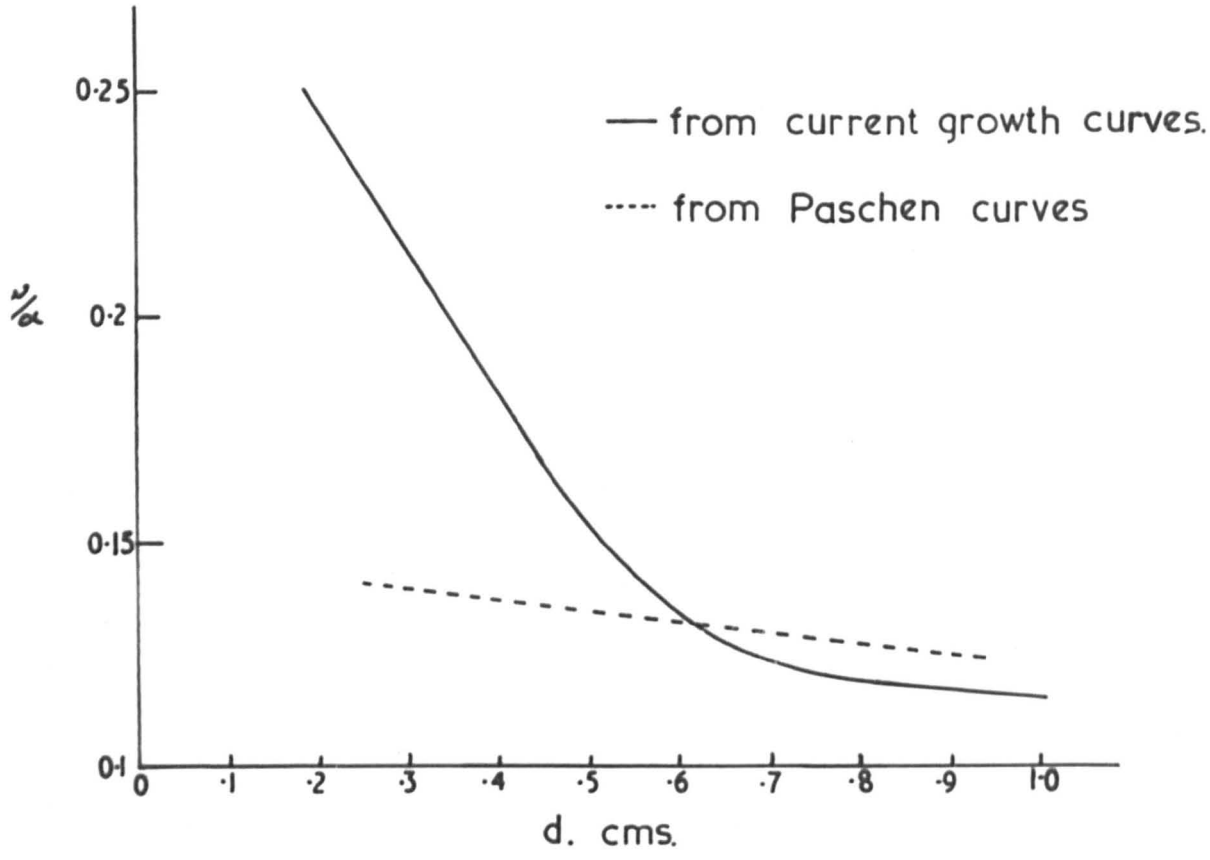

Variation of ω/α with gap distance, d., obtained by Myatt.

Figure 23.

almost a week at 450°C. Hydrogen was produced by the electrolysis of barium hydroxide solution, dried over phosphorus pentoxide, passed through two heated palladium thimbles and stood over reactor grade uranium turnings, contained in a vitrosil tube, which had been outgassed previously at 1000°C. The hydride of uranium was thus formed which, when heated to 300°C, decomposed with the evolution of pure hydrogen.

Using a Ferranti B.D.M.4. electrometer valve, Davies and Myatt obtained spatial current growth data which was analysed by the Davies-Milne analysis. The values of α/p obtained agreed with Jones and Llewellyn-Jones for $E/p < 100$ volts/cm.mm.Hg., but for higher values of E/p, α/p fell significantly lower showing a saturation value of $\alpha/p = 2.2$ ionizations/cm.mm.Hg. for $E/p > 300$ volts/cm.mm.Hg., Figure 20. The secondary coefficient, ω/α, was calculated from both the $\log_e$ I.v.d. curves and from Paschen curves using the freshly determined values of α/p. It was found that ω/α was a monotonic function of E/p, no photo-electric peaks being evident. From the Paschen curve data, however, curves at different pressures did not coincide so indicating a deviation from Paschen's law. This observation, which corroborated the variation of ω/α with pressure found by Jones and Llewellyn-Jones, was pursued by calculating the variation of ω/α with d using both current growth data and sparking potential measurements. The results, which are given in Figure 23, show that ω/α increases rapidly as d decreases at low values of electrode separation, butat

high values ($d > 0.7$ cms.) ω/α is virtually constant. This may be explained both by an increase in photon loss as the solid angle subtended by the cathode at any point on the anode increases, or by adsorption of photons in the gas since photons will be produced near the anode and must cross the gap to the cathode before they can contribute to the discharge. Myatt favoured the former of these explanations but more recent work by Smith (54) in mercury vapour has indicated that the change in ω/α at low electrode separations is an order of magnitude too high for geometric loss to be the main consideration.

2.2. D.C. Determinations in the Rare Gases

As in the case of hydrogen, the early determinations of the Townsend ionization coefficients in the rare gases were carried out in gases of relatively high impurity content and under doubtful vacuum conditions, judged by present day standards. The negligable reactivity of the rare gases was advantageous in that it could be safely assumed that the gas would not react with the walls of the experimental tube or with the cathode material, but it also rendered the purification of these gases very difficult. The only method of purification known at the time of Gill and Pidduck, (55, 56), Townsend and MacCallum, (57, 58), and Kruithoff and Penning, (59, 60), was the empirical process of estimating which impurities were present and passing the gas over an absorption train so as to remove them. This process, however, would not remove rare gas impurities from another rare gas, e.g. neon from helium.

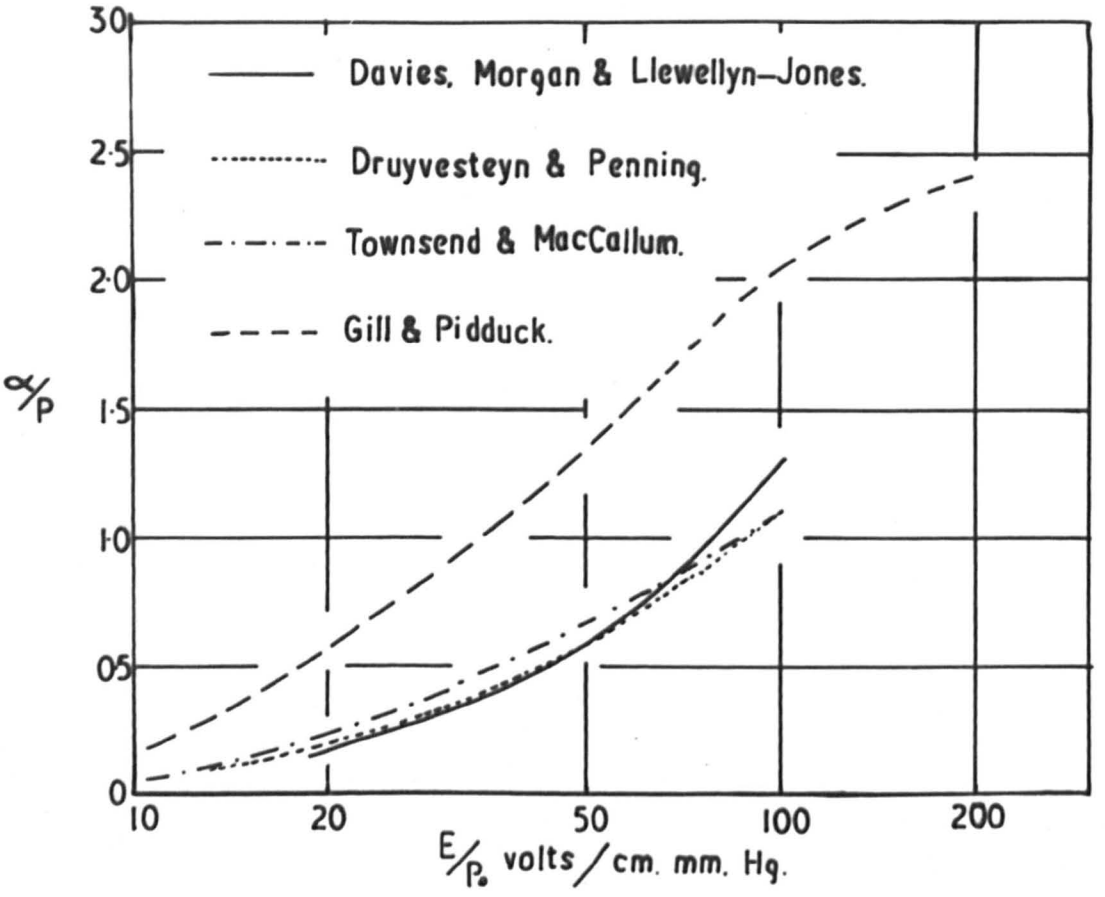

Figure 24.

Previous determinations of the First Ionization Coefficient in Helium.

As early as 1908 Gill and Pidduck determined the primary ionization coefficient in helium. The gas used was admitted as being only 99% pure and further purification was attempted by standing the gas over charcoal at liquid air temperatures. This, however, did not remove neon impurities which tended to give a falsely high value of α/p. Zinc electrodes were used and the quartz window, positioned so as to allow ultra-violet light to fall on to the cathode through a hole in the anode, was sealed to the experimental tube by plastic cement. The apparatus was not air-tight but it was estimated that the leak would not appreciably effect the primary coefficient. Due to inadequate liquid air trapping, mercury vapour was present in the experimental tube along with organic vapours from the "Vaseline" sealing grease. Hence it is not surprising that the values of α/p as a function of E/p obtained from this determination fall significantly above the results of subsequent investigations, Figure 24.

The next determination was that of Townsend and MacCallum who determined the ionization coefficient in neon in 1928, (57), and in helium in 1934, (58). A glass experimental tube was used with parallel plate nickel electrodes of 3.5 cms. diameter. The gas used was first passed over hot copper oxide to remove any hydrogen present and then stood over carbon at -180°C. The system was outgassed at 300 - 400°C and then flushed out with the gas to be used. When the gas was in the system a high frequency discharge was applied with the intention of ionizing any impurities, probably hydrogen.

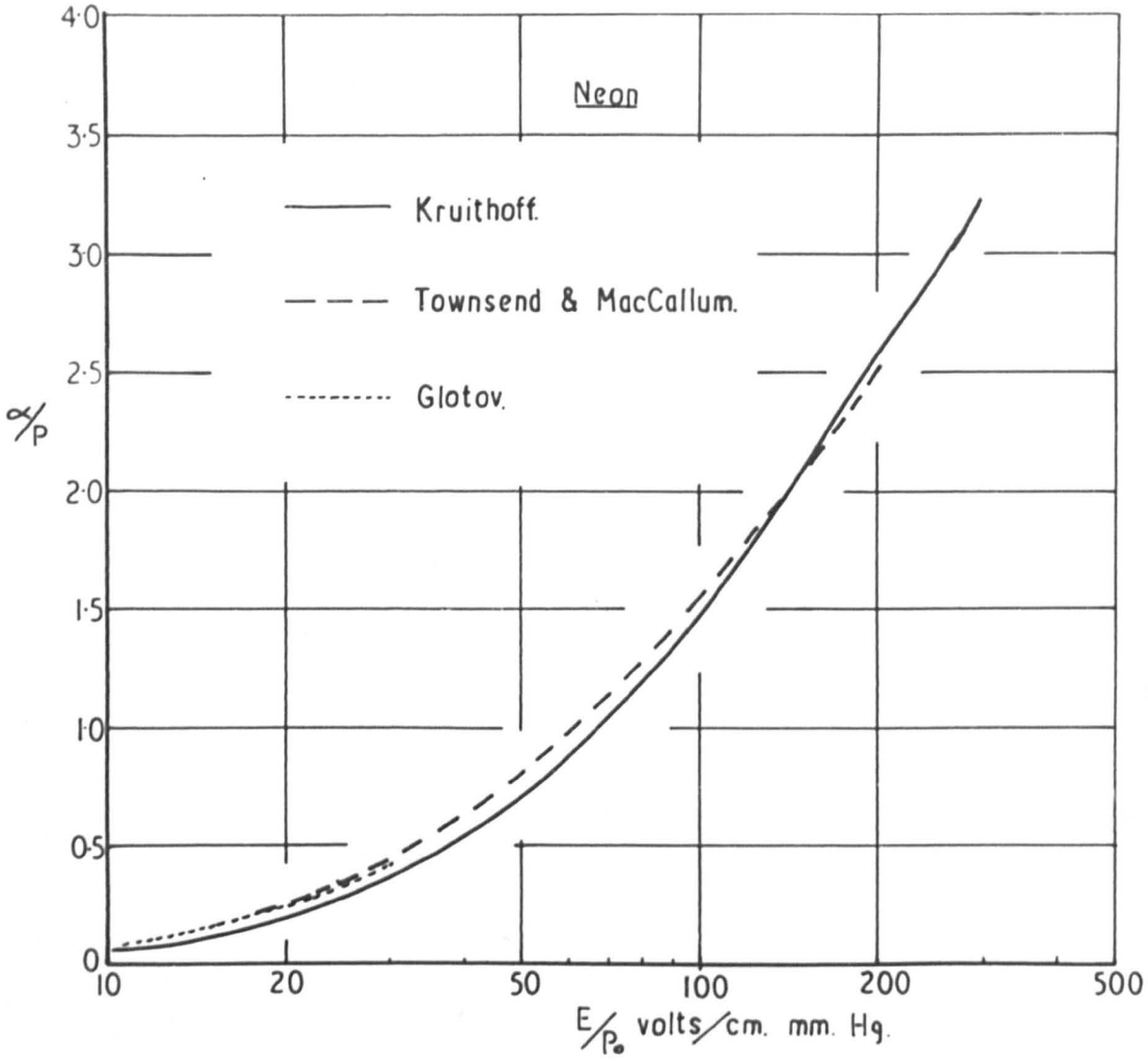

Figure 25.

Previous Experimental Determinations of α/p in Neon.

It was expected that the electrons would be attracted to the walls, so leaving the gas positively charged which would act to repel the impurity positive ions to the walls where they would be absorbed. This also acted as a test for purity since the colour of the discharge changes as the impurity content changes. The main criticism of the method is that once the h.f. discharge is removed, it seems highly probably that the impurity atoms will tend to return to the body of the gas. From the current growth data obtained, values of α/p were found for both neon, Figure 25, and helium, Figure 24, along with values of ω/α in these gases. The values of α/p for helium in the range $12 < E/p < 97$ volts/cm.mm.Hg. fell considerably lower than those of Gill and Pidduck and this can certainly be ascribed to the increased purity of gas obtained. A further reassuring feature of this work is that the sparking potential, V_s, was observed to increase as the gas purity increased as would be expected. The opposite effect was observed by Gill and Pidduck. Curves of ω/α as a function of E/p obtained from this work showed no photo-electric peaks in either gas.

The only comprehensive study of the ionization coefficients of the rare gases is that of Kruithoff and Penning, (59, 60), which was extended by Kruithoff alone, (61). Copper electrodes, 8 cms. in diameter were used, the anode being pierced by 500, 1 mm. holes to allow the ultra-violet light from a hot cathode 500 watt quartz mercury lamp to fall vertically on to the cathode. The cathode could be moved relative to the anode by means of a large bulk metal screw

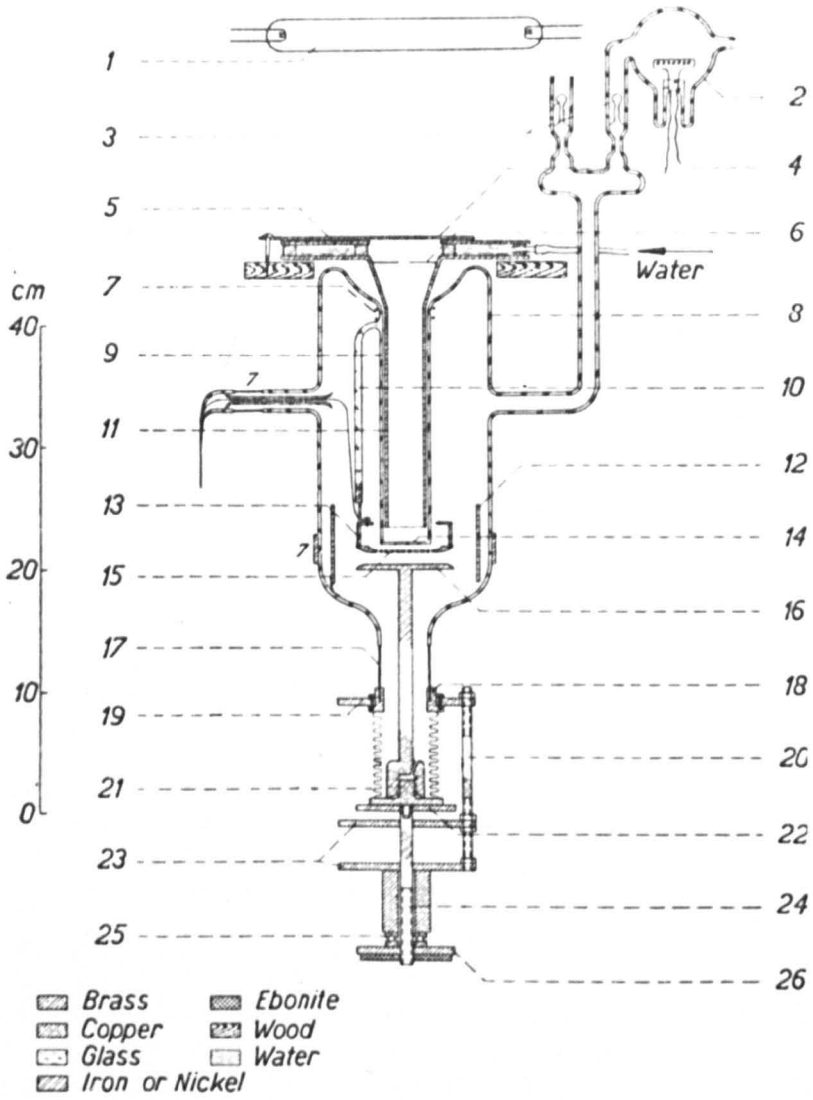

. KRUITHOF and PENNING's tube for measuring the ionization coefficient α in pure rare gases at $p \approx 1$ to 200 mm. Hg. *1* Quartz Hg lamp (500 W); *2* tube with Ba coated wall; *3* thin glass walls which can be broken magnetically; *4* cooled light shutter; *5* cooling device; *6* diaphragm; *7* electrodes for collecting leakage currents; *8* tube; *9* glass to quartz seal; *10* anode support; *11* Cu cylinder attached to 5 protecting 9; *12* electrostatic shield of Cu; *13* fixed anode; *14* quartz window; *15* holes in the anode (500, 1 mm. diameter); *16* movable cathode; *17* chrome-ion ring; *18* to *26* flexible parts and moving mechanism; liquid air traps and pressure gauges are not shown here.

Figure 26.

assembly which was connected to the main body of the glass experimental tube by means of a chrome iron ring and a metal to glass seal, Figure 26. The experimental tube was baked at 400°C for only one hour and then at 470°C for a further half hour which, in the light of present experience, seems hardly sufficient particularly as the tube contained so much bulk metal. The gases to be used were kept in glass bulbs on to the inside of which had been evapourated a barium film which, it was estimated, would absorb all impurities, apart from rare gas impurities, to less than $10^{-4}\%$. Although the argon used contained up to 0.1% neon, the neon up to 0.3% helium, the krypton up to 0.5% xenon, and the xenon up to 0.1% krypton, it was thought that these impurities would have no effect on α/p since the ionization potential of the impurity gas was always higher than the highest excitation potential of the bulk gas. It is not made clear how these impurities were identified. If it were from the fact that the rare gases cannot be perfectly separated by fractional distilation,, then it would seem likely that the neon would contain some argon and the argon may even contain some xenon. Also with so little outgassing of the experimental tube carried out, it seems more than possible that non-rare gas impurities would also be present.

Kruithoff and Penning studied the current growth by observing the variation of current with potential. Since they began their measurements at very small values of gap distance and hence at low values of applied potential difference, details were observed that had not been noticed previously. The current growth curves for

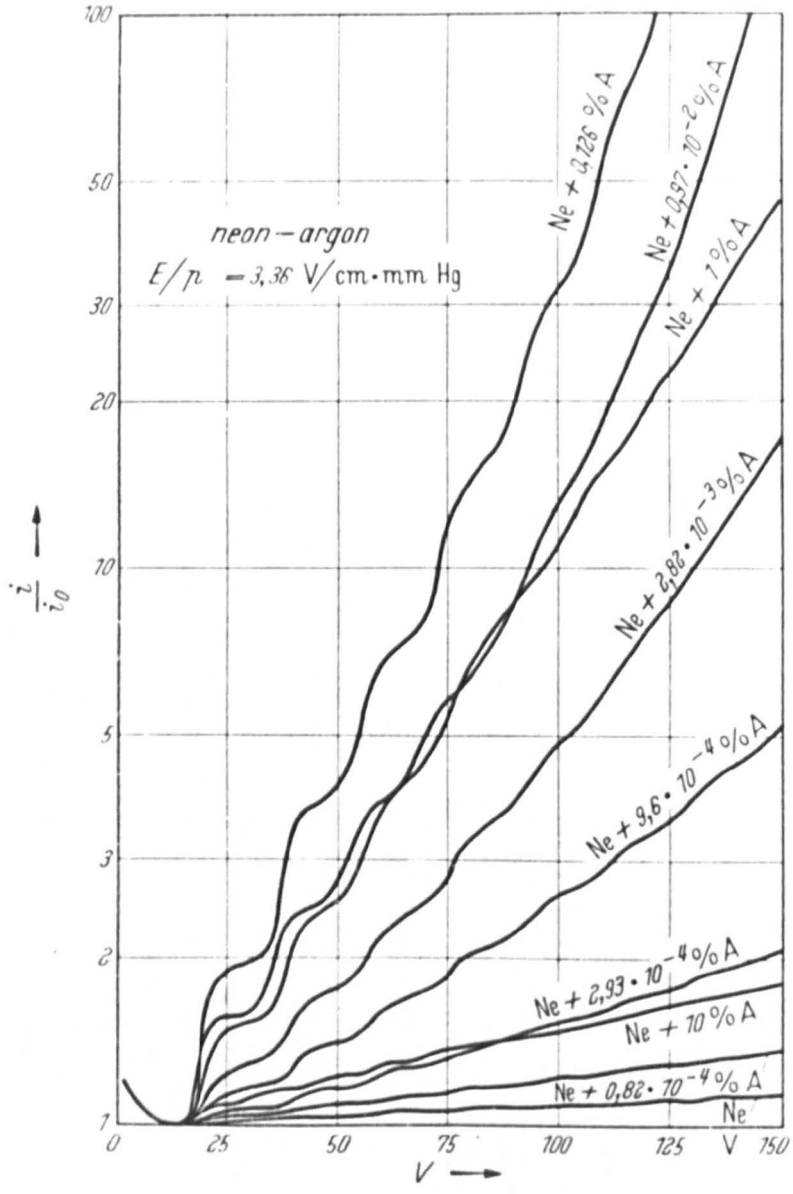

Figure 27.

Kruithoff's Current Growth Curves.

gas mixtures showed a stepwise increase of current with voltage, the size of the step increasing as the percentage of added gas increased. Figure 27 shows these curves for traces of argon added to neon. The stepwise nature of the current growth was credited to the ionization of the argon by the 16.6 e.v. excited state of the neon. When the electrons in the discharge have been accelerated sufficiently to have an energy of 16.6 e.v. they will be able to excite the neon atoms and will themselves be left almost stationary. The excited neon atoms are able to ionize the argon atoms whilst the electrons begin to accelerate in the field once more. After they have gone sufficient distance in the field to excite more neon atoms, a further step is observed in the current growth curve. Direct ionization of the argon was found to be negligable.

The values of η as a function of E/p obtained from this determination, which are given in Figure 28, show that the maximum efficiency of ionization for the various pure gases increases as the ionization potential decreases and as the size of the atom increases and the mean electron energy at which the maximum efficiency of ionization occurs decreases as the mass of the atom decreases, which is to be expected.

The most recent experimental determination of α/p as a function of E/p in helium was made by Davies, Llewellyn-Jones and Morgan at Swansea, (62). The gas used, which was supplied by B.O.C., was estimated as having less than eight parts per million impurity content. No indication is given of how this figure is

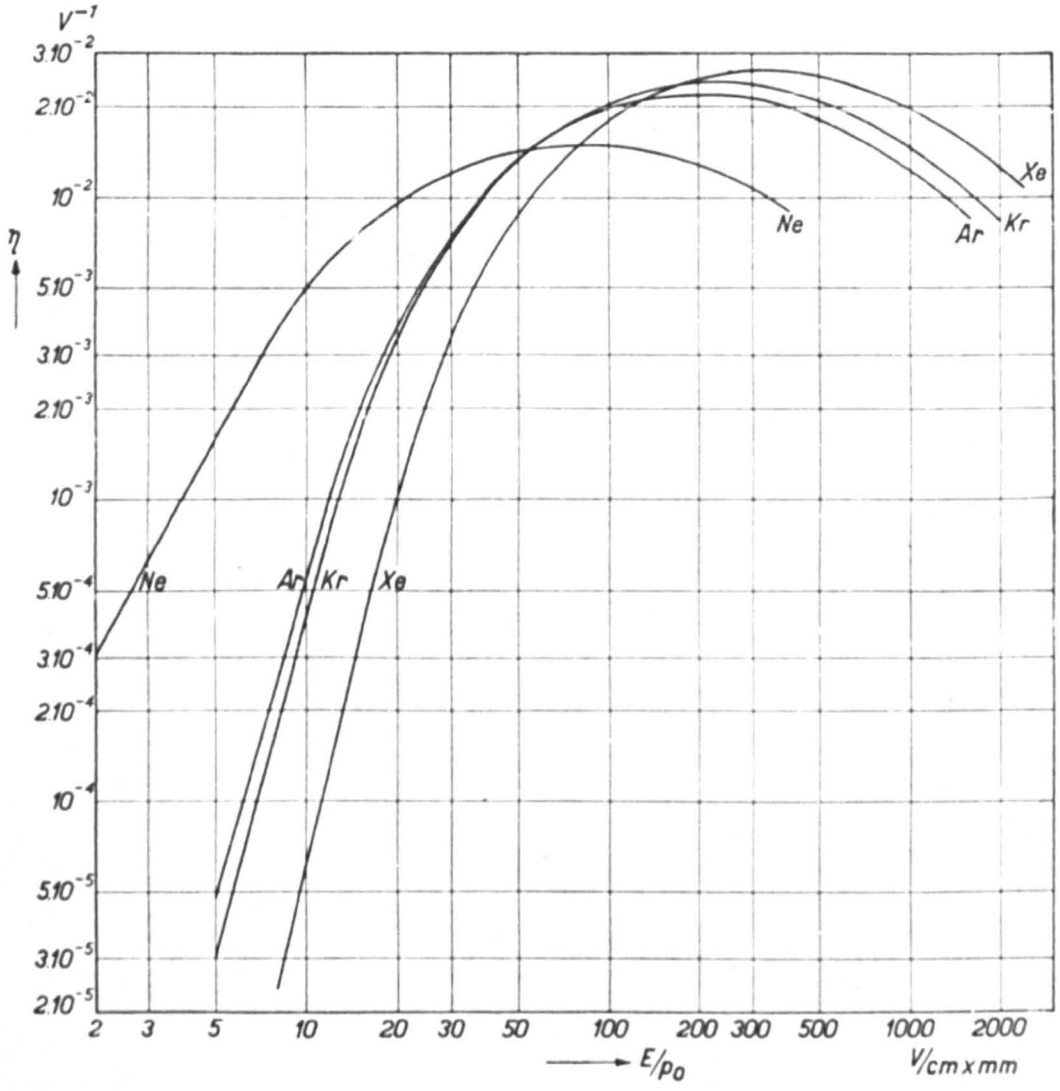

The ionization coefficient $\eta = \alpha/E$ for neon, argon, krypton and xenon.

Figure 28.

obtained. The helium used was purified by being stood over activated charcoal at liquid nitrogen temperatures and then passed through a titanium trap. Doubt as to the final purity of the gas used in the determination rises from two points. Firstly, the figure of eight parts per million of all impurities seems very optimistic since Riesz and Dieke, (63), found that forty five parts per million neon impurity alone were present in "spectroscopically pure" helium. Secondly, the absorption technique used for the purification of the helium will not remove neon which, as indicated above, should be suspected of being the major contaminant. This will tend to give falsely high values of α/p at low values of E/p.

The results obtained from this work are given in Figures 29 and 30. Values of α/p fall below all previous determinations indicating that, despite the above criticism, this work is the most rigorous to date. At E/p_o = 60 volts/cm.mm.Hg. the ionization coefficient is found to be 15% lower than that obtained by Townsend and MacCallum and about 50% lower than that of Gill and Pidduck. The graphs of ω/α v. E/p show distinct photo-electric peaks at E/p = 27 volts/cm.mm.Hg. and E/p = 60 volts/cm.mm.Hg.. The determinations of Davies et al are limited by their only having measured α/p up to E/p = 100 volts/cm.mm.Hg..

2.3. Measurement of A.C. Ionization Coefficients

As has been shown in Chapter I, the first Townsend ionization coefficient η is given by

Experimental values of α/p_0 as a function of E/p_0.

Figure 29.

Experimental values of ω/α as a function of E/p_0.

Figure 30. The Published Results of Davies Llewellyn-Jones & Morgan.

$$\eta = \frac{\nu_i}{\mu E^2}$$

for a gas in a uniform steady field, where ν_i is the frequency of ionization on collision and μ is the electron mobility coefficient.

An analogous ionization coefficient can be obtained for the case where the gas is subject to an ultra-high frequency field. In this case

$$\xi = \frac{\nu_i}{DE^2}$$

where D is the electron diffusion coefficient. From ξ, η may be found since Townsend showed that

$$\frac{\eta}{\xi} = \frac{D}{\mu}$$

Determinations of ξ have been made by Herlin and Brown, (64), MacDonald and Brown, (65), and by Varnerin and Brown (66). The apparatus used in all these determinations was similar to that given in Figure 31. A continuous-wave tunable magnetron was used as the power source, the power being fed into the resonant cavity and measuring devices via a variable power divider. A directional coupler was used to tap off a known fraction of the power which was measured by means of a thermistor element, the resistance of which was measured by a bridge circuit and which indicated the power incident on the cavity. This is analogous to the resistance chain and potentiometer of the d.c. circuit.

The major advantage of this method is that no electrodes are required and hence there are no secondary mechanisms to possibly

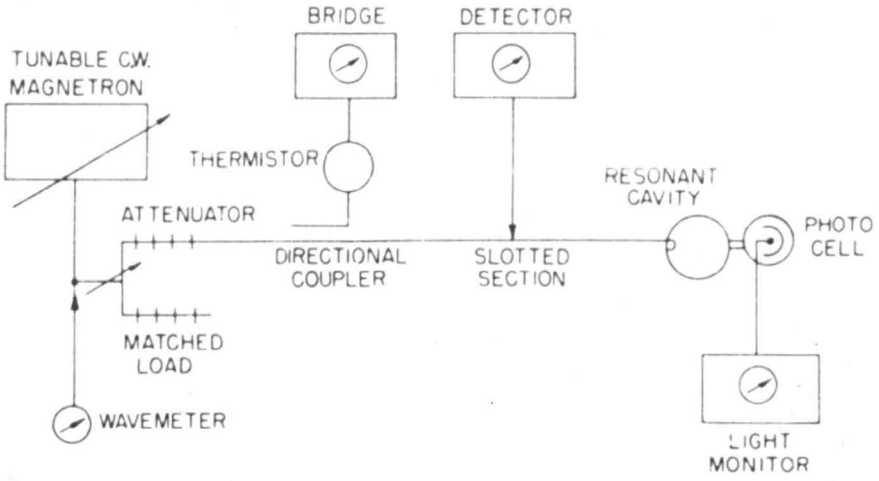

Block diagram of experimental arrangement for measuring steady-state microwave plasma.

Figure 31.

E/p (V/cm mmHg)

Comparison of α/p values. ×, Hale; □, Ayres; —·—·—, Varnerin & S. C. Brown; — ---○---, theory given by Emeléus *et al.*

Figure 31.a

distort the η v. E/p curve. A possible disadvantage is that since the electron energy distributions are different for the a.c. and d.c. cases, discrepancies may occur between the values of η obtained this way and those from d.c. measurements. Varnerin and Brown however found that for hydrogen, for which the mathematics may be simplified, there was good agreement with d.c. measurements and with theoretical evaluations, Figure 31a Later d.c. values, however, have tended to fall appreciably lower at low values of E/p.

2.4. Conclusion and Statement of Problem

In the course of this chapter the most important determinations of the first and second ionization coefficients as functions of the ratio of applied electric field to gas pressure have been summarised for hydrogen and the rare gases. From this it can be seen that appreciable discrepancies exist between all these results in hydrogen and that very little work has been carried out in the rare gases. Indeed no attempt has been made to determine α/p in helium from which all traces of the other inert gases have been removed as well as non-inert gas impurities. The present work is aimed at re-determining the values of α/p for hydrogen using evapourated film parallel plate electrodes, ultra-high vacuum techniques and extremely pure hydrogen and at determining the values of α/p as a function of E/p in helium and neon from which all contaminants have been removed. It is also intended to appraise the effect that the excited and metastable states of the rare gases have on the discharge at low pressures between gold

electrodes and to attempt to estimate the gaseous processes causing these effects.

CHAPTER III

THEORETICAL EVALUATIONS OF THE PRIMARY IONIZATION COEFFICIENT

Theoretical calculations of the values of α/p and of η as functions of E/p present several problems, the most serious of which is the difficulty in determining the exact form of the electron energy distribution, F(ε). This not only varies from gas to gas, but also changes with E/p for any one gas. A further complicating factor is the variation of the mean free path of the electrons, λ_e, with electron energy. This effect, known as the Ramsauer effect, (66), is perhaps most marked for the case of argon, whereas, for the gases involved in this discussion it is only small.

If the electron energy distribution is known, along with the mean free path of the electrons in the gas, λ_e, the electron drift velocity, V_d, and the ionization cross-section of the atom, Q_i, the value of α/p may be calculated at that particular value of E/p. To calculate the variation of α/p with E/p the variation of all the above parameters with E/p must be known. Because of this most early derivations were limited to small ranges of E/p.

3.1. The Electron Energy Distribution

The first attempt to calculate the electron energy distribution in a gas subjected to an applied electric field was made by Pidduck (67), in 1913 and this has been followed by many other attempts, notably by Morse, Allis and Lamar (68), Druyvesteyn(69),

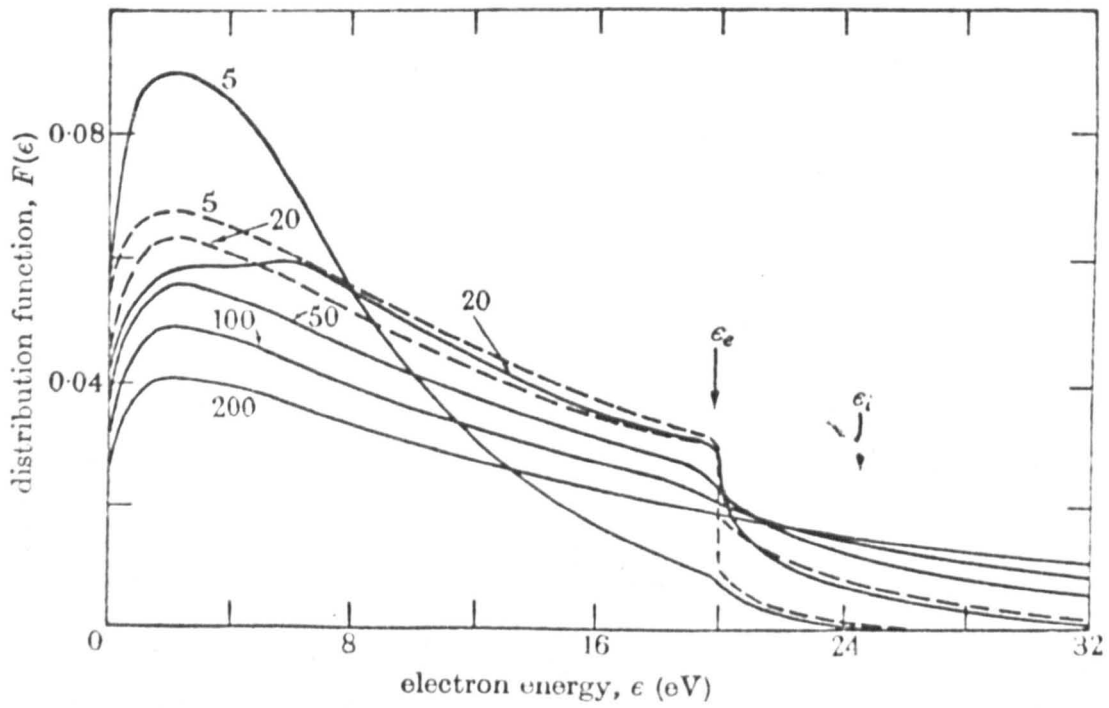

Electron energy distributions for helium at various values of E/p. The distributions at $E/p = 5$ and 20 shown by dashed lines are obtained by neglecting elastic loss.

Figure 32.

Smit, (70), and more recently by Lewis, (71), and Heylen and Lewis, (72). From this work several conclusions may be drawn. If the electron density is low, so that there is little interaction between electrons, the energy distribution will tend towards a Druyvestyn distribution. If, however, the electron density is high and electron-electron events are common, the distribution approaches a Maxwellian distribution. In molecular gases, for example hydrogen, the Maxwellian distribution is a good approximation since these gases have excitation levels, including vibrational levels, widely spread out up to the ionization potential. Hence inelastic losses begin at low energies and these losses are so distributed as to produce an approximately Maxwellian distribution of the form,

$$N(\varepsilon).d(\varepsilon). = C\sqrt{\varepsilon}\ \exp-\left(\frac{\varepsilon}{\bar{\varepsilon}}\right).d(\varepsilon)$$

$$\text{or } N(\varepsilon).d(\varepsilon) = \frac{2}{\sqrt{\pi}}\sqrt{\frac{\varepsilon}{\bar{\varepsilon}}}\ \exp-\left(\frac{\varepsilon}{\bar{\varepsilon}}\right).d\left(\frac{\varepsilon}{\bar{\varepsilon}}\right) \qquad 3.1.$$

where $N(\varepsilon)$ is the number of electrons with energies between ε and $\varepsilon + d(\varepsilon)$ and $\bar{\varepsilon}$ is the mean electron energy.

Druyvesteyn derived a similar function to deal with the situation in which elastic collisions were prevelant. This was principally meant to apply to the case of helium, neon and argon in which the excitation levels all lie within a few e.v.'s of the ionization energy. The Druyvesteyn distribution is of the form

$$N(\varepsilon).d(\varepsilon) = C'\sqrt{\varepsilon}\ \exp.-0.55\left(\frac{\varepsilon}{\bar{\varepsilon}}\right)^2.d(\varepsilon)$$

$$\text{or } N(\varepsilon).d(\varepsilon) = 1.04\sqrt{\frac{\varepsilon}{\bar{\varepsilon}}}\ \exp.-0.55\left(\frac{\varepsilon}{\bar{\varepsilon}}\right)^2.d\left(\frac{\varepsilon}{\bar{\varepsilon}}\right) \qquad 3.2.$$

This distribution is much narrower than the Maxwell distribution predicting the occurence of less high energy electrons

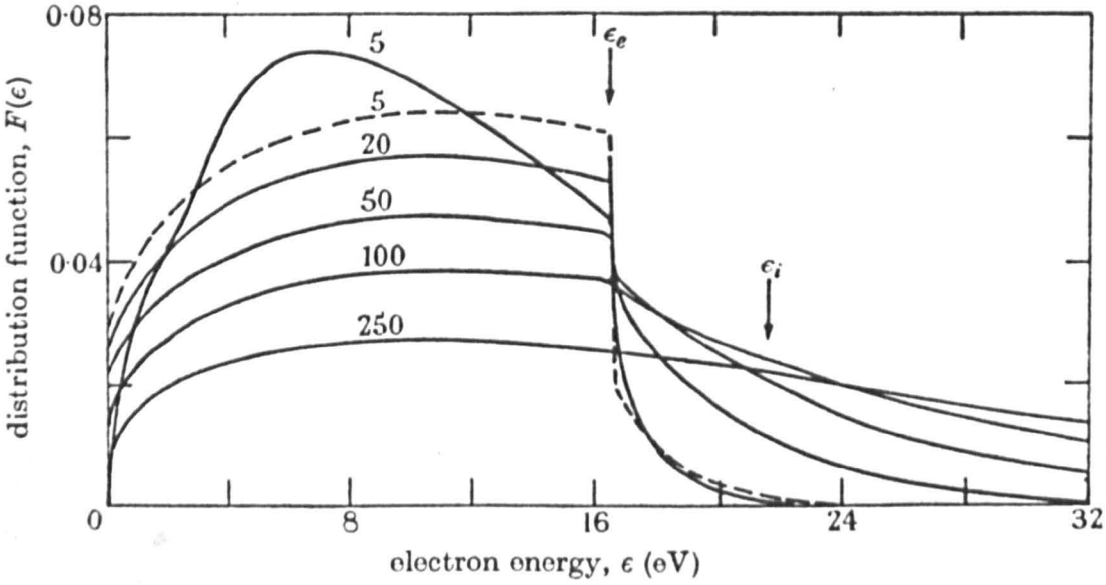

Electron energy distribution for neon at various values of E/p. The distribution at $E/p = 5$ shown by a dashed line is obtained when elastic loss is neglected.

Figure 33.

and hence a lesser degree of excitation and ionization.

If the electron mean free path varies appreciably with energy, the distribution will be distored obeying neither the Maxwellian expression nor the Druyvestyn equation. For an expression to be obtained which allows for this variation, the cross-sections for elastic scattering, excitation and ionization must all be known as functions of electron energy. This complicates the equations a great deal but Smit, (70), Lewis, (71), and Heylen and Lewis, (72), have all obtained expressions for $F(\varepsilon)$ under these circumstances.

Smit calculated $F(\varepsilon)$ for electrons in helium using a method based on the Boltzmann transport equation. He assumed that in a steady state the number of electrons per second gaining energy, ε, $n'(\varepsilon)$, was equal to the number of electrons per second loosing energy, ε, $n''(\varepsilon)$

i.e. $$\sum n'(\varepsilon) - \sum n''(\varepsilon) = 0 \qquad 3.3.$$

where the summation is over all possible electron processes.

An alternative method used by Holstein, (88), Morse, Allis and Lamar, (68) and Margenau, (73), was to consider one possible process and to calculate the change in the number of electrons per second with energy between ε and $\varepsilon + d\varepsilon$ as a result of this one process. The increase in electrons with energies in this range is then given by

$$[n_1(\varepsilon + d\varepsilon) - n_2(\varepsilon + d\varepsilon)] - [n_1(\varepsilon) - n_2(\varepsilon)] = \frac{d(n_1 - n_2)}{d\varepsilon}$$

which in the steady state for all such processes will be zero, hence

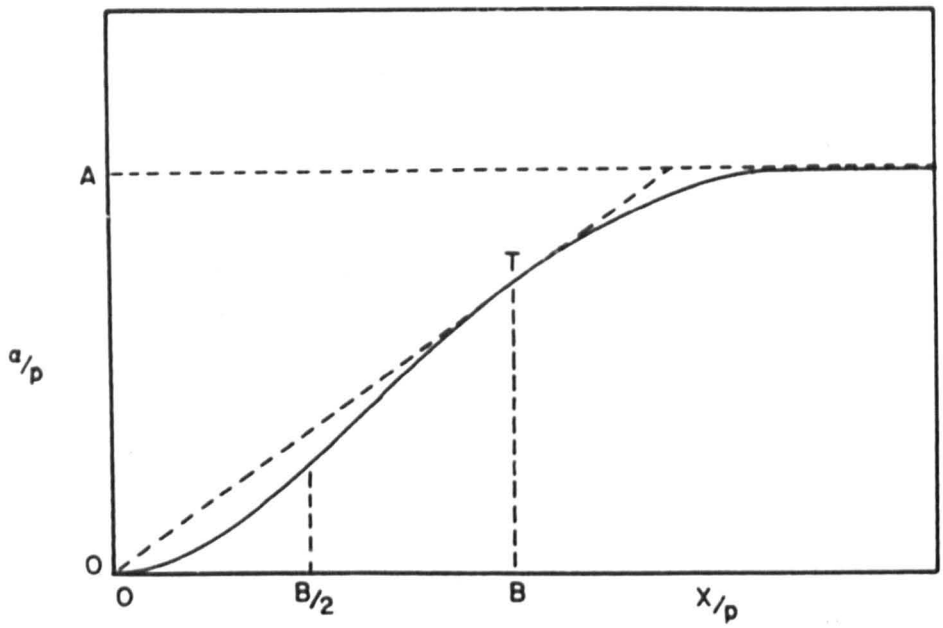

Characteristic curve for α/p, plotted against X/p over an extended range of X/p values. Note that the scale of plotting for real curves of α/p is so compressed near the origin that it does not indicate that α/p has zero values out to considerable values of X/p, e.g., 20 in air, 10 in H_2, and 2 in A. Real α/p curves do *not* start at the origin. Illusions from this scale of plotting have led to serious complications. However, in the interest of saving space, the curve here shown is that corresponding to an analytical form $\alpha/p = A\ \epsilon^{-Bp/X}$.

Figure 34.

$$\frac{[d\ (n_1 - n_2)]}{d\varepsilon} = 0 \qquad 3.4.$$

Comparing 3.3. and 3.4. it may be seen that both are of the same form, so indicating that Smit's assumptions were justified.

From this starting point Smit calculated the value of $F(\varepsilon)$ for values of E/p from 3 to 10 volts/cm.mm.Hg..

This work was extended by Lewis in 1958, (71), and by Heylen and Lewis in 1963, (72). Lewis initially simplified the equations by neglecting losses due to elastic collisions but Heylen and Lewis allowed for all possible mechanisms. Distribution functions were calculated for He, Ne and Ar in the range $5<E/p<250$ volts/cm.mm.Hg.. It was observed that at low values of E/p, ($E/p < 20$ volts/cm.mm.Hg.) helium has an almost Maxwellian distribution whilst neon approaches Druyvestyn. Neon, however, is found to have more electrons at energies above the excitation potential, (16.6 e.v.) than would be expected from the Druyvestyn equations.

From the values of $F(\varepsilon)$ obtained (Figures 32 and 33), the diffusion coefficients and the mobilities were deduced. These latter were found to agree well with experimental "time of flight" measurements of Bradbury and Nielson. The values of α/p as $f(E/p)$ calculated from this approach will be given below.

3.2. Theoretical Evaluation of α/p as f.(E/p)

α/p v. E/p curves are characterised by an elongated, horizontal S shape, a typical example of which is given in Figure 34. The value of α/p rises slowly at first, since at low values of E/p

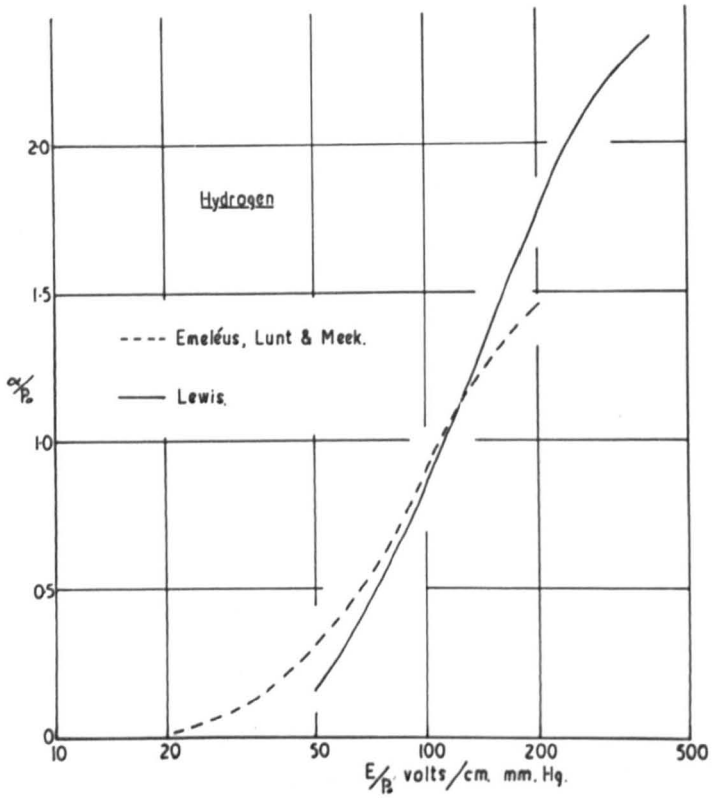

Figure 35. Theoretical Values of α/p in Hydrogen.

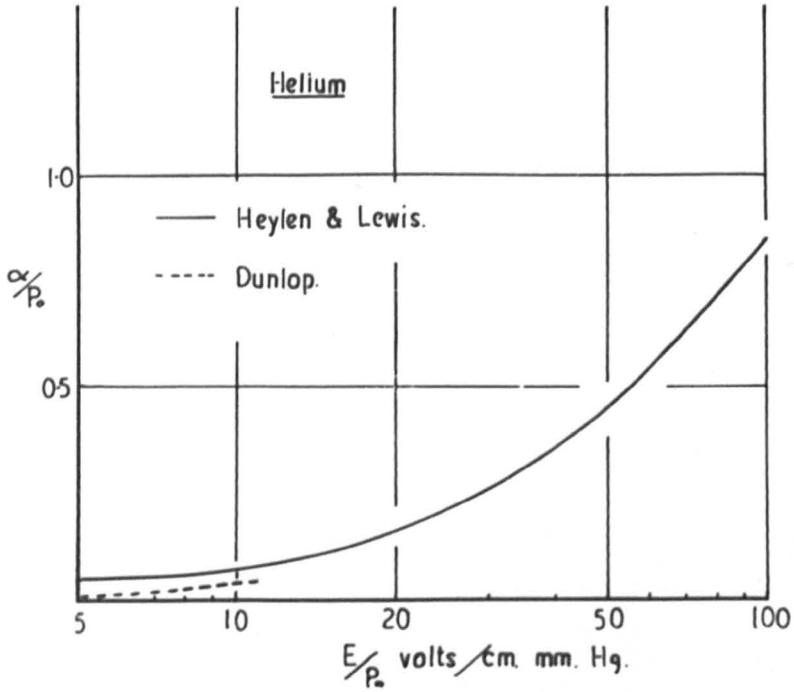

Figure 36. Theoretical Values of α/p in Helium.

there are few high energy electrons in the electron energy distribution and hence there is little ionization. As E/p increases so the number of electrons capable of ionizing by collision increases, but the cross-section for ionization by impact decreases. Of these two variables, the former seems to be the prevalent factor, however, and the value of α/p increases more rapidly with E/p at higher E/p. At still higher values of E/p the second factor becomes most important and the curve passes through a point of inflexion, at a value of E/p characteristic of the gas, and then tends to level off. At still higher mean electron energies, the probability of ionization, P_i, tends to decrease much more rapidly and hence α/p would be expected to decrease. This effect has not been observed. As the electron energy distribution changes from gas to gas and varies with E/p for one gas no general solution of α/p as $f(E/p)$ is possible for all gases or over a wide range of E/p for one gas.

Von Engel and Steenbeck, (74), attempted a theoretical description by considering an electron swarm moving in a uniform field. Those electrons with energies above the ionization energy, V_i, are able to ionize. If the number of ionizing collisions per electron per second is ν_i and V_d is the electron drift velocity, i.e. the distance an electron moves in one second in the direction of the field, then

$$\alpha = \frac{\nu_i}{V_d}$$

From a consideration of the kinetic theory and applying Maxwell's

distribution

ν_i is proportional to $pT_e^{\frac{1}{2}} \exp.\left(\frac{-eV_i}{kT_e}\right)$

where T_e is the electron temperature in ^{o}K.

Also,

T_e is proportional to E/p

V_d is proportional to $(E/p)^{\frac{1}{2}}$

Hence, since α is proportional to $\frac{pT_e^{\frac{1}{2}}}{V_d} \exp.\left(\frac{-eV_i}{kT_e}\right)$

α/p is proportional to $\exp.\left[\frac{-V_i}{(E/p)} \cdot \text{constant}\right]$

or since V_i is a constant

$$\alpha/p = A \exp.\left[-\frac{B}{(E/p)}\right] \qquad 3.5.$$

which is of the same form as equation, 1.2. This equation can be made to fit the observed data over limited ranges of E/p by the insertion of suitable values of the constants A and B. The form of the equation breaks down, however, when $\alpha/p = 0$, since it predicts that this should occur when $E/p = 0$. In practice, it is found that E/p is finite when $\alpha/p = 0$, e.g. in hydrogen this threshold occurs at $E/p = 10$ volts/cm.mm.Hg..

A more rigorous expression may be derived by considering the frequency of ionization per electron, ν_i, to be equal to the velocity of the electron, V, divided by the distance an electron must travel before it undergoes an ionizing collision, l_i.

i.e. $\nu_i = \frac{V}{l_i} = V \,.p.\, P_i$

If the electron velocity distribution is $f(u)$ then,

$$\gamma_i = p \int_{u_i}^{\infty} P_i . V . f(u) . du$$

where u_i is the ionization potential

Since

$$V = \left(\frac{2e}{300m}\right)^{\frac{1}{2}} u^{\frac{1}{2}}$$

and $$\alpha = \frac{\gamma_i}{V_d}$$

$$\alpha/p = \left(\frac{2e}{300m}\right)^{\frac{1}{2}} \frac{1}{V_d} \int_{u_i}^{\infty} P_i \, u^{\frac{1}{2}} f(u) \, du \qquad 3.6.$$

Emeleus, Lunt and Meek, (75), used 3.6., and using a Maxwellian distribution to give

$$f(u) = c u^{\frac{1}{2}} \exp. \left[-\frac{3}{2} \frac{u}{\bar{u}}\right]$$

where c. is a constant, obtained the expression

$$\alpha/p = \frac{1.23 \times 10^8}{V_d} . \bar{u}^{-\frac{3}{2}} \int_{u_i}^{\infty} P_i \, u \exp.\left[-\frac{3}{2} \frac{u}{\bar{u}}\right] . du. \qquad 3.7.$$

This gave good agreement with experimental results in hydrogen, nitrogen and air but in argon and neon discrepancies of up to four orders of magnitude were evident. The conclusions drawn from this is that in hydrogen, nitrogen and air $f(u)$ is close to Maxwellian but, as would be expected, the Ramsauer effect tends to distort the energy distribution in argon.

Deas and Emeleus, (76), confirmed these results by applying a form of $f(u)$ which allowed for elastic collisions of the electrons.

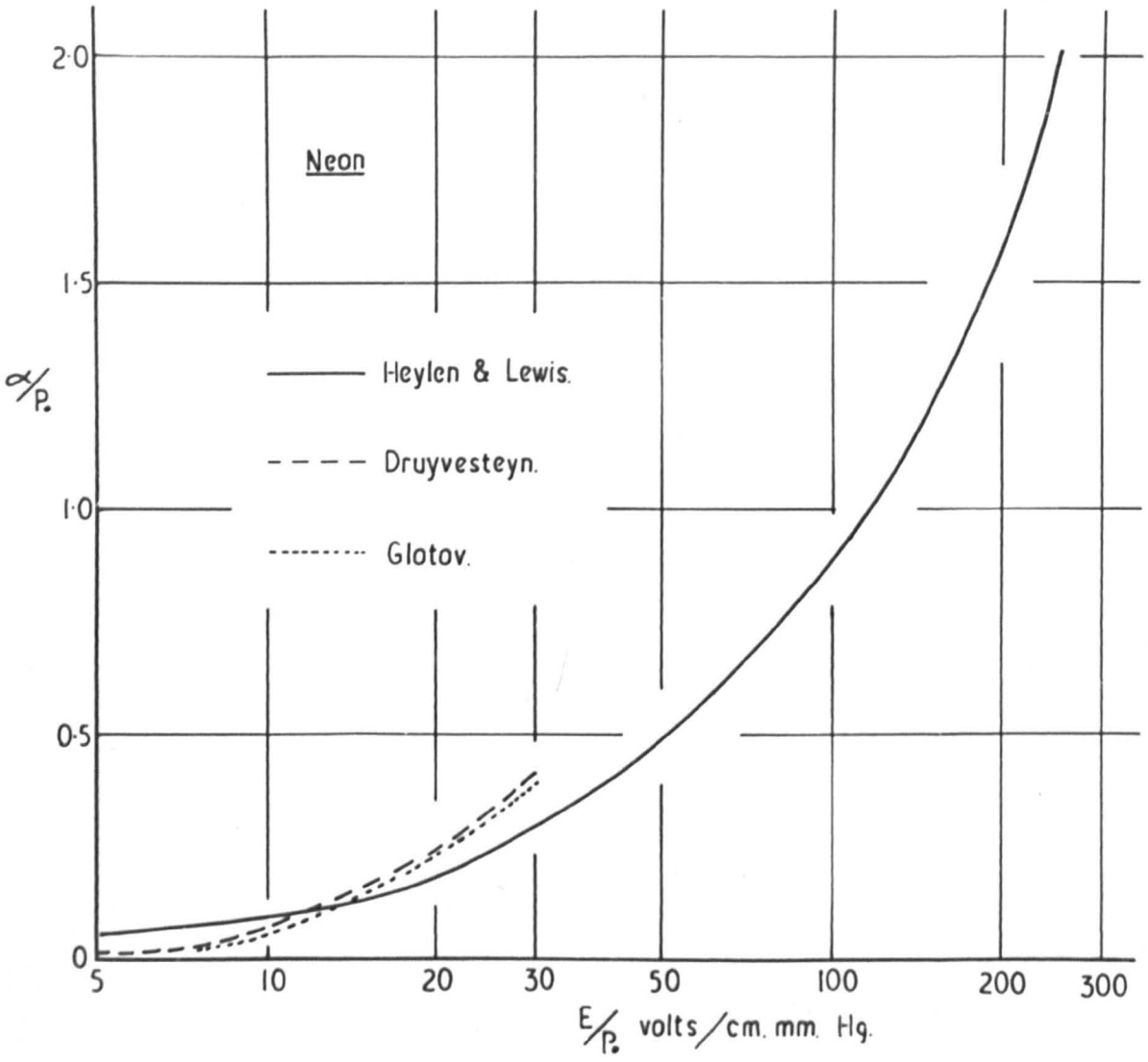

Figure 37.

Theoretical Evaluations of α/p in Neon

This was done by taking

$$f(u) = Cu^{\frac{1}{2}} \exp. \left[- \frac{0.55\ u^2}{\bar{u}^2} \right]$$

where C is the constant. The disparity between observed and calculated data for argon and neon could not be removed by applying this distribution.

Druyvesteyn, (69), obtained much closer agreement for the case of neon by deriving a velocity distribution which allowed for all types of collisions and by assuming that the probabilities of excitation and ionization are directly proportional to the mean electron energy. The values obtained from this derivation are given in Figure 36.

The form of $F(\varepsilon)$ derived by Smit (70), was used by Dunlop, (77) to calculate values of α/p and V_d in helium. Only poor agreement was reached, however, with the drift velocity measurement of Bradbury and Nielson, (78), whilst α/p fell below the extrapolated values of Townsend and MacCallum, (57, 58). More recent experimental values also fall below these, however.

The latest calculated values of α/p in hydrogen, helium and neon are those of Lewis, (71), and of Heylen and Lewis, (72). The distribution used has been outlined in the preceding section whilst the result obtained are given in Figures 35, 36 and 37. These are found to be in very close agreement with experimental values and are certainly the result of the most rigorous analysis to date. Indeed the calculations are complicated enough to warrant

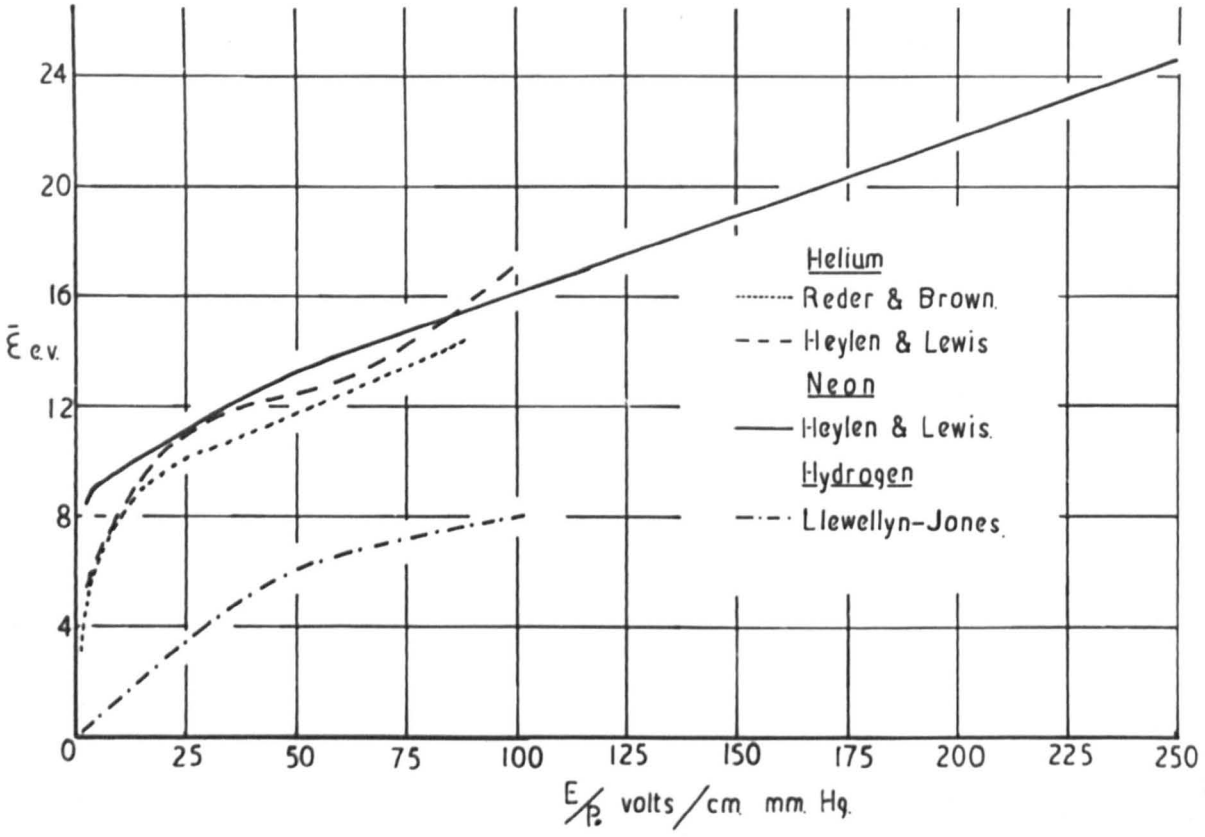

Figure 38.

$\bar{\varepsilon}$ as a Function of E/p.

the use of a computer. However, the range over which calculations have been made is limited, e.g. in helium the range is only from E/p = 5 volts/cm.mm.Hg. to E/p = 100 volts/cm.mm.Hg., and this has had to be done by taking a different value of of $F(\varepsilon)$ for each value of E/p.

3.3. $\bar{\varepsilon}$ as a Function of E/p.

Since α/p and η are always considered as functions of E/p it is useful in order to compare the variations of α/p and η with E/p with the probability of ionization and efficiency of ionization with $\bar{\varepsilon}$, to know the variation of mean electron energy with E/p. This has been attempted experimentally by Townsend, (89), for a very limited range of E/p at low E/p and theoretically by Heylen and Lewis, (72), for the d.c. discharge. For the a.c. distribution experimental determinations has been carried out by Llewellyn-Jones, (91), and by Reder and Brown, (90). These are given in Figure 38. Since the d.c. and a.c. distributions are different it is not logical to expect the curves of $\bar{\varepsilon}$. v. E/p. to coincide for the two cases. This is observed. An attempt will be made to determine $\bar{\varepsilon}$ as $f(E/p)$ from the results of the work described in this thesis.

3.4. Conclusion

In the course of this chapter it has been shown that the variation of α/p with E/p is not a simple function but is dependent upon many factors which themselves vary with electron energy. It is believed, however, that the derivation of Heylen and Lewis is close to the experimental situation and this belief has been strengthened

by the results presented in this thesis.

CHAPTER IV

GAS PURIFICATION - EXPLANATION OF TECHNIQUES

Ionization coefficients are critically dependent upon the purity of the gas. For this reason it is of paramount importance that the gas used should be as pure as possible since a few percent impurity content can increase α/p by as much as 50%. An increase in α/p may be affected by the ionization of the impurity atoms by photons emitted from the decay of an excited atom of the main gas, provided that the excited states of the main gas are at a higher energy level than the ionization level of the impurity gas. Metastable states can also cause additional ionization by direct collision of the metastable atom with an impurity atom if the potential energy of the metastable atom is greater than the ionization energy of the impurity. Since the metastable atom can undergo 10^8 collisions during its life-time it will tend to make several hundred collisions with impurity atoms even if the impurity is only present in a few parts per million. This effect is of great importance in the rare gases which have high ionization potentials with the excitation and metastable levels very close to the ionization energy, e.g. traces of argon, with an ionization potential of 16.0 e.v. in neon, with a metastable state at 16.6 e.v., can be a very serious contaminent.

In this case

$$Ne^* + A \longrightarrow Ne + A^+ + e$$

where Ne^* represents the metastable neon atom.

The variation in the conductivity of a gas due to contaminants, which is reflected in this change in α/p, also affects the breakdown potential V_s and correspondingly changes ω/α.

Mercury contamination of the experimental tube which was the cause of so many spurrious results from early determinations of ionization coefficients, is not considered to be a major source of error in the present work since it is very easily eliminated by the inclusion of liquid air traps between the mercury diffusion pump and the ultra-high vacuum system. The main impurities in the case of hydrogen are water vapour, oxygen, nitrogen and carbon dioxide, whilst in the rare gases the chief contaminants are the same with the addition of traces of rare gases other than the main gas.

4.1. Purification of Hydrogen

The hydrogen used in the present work was produced by the electrolysis of dilute barium hydroxide solution. It was then allowed to stand over phosphorus pentoxide for several hours and was then passed through a liquid air trap. This served to remove the vast majority of the water vapour and carbon dioxide impurities. The main purification, however, was performed by allowing the hydrogen to diffuse through two palladium osmosis tubes and then by the reaction of hydrogen with uranium.

Palladium, at a temperature of about 300°C, acts as a semi-permeable membrane when in contact with hydrogen, allowing the hydrogen to diffuse through the metal until the pressure on each side is equal. Dynamic equilibrium is thus attained. This property of

the palladium-hydrogen system is a result of the small size of the hydrogen atom, about 1.2 Å diameter, and since all other gas atoms are larger, e.g. nitrogen 1.5 Å, oxygen 1.4 Å, only hydrogen can undergo this osmosis. Purification of hydrogen in this way has been used in many previous determinations of ionization coefficients in hydrogen, (39, 42, 43, 47, 51), and has been used in the present determinations as an initial purification.

Darling, (81), has shown that the diffusion rate is greatly reduced if the hydrogen on the high pressure side of the osmosis tube is stationary. It has also been shown by Crompton and Elford, (82), that the palladium tends to crack if it is heated or cooled in an atmosphere of hydrogen due to a phase transition at about 150°C. The palladium should, therefore, be heated to its operating temperature in vacuum. Unfortunately, the nature of the vacuum system prevented the former of these two suggestions being incorporated in the present work and the second paper was published too late. A silver palladium alloy has been reported, (82), which does not have an α - β phase transition and which can hence be safely heated or cooled in hydrogen.

The final stage of hydrogen purification was carried out by standing the now fairly pure hydrogen over reactor grade uranium turnings at 200°C and allowing the uranium to cool to room temperature. In this way uranium hydride was formed by direct combination in accordance with the reaction

$$2U + 3H_2 \rightleftharpoons 2UH_3$$

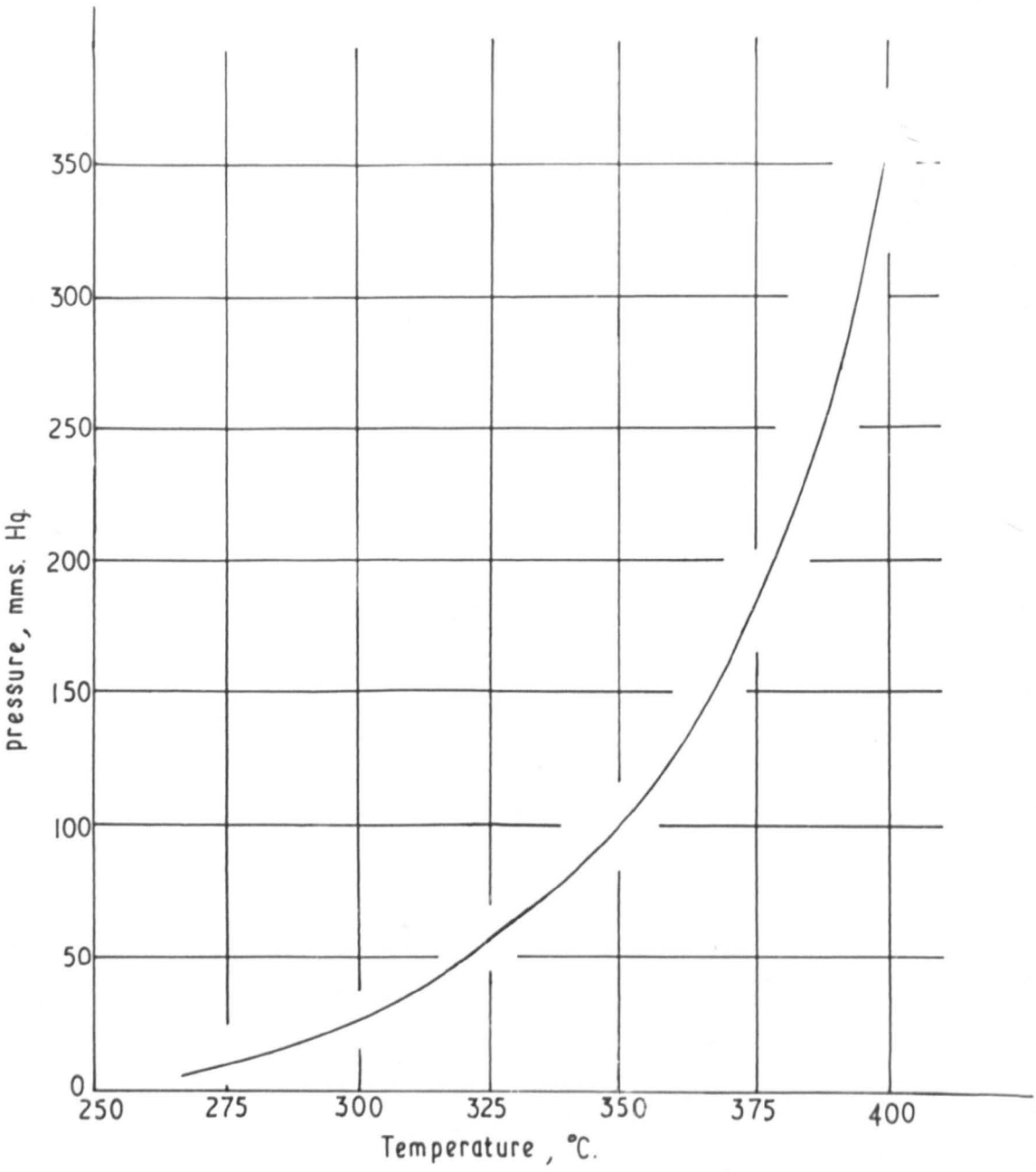

Variation of equilibrium pressure with temperature for the system

$$2UH_3 \leftrightharpoons 2U + 3H_2$$

Figure 39.

When the uranium had been completely converted to the hydride, all the remaining gas was pumped away and the system was sealed off. Pure hydrogen could then be obtained by heating the uranium hydride. As may be seen from Figure 39, the equilibrium pressure of this system is a sensitive function of temperature and hence the hydrogen pressure in the sealed off system could be adjusted by varying the temperature of the uranium hydride.

4.2. Purification of Helium and Neon

Both the helium and neon used in the determinations were drawn initially from commercial B.O.C. samples. These were prepared from air by a complex liquefaction and rectification process. The most volatile fraction contains nitrogen, neon and helium with oxygen, argon, krypton and xenon left in the residue. Removal of nitrogen from the volatile fraction gives a neon-helium mixture. Further purification is obtained by selective adsorption on activated charcoal. In this process the charcoal, if kept at -190°C, will adsorb all gases except helium whilst at -100°C neon will also not be adsorbed. Hence it may be seen that the chief impurity in helium will be neon and the main impurity in neon will be helium. In each case a few parts per million of nitrogen may be present. Although such samples are quoted as being "spectroscopically pure" a rigorous analysis by Riesz and Dieke, (63), has shown that there are 45 parts per million neon impurity alone in spectroscopically pure helium, so supporting the above conclusions.

During the course of the preliminary experiments the

commercial gas was used after being purified over activated charcoal at the appropriate temperature. However, although this would remove any traces of nitrogen, oxygen or carbon dioxide it would not remove helium impurity from neon or neon impurity from helium. Indeed no adsorption method of purification can be absolutely satisfactory unless the exact nature of all the contaminants is known.

In order to obtain helium and neon containing impurities of less than one part in 10^8 a glow discharge was run in the gas in a 3.5 cm. bore, 50 cm. long glass tube, containing an electrode at each end, attached to the system by means of a side arm situated close to one of the electrodes. The discharge was run in such a direction that the cathode was the electrode remote from the ultra-high vacuum system. This whole assembly was placed on the system as far away from the experimental tube as possible.

When a glow discharge is run in a gas mixture it is found that the minority gas is drawn to one electrode and held there by the electric field. In all but one recorded case the impurity gas is attracted to the cathode. This phenomenon, known as cataphoresis, was discovered by Baly, (83), in 1893 and has been studied theoretically by Druyvesteyn, (85), and experimentally by Oskam, (84), and Riesz and Dieke, (83). In the course of this latter work currents of from 10 mA to 25 mA were passed through commercial "spectroscopically pure" helium containing neon impurity and the intensity of the 6402Å spectrum line of neon was compared with the 5047 Å spectrum line of helium at a point near to the cathode. It was observed that the

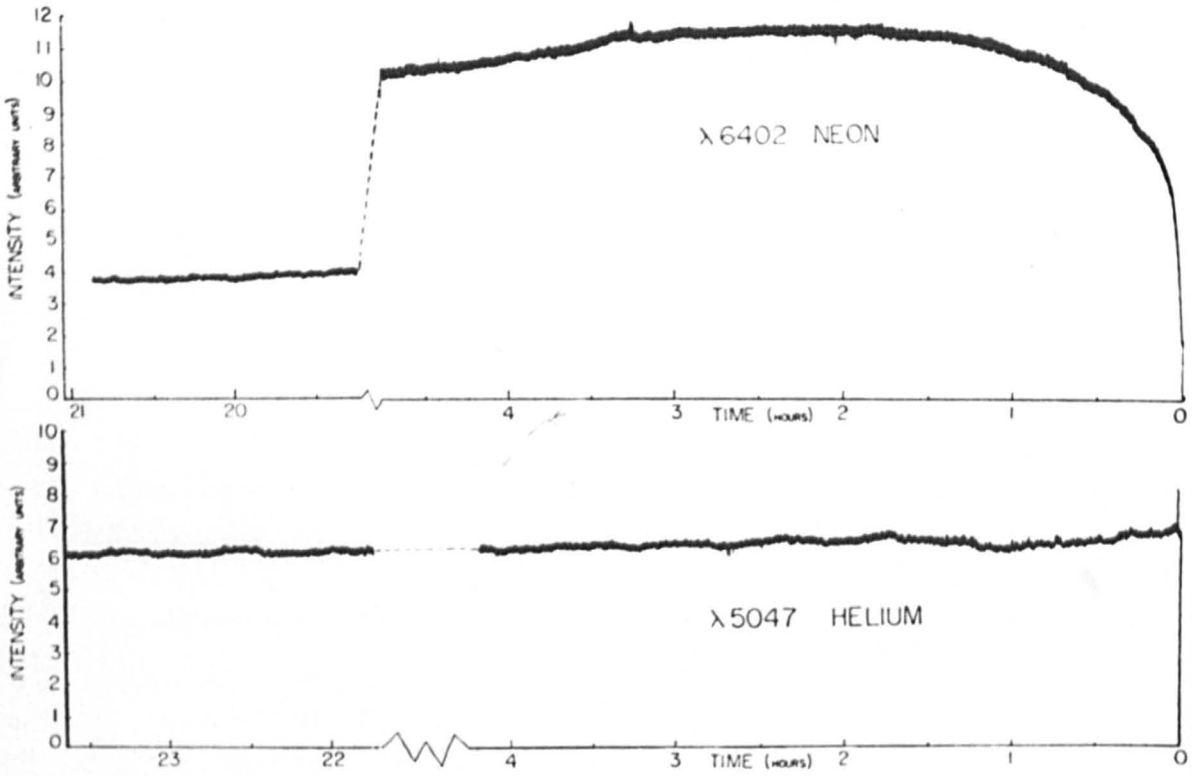

10 mm PRESSURE 25 ma dc CURRENT
MEASUREMENTS 6 cm FROM CATHODE
BOTTLE SAMPLE OF HELIUM

Figure 40.

intensity of the neon line at this point increased while the intensity of the helium line remained constant so indicating an increase in the neon concentration around the cathode which reached equilibrium in about 2 hours, Figure 40. The fall in the neon concentration at the cathode after about 19 hours is explained as being due to clean up of the neon into the cathode. The process of cataphoresis increases rapdily with increasing pressure and with increasing current and decreases as the mass of the atoms increase.

The mechanism by which this process occurs is readily explained if the impurity gas has a lower ionization potential than the bulk gas. In this case the impurity atoms may be ionized by photons from the decay of excited atoms of the bulk gas or by direct collision with metastable atoms of the bulk gas, so long as the excited and metastable states have energies higher than the ionization energy of the impurity. Also charge transfer between the ions of the bulk gas and atoms of the impurity gas may contribute to the ionization. Once ionized the impurity positive ion will move to the cathode where it will give up its charge and diffuse back into the gas. It will soon be reionized, however, and be drawn back into the cathode. In this way the impurities will be held within about 10 cms. of the cathode.

The atomic processes operating when the impurity has a higher ionization potential than the bulk gas, e.g. helium impurity in neon, is not as clear. The impurity is still drawn to the cathode and hence must be ionized. Oskam, (84), has shown that in this case

the separation is due to the formation of hybrid ions such as $Ne\,He^+$ which is formed by the triple impact of Ne^+ with two helium atoms. In this way the helium impurity forms part of an ion and is drawn to the cathode. Similar hybrid ions are formed in other gas mixtures. It seems probable that these hybrid ions will also be formed in the case in which the impurity gas has a lower ionization potential than the bulk gas. Since the cross section for charge transfer is high compared with the cross section for the necessary three body collision to form a hybrid ion, however, it would appear of only secondary importance in this case. This is particularly so in the case of a mixture of two rare gases for which the ionization potentials are so close, e.g.

He, 24.6 e.v.; Ne 21.6 e.v.

Conclusion

In the course of this chapter the techniques of the gas purification have been explained. In both hydrogen and the rare gases an attempt has been made during the present work, to achieve gas purity corresponding to a maximum impurity content of one part in 10^8 and it is believed that this has been obtained. It is now necessary to consider the apparatus and methods used to achieve both high purity of gas and high accuracy of all measurements.

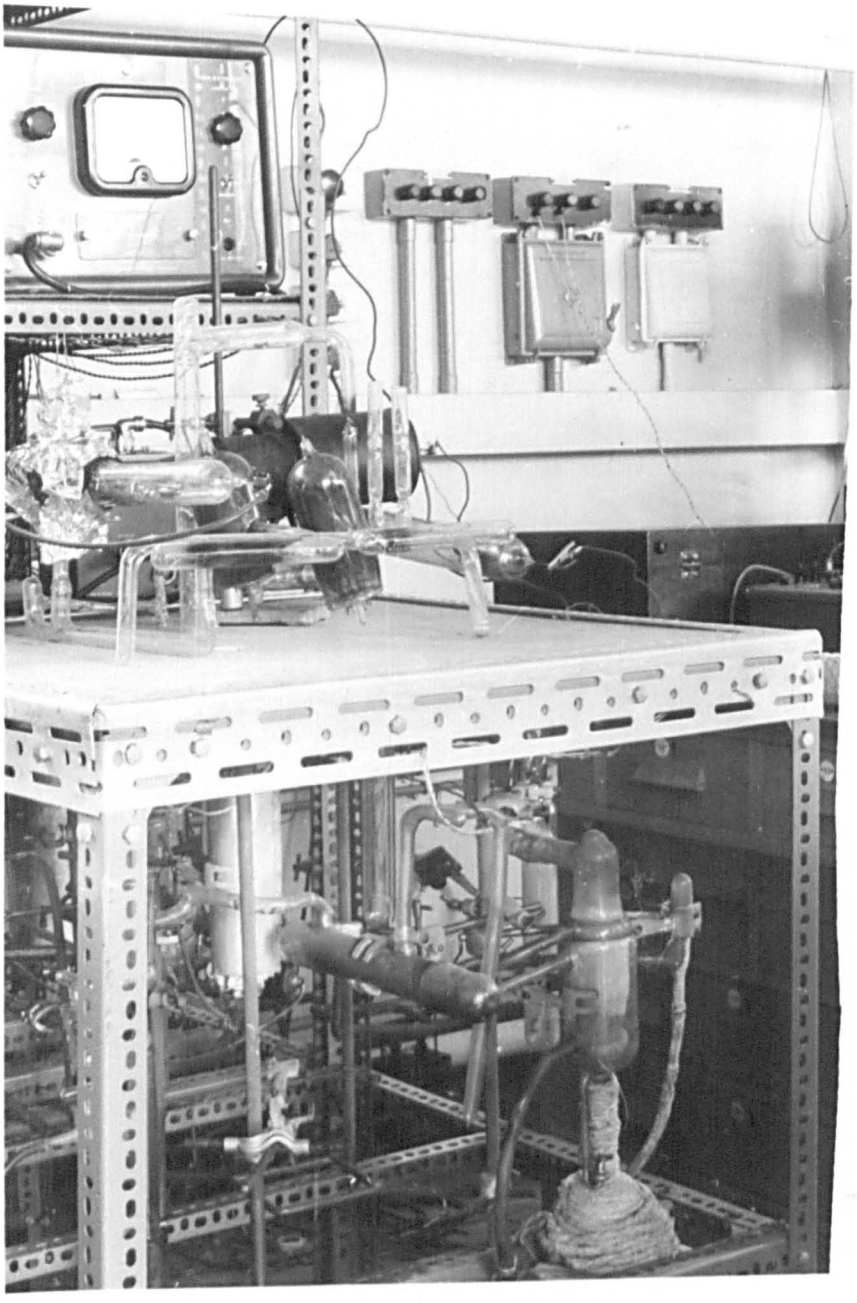

Figure 41.

General View of Apparatus.

CHAPTER V

THE EXPERIMENTAL APPARATUS

The experimental apparatus, a general view of which is shown in Figure 41, may be considered in two stages, firstly the vacuum system made almost entirely of pyrex glass, consisting of the experimental tube, the ultra high vacuum system, the conventional high vacuum system and the gas supply system, and secondly, the electrical circuitry used to supply and measure the stable potential difference across the experimental tube and to measure the pre-breakdown currents flowing in the gas. For the sake of economy, both the vacuum systems were backed by the same backing pump. Both the ultra-high vacuum system and the gas supply system had to be altered when different gases were used and where such adaptation was necessary this will be made clear in the relevant sections. The high tension supply and measuring circuits were the same for all the gases as was the conventional high vacuum system.

5.1. The Experimental Tubes

The experimental tubes, photograph and line diagram of which are shown in Figures 42 and 43, were constructed as far as practicable from pyrex glass so that rigorous outgassing techniques could be employed. The anode and the cathode consisted of an evaporated gold film on a glass disc substrate which had been ground perfectly flat and then flame polished so producing a smooth homogeneous surface. To eliminate edge effects around the cathode

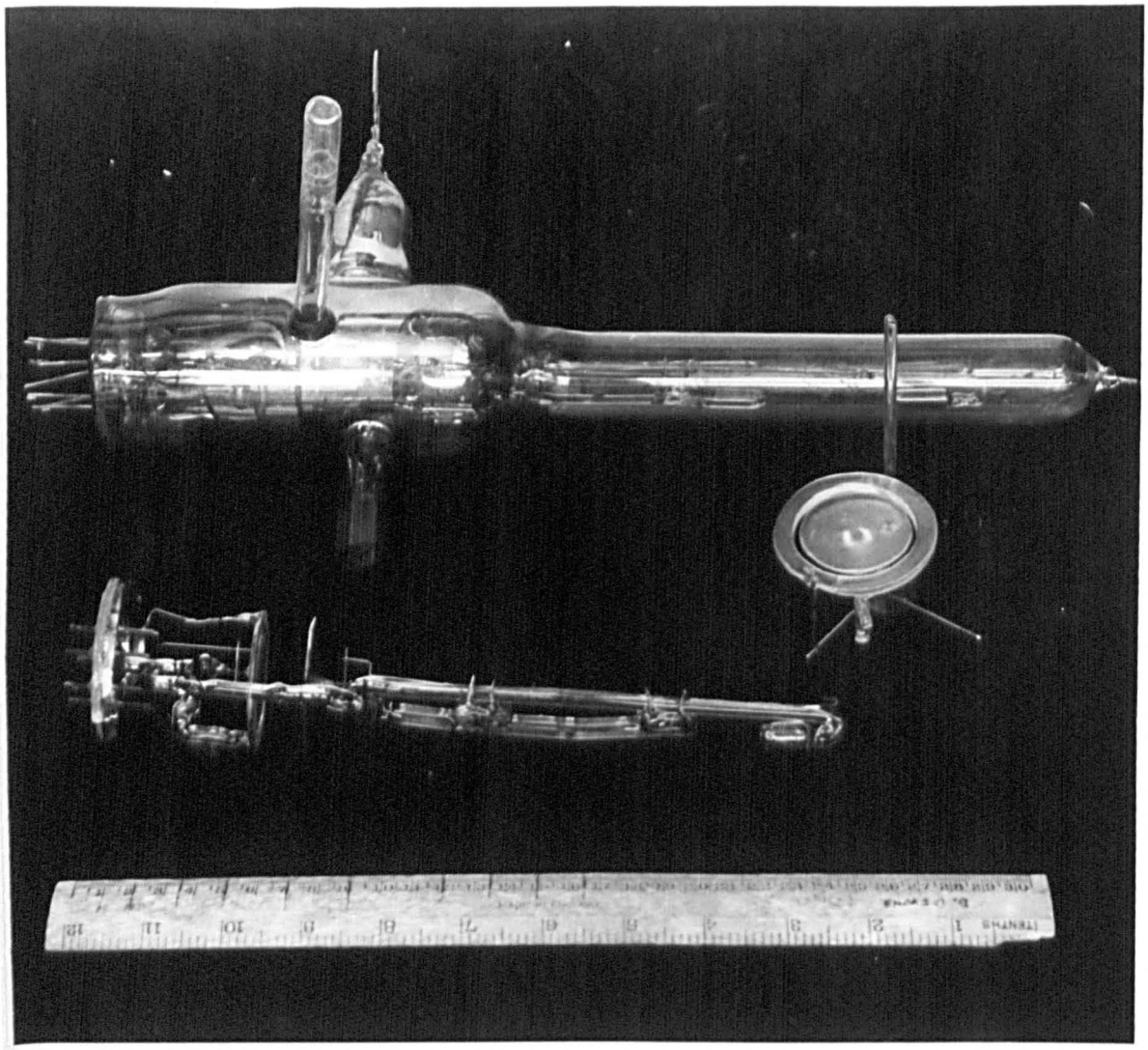

Figure 42. The Experimental Tube.

it was surrounded by a separate guard ring consisting of a gold film evaporated on to a ground, flame polished anular glass substrate. The gap between the guard ring and the cathode was always kept to a minimum and was less than 0.5 mms. in all the tubes used. One of the chief difficulties in developing this type of tube was to evolve a method of obtaining a movable anode without the use of a bulk metal screw assembly as had been used in many previous determinations. This was overcome by attaching a 5 mm. diameter glass rod to the anode, vertical to the anode, with an iron slug enclosed in glass, mounted at the other end. This was supported horizontally by an 8 mm. diameter glass rod attached to the pinch of the tube and held in place by means of two V shaped notches mounted on the support. Hence by means of a movable solenoid around the outside of the tube, the iron slug, and hence the anode, could be moved, so changing the inter-electrode gap distance. Great care had to be taken in the construction of the electrode assembly in order to ensure that the electrodes were perfectly parallel in all positions of the anode. The electrode of the earliest tubes were 2.2 cms. diameter, whilst the third and fourth experimental tubes had electrodes of 3.4 cms. and 3.8 cms. diameter respectively. An attempt was made to construct a tube with electrodes of 6 cm. diameter. This tube was unsatisfactory, however, since at large values of d (> .7 cms.) the discharge tended to pass from the anode to the walls of the tube. Also the weight of such large electrodes made it very difficult to move them by a magnet from outside the tube and to keep them within the V groove

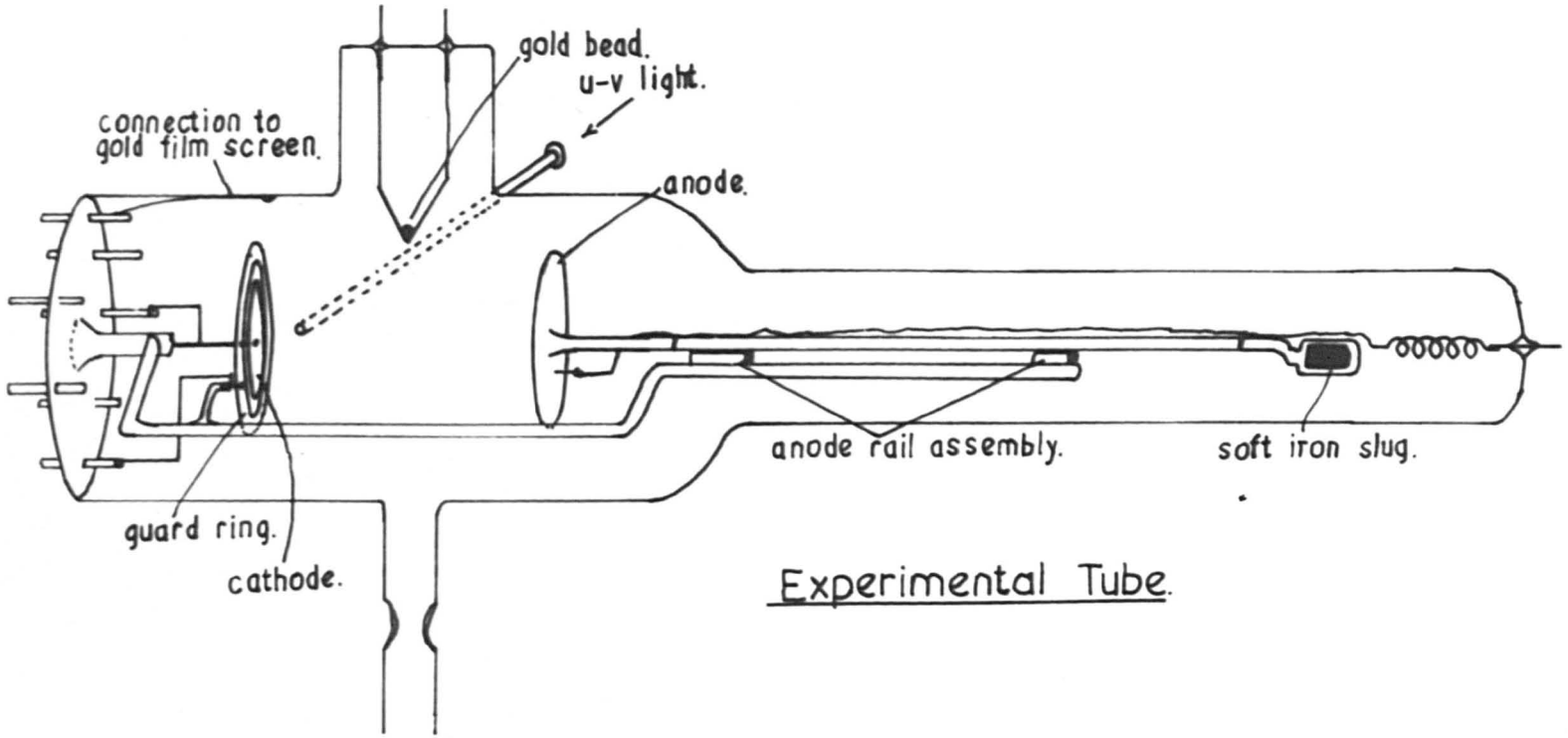

Experimental Tube.

Figure 43.

of the support. Hence the experimental tubes used for the determinations in the rare gases reverted back to electrode diameters of around 3.8 cms.

The gold which formed the final electrode surface was deposited by Joule heating of a gold bead supported in a V notch in a tungsten filament. This gold bead was made from fine gold wire wound around the tungsten filament and then melted in a flow of hydrogen. This process both formed the necessary bead of gold around the filament and cleaned the gold. The filament was spot welded to two work hardened nickel supports which held it in place within the tube, electrical contact being made via two tungsten to glass seals through the glass envelope. In the first three tubes used the gold bead was not shielded and hence the gold film was deposited evenly over the electrodes and over the walls of the tube. This produced a tendency for sparks to pass between the anode lead and the walls of the tube. To overcome this, later tubes had shielding around the gold bead to prevent gold being evaporated on to the walls near the section of the tube where the tube narrows. Also glass beading was put over the anode high tension lead. No attempt was made to prevent the gold evaporating on to the walls between the electrodes since this was used as a screen, being kept at earth potential throughout the measurements, so preventing charge build-up which would occur if the glass were bare. A window was formed in the film due to the shadow thrown by the glass rod which connected the anode support to the pinch. This window enabled the inter-electrode gap distance to be measured by means of a travelling microscope, which

was calibrated to 0.0001 cms, which meant that the gap distance could be measured to an accuracy of 0.5% at the lowest values of d. The position of the gold bead inside the tube was such that it was mid-way between the electrodes at their furthest apart position and also the distance of it from either electrode had to be greater than the maximum inter-electrode gap used during the determinations so that it would not distort the field.

A quartz window was attached to the side of the experimental tube in such a position that ultra-violet light incident upon it would fall on to the cathode. This radiation was used to produce the initial photo-electric current I_0. This will be discussed in more detail in section 5.7.

The leads from the guard ring and the cathode were spot welded to two of the pins on the pinch as was the spring contact which served to earth the gold film screen on the wall of the tube. This presented the danger that, if gold was evaporated on to the pinch, the cathode might be short circuited to earth. To avoid this, small glass cones were placed over the pins on the pinch so that the base of each pin was shielded from the gold evaporater.

5.2. The High Vacuum and Ultra-High Vacuum Systems

The purpose of this part of the apparatus was to obtain the lowest pressure possible so that any pure gas which was then introduced would not be contaminated by any air left in the experimental tube or in the auxiliary equipment. A pressure of 5×10^{-7} mm.Hg. was obtained initially by means of a three stage mercury diffusion pump

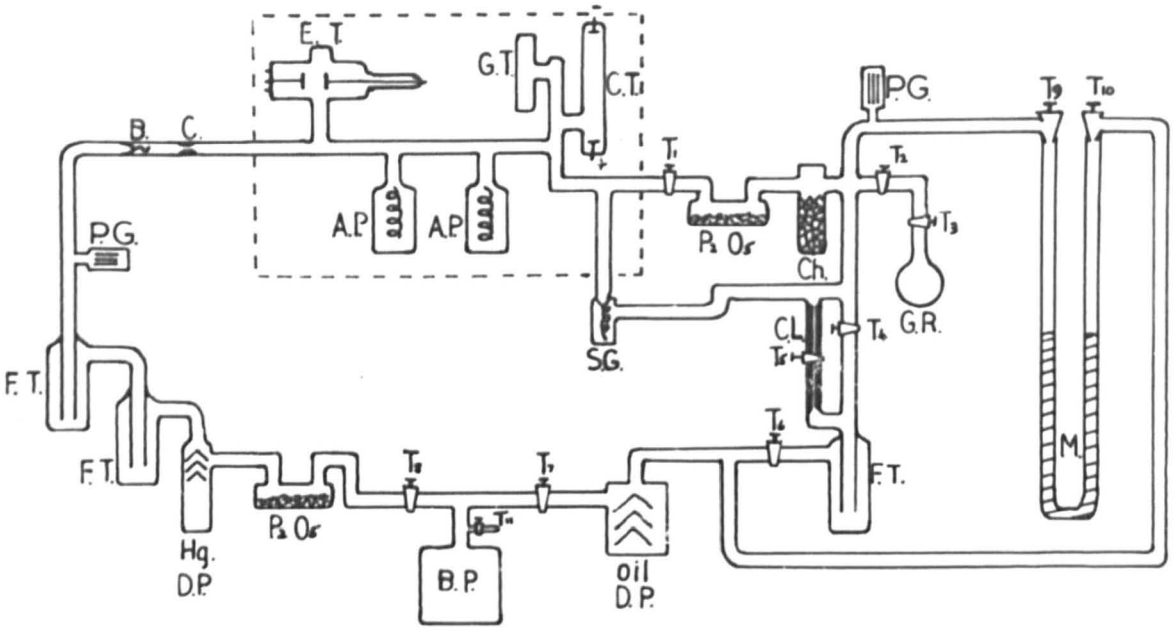

T_1- T_{10} -	GREASED TAPS.	E.T.	EXPERIMENTAL TUBE.
F.T.	FREEZING TRAP	A.P.	ALPERT PUMP
D.P.	DIFFUSION PUMPS.	G.T.	GETTER TUBE.
B.P.	BACKING PUMP	C.T.	CATAPHORESIS TUBE.
M.	MANOMETER.	G.R.	GAS RESERVOIR.
B.	BREAKER	Ch.	ACTIVATED CHARCOAL.
C.	CONSTRICTION.	S.G.	SPIRAL GAUGE.
C.L.	CAPILLARY LEAK.	P.G.	PENNING GAUGE.

-----OVEN BASE.

Figure 44.

The Vacuum System.

backed by a rotary backing pump. A phosphorus pentoxide trap was included in the system between the backing pump and the diffusion pump which absorbed water vapour from the system as well as preventing back diffusion of the backing pump oil. On the high vacuum side of the diffusion pump were two liquid nitrogen traps connected in series to prevent any mercury vapour from the diffusion pump distilling over into the ultra-high vacuum system. A Dewar vacuum flask containing liquid nitrogen was kept around at least one of these at all times during the determinations.

The ultra-high vacuum system was connected to the conventional vacuum system by means of one of several constrictions and breakers. These "pig's-tails" breakers consisted of a closed piece of glass tube, the closed end of which had been drawn out in a fine, very thin, sealed point, butt jointed to an open glass tube. To open these breakers a small iron slug, enclosed in glass to prevent it outgassing into the system, was included inside the system. The system could be opened up by striking the fine point of the breakers with this slug which could be moved from outside the system by means of a magnet. In this way the use of greased taps was eliminated on the high vacuum side of the diffusion pumps since the ultra-high vacuum system could be isolated by melting the glass at one of the constrictions and opened up again by breaking one of the "pig's tails" breakers.

The ultra-high vacuum system for the hydrogen determinations consisted of a getter tube, an Alpert inverted ionization pump, a

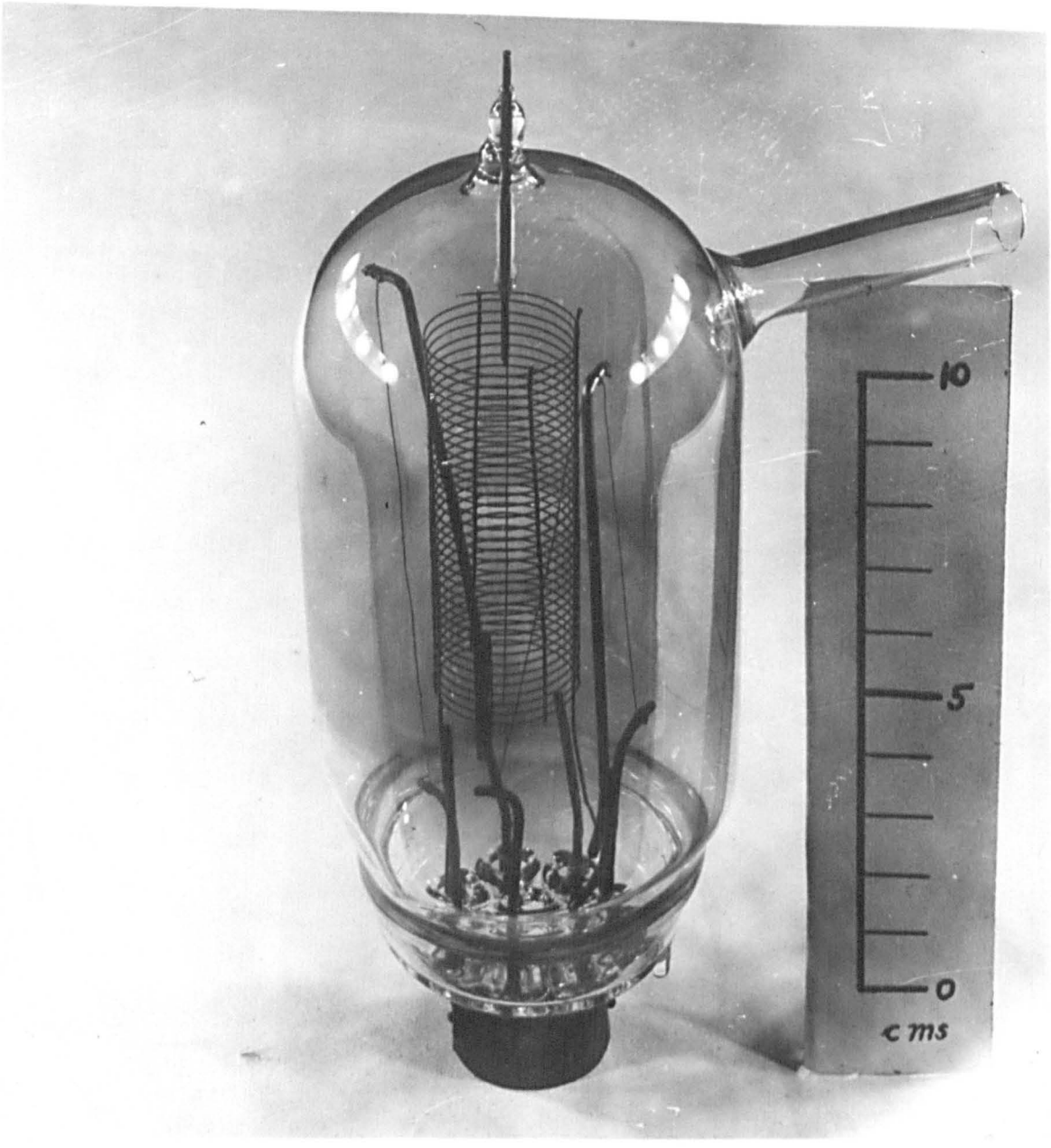

Figure 45.

Alpert Pump.

vitreosil glass side arm containing reactor grade uranium turnings which was surrounded by a small cylindrical oven and the experimental tube. On later systems an additional side arm was added around which could be placed a Dewar flask containing liquid nitrogen. The system used for determinations in the rare gases was slightly different. Two Alpert pumps were used, the vitreosil side arm was removed and a glow discharge tube was included. Also more than one getter tube was used so improving the gettering action by increasing the area over which the metal was deposited.

Barium getters were used consisting of a barium strip, each strip being attached to a small square nickel frame. About eight of these were spot welded to a nickel support and the whole assembly was included in a side arm on the system. The barium strips were heated by radio-frequency eddy current techniques both for outgassing purposes and for the final flashing. The firing of the getters lowered the pressure by as much as a factor of a hundred after the ultra-high vacuum system had been isolated.

Further pumping was carried out by means of a Bayard-Alpert type inverted ionization pump and gauge, (86), as shown in Figure 45. It consists of a spiral molybdenum grid along the axis of which is a thin tungsten collector, whilst outside the grid are two tungsten filaments. These filaments, when heated, act as a source of thermionic electrons which are accelerated towards the grid since the grid is kept at 120 volts with respect to the filament. Most of the electrons which will have approximately 120 e.v. energy at

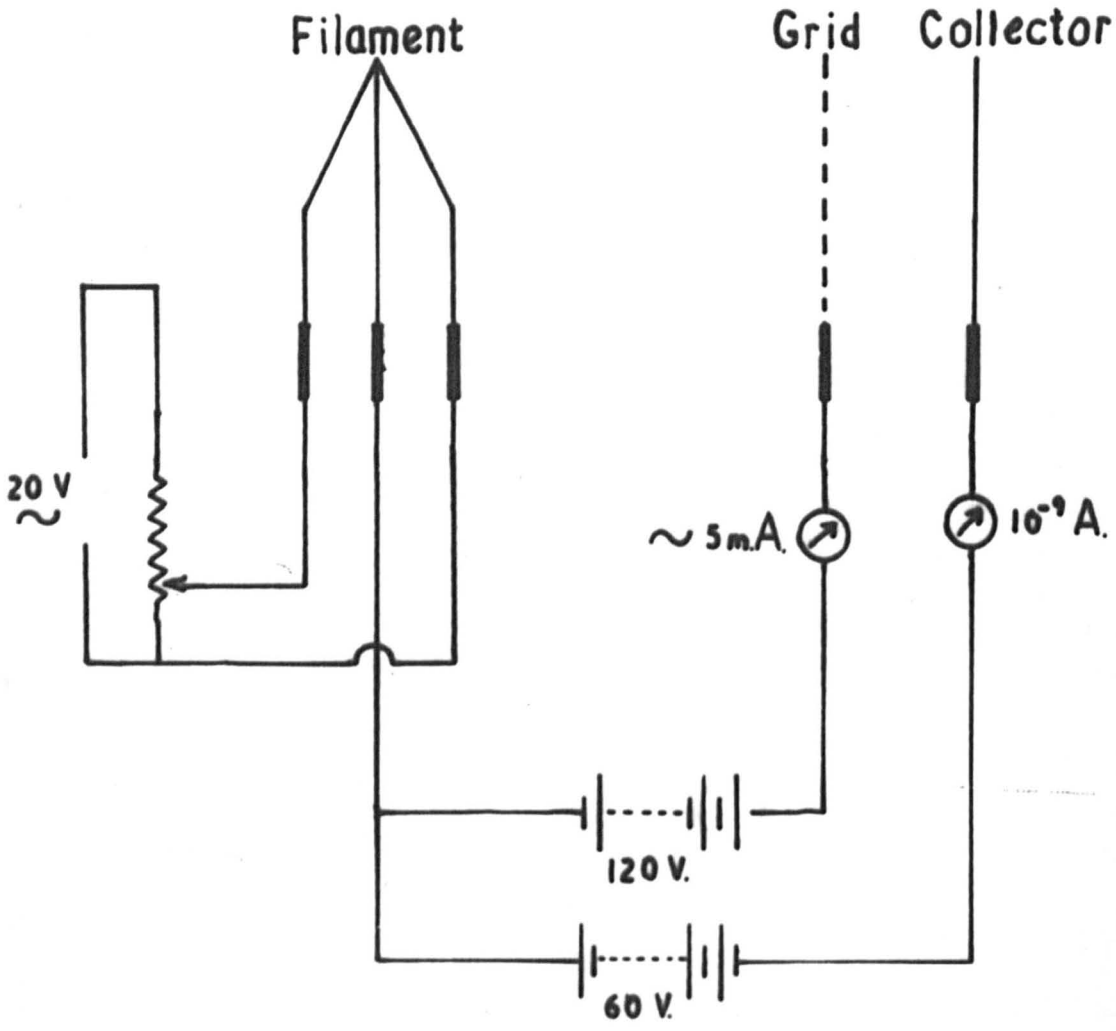

Circuit for Alpert pump

Figure 46.

this point will pass through the open structure of the grid and enter the region between the grid and the collector. Within this space they will be decellerated since the collector is kept at - 60 volts relative to the filament, i.e. - 180 volts with respect to the grid, and will eventually return to the grid. Whilst they have enough energy, however, these electrons will ionize any gas atoms present and so form positive ions which will be drawn to the collector. Hence a milliameter in the grid circuit will register the electron current whilst the microameter in the collector circuit will show the positive ion current. Assuming the electron current to be constant, therefore, the positive ion current will be proportional to the gas pressure. Using the Alpert gauge as a continuous pump and gauge the calibration used in the present measurements was

$$p = \frac{1}{10} \frac{I_c}{I_g}$$

where p is the gas pressure, I_c is the collector positive ion current, and I_g is the grid electron current. Although the sensitivity of such a gauge varies from gas to gas the above calibration was used for all three gases considered since measurements of the pressure were only needed to an accuracy of an order of magnitude. The circuit used with the Alpert pump is given in Figure 46.

The side arm containing uranium turnings used to purify the hydrogen, consisted of a vitreosil tube joined to the pyrex system by means of graded seals. A cylindrical oven was placed around the outside of this tube in order to first outgass the uranium

and later to decompose the uranium hydride. The oven was run off an a.c. mains supply via a "Variac" auto-transformer.

During the course of the measurements in hydrogen, it was suggested by Haydon, (87), that pyrex glass gives out water vapour even after it has been rigorously baked. To counteract this, a side arm was added to the ultra-high vacuum system which could have a Dewar flask containing liquid nitrogen placed around it. This arrangement would trap any water vapour formed in the sealed-off system. However, measurements both with and without the precaution were identical and hence this arrangement was not incorporated on later systems.

In order to purify the rare gases by the process of cataphoresis a glow discharge tube formed part of the ultra-high vacuum systems for determinations in helium and neon. This consisted of a 3.5cm diameter glass tube, 50 cms. long, with an electrode at each end. The anode was made of a thin nickel disc, 2 cms. in diameter. The shape of the cathode was varied since trouble was experienced in getting the discharge to start. At first a thin nickel disc was tried, then a pointed piece of tungsten strip, and finally a tungsten disc. This latter proved the most successful since it was sputtered away less than the nickel and was more substantial than the strip. The glow discharge tube was connected to the system by means of a side arm situated near to the anode since the impurities tend to concentrate near the cathode and hence the cathode needs to be as remote as possible from the system.

The whole ultra-high vacuum system was built above an asbestos

table so that the whole system could be covered by an oven and baked for long periods at 470°C.

5.3. Hydrogen Supply System

The hydrogen supply system, in which the hydrogen was produced and the initial purification was carried out, was evacuated by means of a two stage oil diffusion pump backed by a rotary backing pump which together enabled a pressure of less than 10^{-6} mm.Hg. to be obtained. The residual gas pressure in this system was not accurately measurable since the only gauge used was a cold cathode Penning gauge. This gauge consisted of two flat nickel discs, about 1.5 cms. in diameter, 1 cm. apart with a nickel wire ring between them. The discs were made 2000 volts negative with respect to the ring, and a strong magnetic field was applied normally to the discs by means of a strong horseshoe magnet clamped around the outside of the gauge. Electrons emitted from the discs when breakdown occured were then drawn towards the ring anode by the electric field and moved in a helical path due to the magnetic field. This spiral motion of the electrons enabled them to ionize more gas atoms than if they had moved directly to the ring, so increasing the ionization current. Since the amount of ionization will be proportional to the gas pressure, the current flowing, as recorded on a microameter, will be a measure of the gas pressure. This gauge was used with the calibration curves given in Appendix 3.

Hydrogen was produced in this system by the electrolysis of a very dilute solution of barium hydroxide in distilled water.

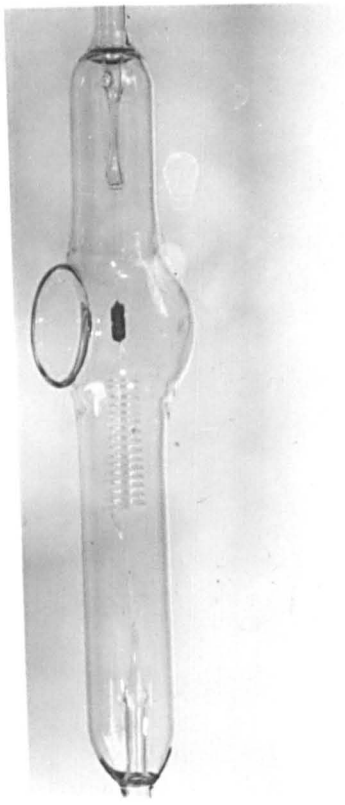

PRESSURE MEASUREMENT WITH SPIRAL GAUGE.

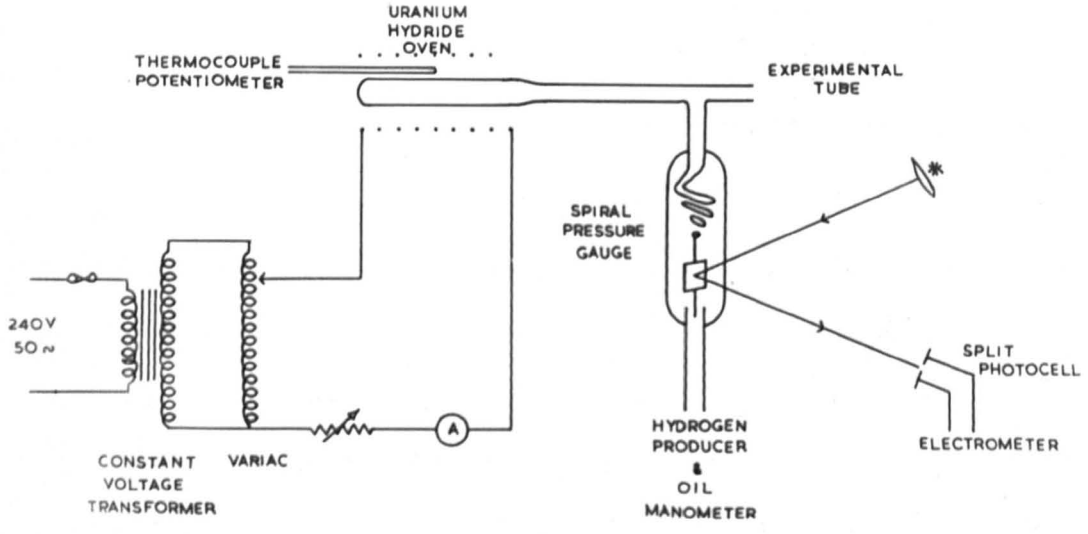

Figure 47.

The water used was first boiled to remove any carbon dioxide it may contain and then, whilst the water was still hot, the barium hydroxide was dissolved in it. Hydrogen from the voltameter was passed into two phosphorous pentoxide traps where it was allowed to stand for 14 hours in order to remove all traces of water vapour. It was then allowed to diffuse through a palladium thimble kept at 250°C, by means of a cylindrical oven placed around the outside of the pyrex tube. From this point it could be passed either into a reservoir for future use or, via a liquid air trap and a further palladium thimble, into the ultra-high vacuum system.

It was necessary for the pressure of the hydrogen in the ultra-high vacuum system and experimental tubes to be measured accurately. Because of the high purity of the gas required it was not feasible to make direct measurements on this system as some impurity would certainly be introduced. To overcome this difficulty a glass Bourdon type pressure gauge,as shown in Figure 47, was incorporated between the gas supply system and the experimental tube. This gauge consisted of a fine glass spiral with a small plane mirror attached to the spiral suspension. When a difference in pressure was apparent across this spiral the force tended to twist the spiral so turning the mirror. Hence an optical lever could be used to determine when the pressures on each side were equal. The reflected spot was arranged to fall on to a divided photo-cell, the two halves of which were only 0.5 mms. apart. The currents from the two halves of this photo-cell were opposed and the net current was passed into

a single tetrode electrometer. The photo-cell, which was movable in a horizontal direction, was adjusted so that when the pressures on each side were equal no current flowed and in this way the arrangement acted as a very sensitive null indicator. In practice it was found that one photo-cell was more sensitive than the other and to overcome this a high leakage resistance was connected between the terminal of this photo-cell and the common base terminal. In order to obtain maximum sensitivity the light source was suitably masked to give a square image on the photo-cells of the same size as one of the photo-cells. Using this arrangement, a pressure difference between the gas supply system and the experimental tube of 0.001 mm.Hg could be detected. Hence if the pressures on the two sides of the apparatus were equal the pressure in the experimental tube could be measured by measuring the pressure in the gas supply system. This was done by means of a three metre oil manometer containing D.C. 703 silicon based oil. If, by any accidental fracture of the vacuum apparatus, one part of the system should be let down to air while the rest of the apparatus was under vacuum, the manometer oil would be forced over into the oil diffusion pump. To avoid having to strip down the pump in such a contingency the same oil was used in both manometer and pump.

To remove hydrogen from the gas supply system very slowly, in order to equate pressures, a fine capillary leak was included between the system and the pumps. In parallel with this was a conventional greased tap which could be used to open or isolate this

system.

5.4. Helium and Neon Supply System

The vacuum system used for the supply and the initial purification of helium and neon was adapted from the hydrogen system and was hence very similar to that used for the hydrogen supply. The barium hydroxide voltameter was replaced by a B.O.C. one litre pyrex glass flask containing the gas at one atmosphere pressure, connected to the system via two greased taps. The neck of the flask was sealed by means of a "pig's tail" breaker so enabling the flask to be opened in vacuum by dropping a soft iron slug enclosed in glass on to the breaker. When the tap nearest to the flask was opened, gas was admitted to the space between the taps. If this tap was now closed and the second tap was opened, a controlled volume of gas was admitted to the initial purification part of the system. The pressure in the gas system could be set at a convenient value by doing this several times. The gas was then stood over phosphorus pentoxide and over activated charcoal at -190°C for 14 hours after which it was admitted to the ultra-high vacuum system via a greased tap. All greased taps in this system were greased with Apiezon 'N' grease having a vapour pressure of 10^{-9} mm.Hg at room temperature.

Pressure measurements in both helium and neon was the same as for hydrogen as was the evacuating equipment.

5.5. The High Tension Supply

Since fluctuations of the high tension supply will produce changes in the magnitude of the ionization currents measured, the

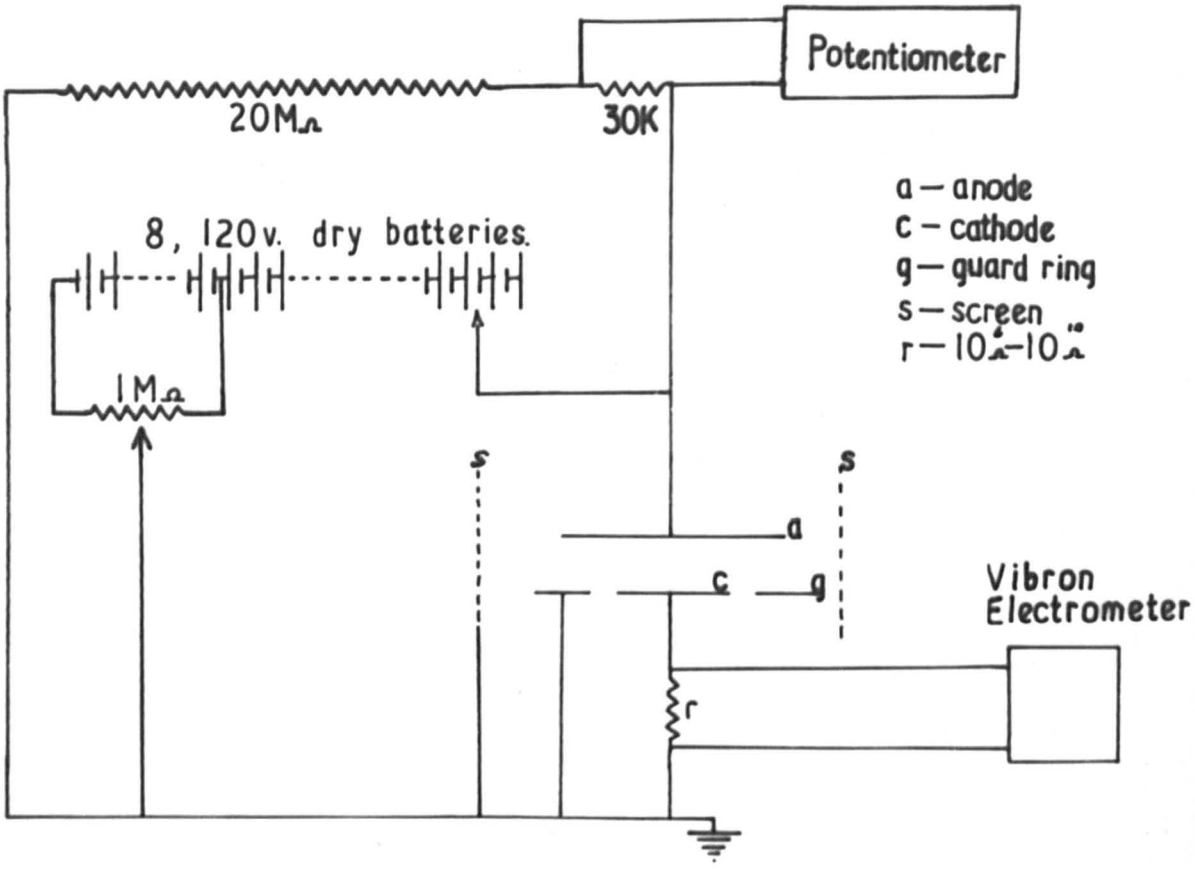

H.-T. Supply to Tube.

Figure 48.

stability of this supply was of great importance in the present work. For this reason a bank of eight 120 volt dry batteries, connected in series, was used with provision for tapping off the required number by means of a selector switch, so giving voltages from 0 to 840 volts in steps of 120 volts. The negative end of these batteries was connected to the positive end of a 1 MΩ potentiometer which had a further 120 volt dry battery in parallel with it. Fine voltage adjustment was allowed for by means of a further 1 MΩ potentiometer with a 9 volt grid bias battery across it, the negative end of which was earthed. This circuit is given in Figure 48. In this way any voltage from 0 to 840 volts could be obtained to an accuracy of $\pm \frac{1}{2}$ volt. Provision was made at the positive end of the battery bank for the addition of further H.T. batteries in case higher voltages were required.

The H.T. was measured by means of a resistor chain in parallel with the experimental tube. This chain consisted of 10, 1 MΩ resistors plus a 30 KΩ resistor. Each of these resistors was accurately calibrated against a standard 1 MΩ resistor. The full H.T. was connected across this chain and the voltage drop across the 30 KΩ resistor was fed into a potentiometer where it was measured by comparison with a Weston Standard cell. The H.T. voltage was thus the voltage across the 30 KΩ resistor multiplied by the ratio of the resistance of the 10 MΩ section to the resistance of the 30 KΩ resistance. The accurate values of the resistors used and the conversion factor are given in Appendix 5. The resistance chain was

put into a sealed glass tube which was evacuated to reduce leakage currents to a minimum.

The output from the batteries was connected to the anode of the experimental tube by means of co-axial cable which was well screened. This screening was all connected to the negative end of the batteries which was earthed. An accuracy of better than 1% was achieved by the arrangement and a highly stable H.T. supply was obtained.

5.6. Current Measurement

Since the values of the Townsend ionization coefficients are found by determining the manner in which the current flowing in the gas varies with gap distance it is clearly of the utmost importance that the current is measured to a high degree of accuracy. The circuit used to measure the prebreakdown currents is given in Figure 48.

The current through the experimental tube was measured by means of a Vibron A33B resistance unit connected in series with the experimental tube in the cathode circuit. In parallel with this resistance box was a Vibron 33B electrometer which could measure small d.c. potentials in the range of 1 millivolt to 1 volt from sources of very high internal resistance. This meant that, since the resistance in the resistance box could be selected from $10^{10}\Omega$, $10^{8}\Omega$ or $10^{6}\Omega$, currents of from 10^{-13} amps to 10^{-6} amps could be measured. An estimated 2% maximum possible error is claimed by the manufacturers of the instrument. For the measurements in neon and

for some of the measurements in helium, this electrometer was replaced by a Vibron 33 C with a A33C resistance box. It was found that this instrument was much less sensitive to external a.c. fields whilst being able to measure currents as low as 10^{-15} amps.

Most fluctuation of the electrometer reading was found to be due to friction and strain in the input lead. This lead was thus securely clamped to the frame of the apparatus and was screened by means of copper pipe which was earthed via an iron stake driven into the ground outside the laboratory. Microphony in this lead was reduced by using special non-microphonic lead and by keeping the length of the lead down to a few inches only. The inter-electrode gap was shielded from stray fields by the evaporated gold film around the inside of the tube. This film was earthed as was the metallic foil shielding that was wrapped around the outside of the tube.

Zero drift was found to be non-existent after the electrometer had been allowed to warm up for about 24 hours, although prior to this some drift was observed.

5.7. Production of Initial Photo-Electric Current

Throughout the work described in this thesis the initial photo-electric current, I_o, was produced by shining ultra-violet light on to the cathode through a quartz window built in the side of the tube. For electrons to be emitted by such radiation

$$h\nu \geq e\phi$$

where h is Planck's constant

ν is the frequency of radiation

ϕ is the work function of the surface.

The number of electrons coming from the electrode surface in unit time will be proportional to the intensity of the radiation. Also the value of I_0 will be dependent upon the velocity with which they are emitted which in turn is proportional to $(h\nu - \phi)$. For these reasons it is clearly important that both the frequency and the intensity of the radiation should be constant.

The ultra-violet light was obtained from a low pressure mercury glow discharge lamp, the output of which was rated at 100 watts at 1,100 volts. The voltage supply was obtained from a step-up transformer in series with a constant voltage mains transformer in order that a constant voltage was applied to the lamp at all times, so giving a constant intensity.

High pressure mercury lamps produced large quantities of ozone which absorb ultra-violet radiation. Hence variations in the concentration of the ozone between the lamp and the tube can cause variations in the intensity of the light received at the cathode and so vary I_0. The low pressure lamp used did not produce appreciable quantities of ozone.

The radiation emitted by the low pressure lamp was almost exclusively at a wavelength of 2536 Å. The following table gives the full spectrum and the relative intensities of each line.

Wavelength, Å	Intensity, μwatts/sq.cm. 1 metre from lamp.
5780	0.17
5461	1.05
4358	1.2

4047	0.47
3650	0.65
3342	0.04
3132	0.71
3022	0.07
2967	0.22
2894	0.05
2804	0.02
2652	0.07
2536	120.0
2482	0.03

Taking the work function of the cathode surface as 4.5 e.v., radiation of wavelengths less than 2747 Å is required to cause electron emission. Hence from the above table it may be seen that 99.92% of all electron emitting radiation occurs at 2536 Å and the lamp may be considered as virtually a monochromatic source.

CHAPTER VI

EXPERIMENTAL PROCEDURE

6.1. Vacuum Techniques

All the glassware used in the vacuum system was washed in nitric acid before the system was built in order to remove all traces of grease and surface dirt. Any parts which had to be added to the system later were similarly treated. The system was initially evacuated to a pressure of 10^{-3} mm.Hg by means of a rotary backing pump. At this stage the majority of leaks could be found by the use of a "Tesvac" high frequency leak detector.

The pressure in the gas supply system was then reduced to 10^{-5} mm.Hg. by means of an oil diffusion pump. Since this system could not be baked in an oven the glass was heated in a gas flame from a small hand torch, after which the pressure was reduced to less than 10^{-6} mm.Hg. At this pressure the Penning gauge ceased to operate. The oil in the manometer was boiled several times by applying a gas flame to it, to remove any air that may have been absorbed whilst it had been exposed to the atmosphere. The system was then isolated and any subsequent rise in pressure noted over a period of several days. If the pressure did rise the system was opened to the pumps and the leak detected and sealed.

A three stage mercury diffusion pump was used to reduce the pressure in the ultra-high vacuum system to 10^{-7} mm.Hg. This system was then covered by a large oven and baked for 24 hours at a temperature of between 450°C and 475°C. When this was done the pressure

rose to about 10^{-3} mm.Hg., as the glass outgassed, but gradually decreased until the Penning gauge once more ceased to operate, that is, a pressure of less than 10^{-6} mm.Hg. The oven was then removed and all the metal within the system was heated to red heat either by passing a current through it where this was possible, or by r.f. eddy current heating. When no more gas appeared to come off the metal, the oven was replaced over the system and the system was once more baked at 460°C for about three days. At the end of this period the oven was removed and the ultra-high vacuum system was isolated from the pumps by means of one of the constrictions included for this purpose. During the baking process prior to the determinations in hydrogen, the uranium turnings were baked at 900°C with occasional bursts at 1000°C and the palladium thimbles were heated at 250°C. Throughout the evacuating process Dewar flasks containing liquid nitrogen were kept around the cold traps to prevent any mercury distilling over into the experimental tubes from the mercury diffusion pump. The pressure of the isolated system was noted for several hours to confirm the absence of any leaks. If the pressure rose the system was opened to the pumps, the leak detected and sealed and the system once more isolated. If no pressure rise was observed the uranium hydride was formed from the uranium in the system as described in 6.2.. Four of the getters were then flashed, so reducing the pressure by up to a factor of 100. With the pressure in the tube between 10^{-9} mm.Hg. and 10^{-8} mm.Hg. a current was passed through the gold bead in the experimental tube until the gold became molten

and was evapourated on to the electrodes and the walls of the tube, leaving only a narrow window through which the inter-electrode gap distance could be measured. The rest of the getters were then fired, and the Alpert pump, which until now had been used only as a gauge, was turned on and a filament current of between 1mA and 10mA was passed for several days. In this way a pressure of less than 5×10^{-10} mm.Hg. was obtained.

6.2. Purification of the Hydrogen

The hydrogen used was obtained from a voltameter containing a dilute solution of barium hydroxide. It was then allowed to stand over phosphorus pentoxide for several days to remove any water vapour present, and was then passed through the first of two heated palladium osmosis tubes. Following this the hydrogen could be either stored in a previously evacuated reservoir or passed directly through a second heated palladium osmosis tube into the ultra-high vacuum system. Final purification of the hydrogen was performed by means of the uranium turnings contained in a vitreosil tube connected to the ultra-high vacuum system via a graded seal and a constriction. As stated in section 6.1., the uranium was baked at 900°C for several days to remove all traces of absorbed impurity, after which time the gas pressure above the uranium was of the order of 10^{-7} mm.Hg.. Now if uranium is stood in an atmosphere of hydrogen the hydride is formed so

$$2U + 3H_2 \rightleftharpoons 2UH_3 - \Delta H$$

where ΔH for this reaction is 30.4 Kcals/mole. Since the hydride is

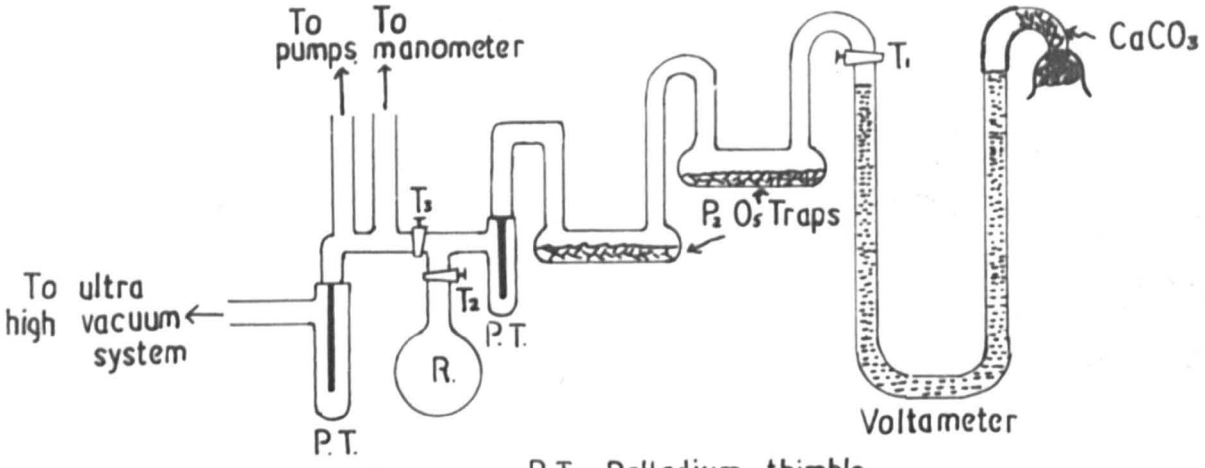

P. T. – Palladium thimble.

R – Reservoir

T_1 – T_3 – Greased taps.

The Hydrogen Supply System.

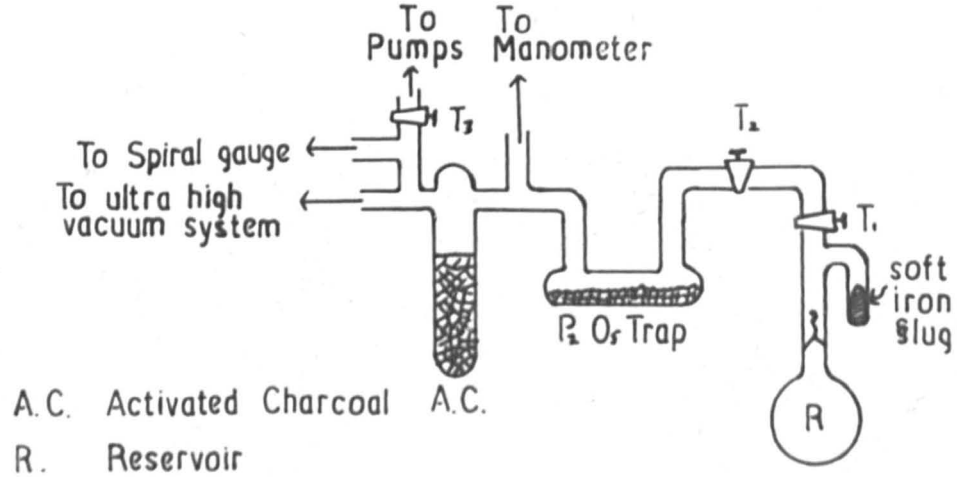

A.C. Activated Charcoal

R. Reservoir

T_1 – T_3 Greased taps

The Rare Gas Supply System.

Figure 49.

formed with the evolution of heat energy it is obvious that raising the temperature of the hydride will cause the reaction to be reversed. In this way very pure hydrogen can be obtained and the hydrogen pressure will be proportional to the temperature of the uranium hydride. Hence the pressure in the isolated system can be controlled.

With this in mind, therefore, hydrogen was allowed to diffuse through the palladium thimble between the gas supply system and the ultra-high vacuum system and to stand over the uranium. When sufficient hydrogen had been absorbed the system was opened up to the pumps by means of a "pigs-tail" breaker and the excess hydrogen was pumped away. Then, as described in 6.1., the system was sealed and ultra-high vacuum techniques applied and the electrode surfaces were put down. Since at this stage extremely pure hydrogen was present in the experimental tube and clean gold electrode surfaces had been laid down, measurements of the spatial growth of ionization and of sparking potentials could be made.

6.3. Purification of Helium and Neon.

Samples of helium and of neon were contained in 1 litre pyrex flasks sealed to the gas supply system and separated from the rest of this system by two greased taps, Figure 49. When the whole system had been evacuated to a pressure of less than 10^{-6}mm.Hg., the flask was opened by dropping a soft iron slug enclosed in glass on to the "pig's-tail" breaker included in the neck of the flask. The tap nearest to the flask, T_1, was then opened allowing the gas to fill the volume between the two taps. This tap was then closed

and the second tap, T_2, was opened so allowing a controlled volume of gas into the system. By repeating the process several times, the gas pressure in this system could be adjusted to any required value. The helium or neon was then stood over activated charcoal at -190°C and over phosphorus pentoxide for 24 hours and was then passed into the ultra-high vacuum system. A 15mA glow discharge was run in a side arm attached to the ultra-high vacuum system in order to purify the gas further by the process of cataphoresis which is described in 4.2.. The power for this glow discharge was obtained from a 0-500 volt d.c. power pack which would give up to 100mA. The discharge was run throughout the determinations in order to keep all impurities in the side arm and away from the experimental tube.

6.4. Investigation of Spatial Growth of Ionization

As may be seen from Figure 43 at small gap distances, the anode of the experimental tube may cut off some of the ultra-violet light incident upon the cathode. To determine at what gap distance this occurs, the variation of electron current with gap distance had to be investigated in vacuum before any gas was admitted. After the ultra-violet lamp had been allowed to warm up for 24 hours, 100 volts was applied across the tube in order to draw all electrons emitted by the cathode across the gap, and the current flow was plotted as a function of gap distance. The value of d above which the photo-electric current was constant, was noted and in all measurements of current growth in the gas only values of d above this

were used.

To test the stability of the ultra-violet lamp, and to determine the constancy of I_0 with time, the value of I_0 was noted at a constant value of d and with 100 volts across the electrodes, over a period of 24 hours.

Pure gas was now admitted to the experimental tube at a pressure of about 10 mm.Hg.. In the case of hydrogen, this was done by heating the uranium hydride and in the case of the rare gases by opening the tap between the ultra-high vacuum system and the gas supply system, allowing some gas to flow into the experimental tube and then closing the tap. The pressure in the gas supply system was then reduced to the same pressure as that in the experimental tube, as indicated by the spiral gauge and the single tetrode electrometer, by means of the capillary leak to the pumps. The gas pressure was measured accurately in the gas supply system from the oil manometer by means of a cathetometer and this value in cms. of oil at room temperature was converted to the pressure in mms. Hg. at $0^{o}C$, p_o.

Once the pressure had been set and accurately measured the inter-electrode gap distance, d, was adjusted to the minimum usable value as indicated by the photo-electric current v. gap distance curve, previously determined. This smallest value of d was found to be about 2 mms. for most of the tubes used. The gap distance was measured, using a travelling microscope, by viewing the electrodes through the window in the gold film on the inside of the

tube. A window was also left in the metallic foil screening around the outside of the tube. Several readings of each gap distance were taken and the mean value of d calculated. In this way d could be measured to an accuracy of $\pm$ 0.5% at the smallest values of d and to $\pm$ 0.1% at large values of d. In order to make this measurement as accurate as possible the elctrodes were illuminated by visible light from a powerful reading lamp situated alongside the travelling microscope.

With the gap width, d, known and the measured pressure at room temperature reduced to the corresponding pressure at 0°C, p_o, the voltage necessary to give the required value of E/p_o was calculated from the expression

$$V = (E/p_o)\ p_o.d.$$

The high tension supply was then adjusted to give this voltage which was measured by means of the potentiometer. This output was connected across the tube and the subsequent current flow in the gas was measured using the "Vibron" electrometer and resistance box. The electrode gap was then increased, the required potential to keep E/p_o constant calculated and applied to the tube and the corresponding current measured. This procedure was repeated until about 20 values of current at the corresponding value of gap distance had been obtained and the curve of $\log_e$ i.v.d., which was plotted as the points were taken, showed pronounced upcurving. During these determinations of pre-breakdown currents, breakdown itself was never allowed to occur since if it did the cathode surface might be

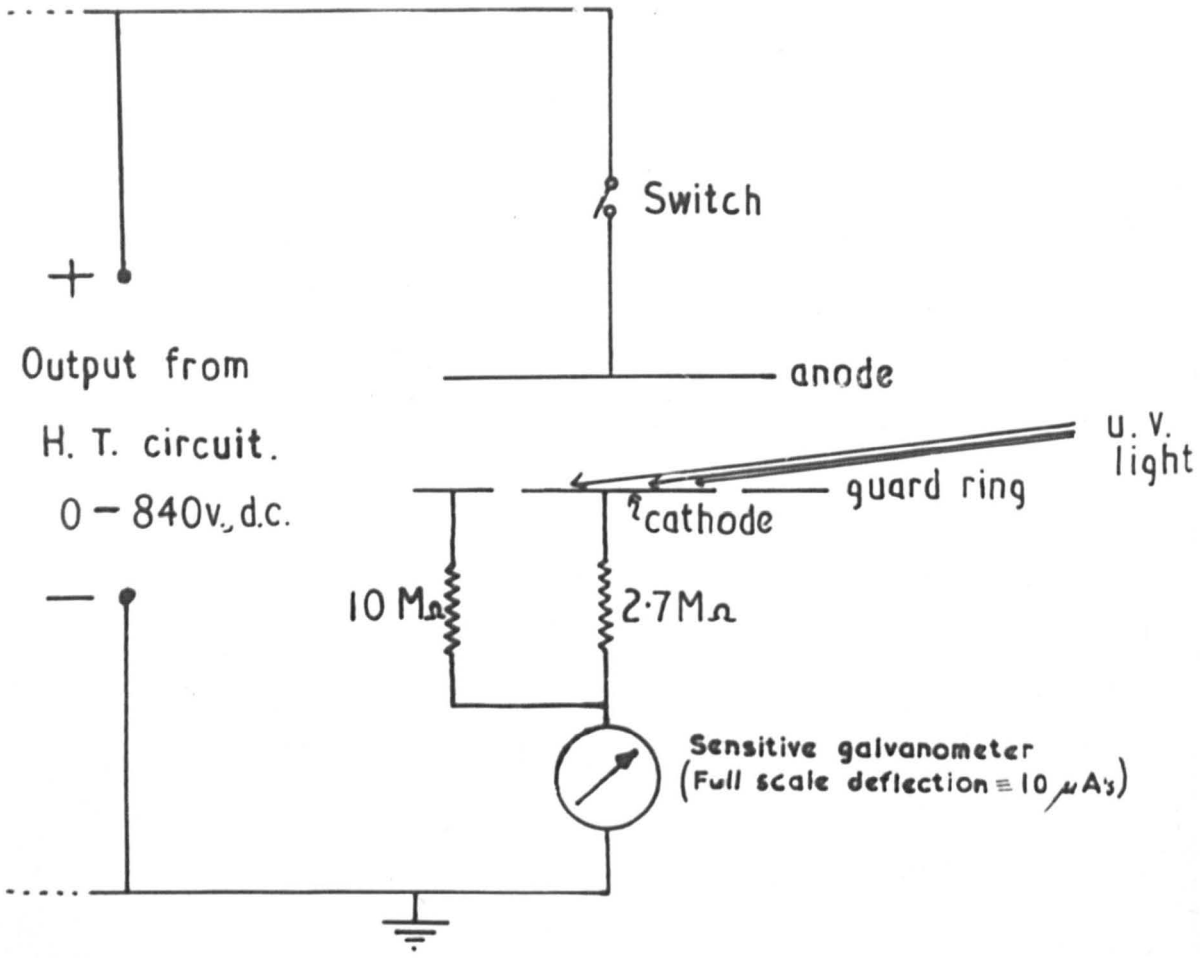

Circuit used for measuring Sparking Potentials

Figure 50.

changed. The resistance of the resistance box in series with the tube was kept constant during the taking of each curve since discontinuities were apparent in the $\log_e$ i.v.d. curve when this resistance was changed. The value of I_o was at all times kept below 10^{-11} amps since the current increased by a factor of 10^3 over a typical current growth curve and space charge effects, which set in at around 10^{-8} amps, had to be eliminated. Only during breakdown were currents of more than 10^{-8} amps allowed to flow.

For a full range of E/p_o from 10 volts/cm.mm.Hg. up to 1000 volts/cm.mm.Hg., the gas pressure in the experimental tube had to be varied from 26 mm.Hg to 0.6 mm.Hg respectively. About four values of α/p_o were determined for each value of E/p_o. Agreement was obtained for all these measurements to within 5% at high E/p_o and to 2% at medium values of E/p_o. In most of the measurements the increase in d between successive measurements was random but for the determinations in which the Haydon and Robertson analysis was to be used the increase in d was kept constant.

6.5. Measurement of Sparking Potentials

After all the pre-breakdown current measurements had been taken the breakdown characteristics of the cathode-gas system were investigated. The circuit used for this is given in Figure 50. The positive of the high tension supply was applied to the anode via a tapping key enclosed in perspex for safety. The cathode was connected to earth through a 2.7 MΩ resistor and a Cambridge spot galvonometer, which had a maximum sensitivity of 10^{-8} amps per scale

division, while the guard ring was connected to earth through a 10MΩ resistor. The technique used to determine the breakdown potential of a given gap was to increase the applied potential in steps of one volt, keeping each voltage across the gap for about 10 secs. Breakdown was evident by a sharp increase of the current flow from about 10^{-8} amps up to about 10^{-6} amps. This final current flow was only dependent upon the external circuit. When breakdown occured a positive ion layer would be formed on the cathode so reducing the apparent work function and reducing V_s. In order to obtain the correct value of V_s several minutes were allowed to elapse between successive measurements in which time the ultra-violet radiation incident upon the cathode would remove the positive ion layer.

In hydrogen a dark discharge was noted but in helium and neon the discharge was often luminous. The value of the breakdown potential was recorded at constant pressure and varying gap distance and at constant gap distance and varying pressure. Curves of sparking potential, V_s, against the product of the spark gap distance and pressure, $p_o d_s$, were plotted from which the values of the Townsend second ionization coefficient could be determined.

6.6. Conclusion

In the course of this chapter the techniques used to process the experimental tube, to purify the gases used, and to obtain the required measurements, have been outlined. It is now necessary to consider the results obtained and the conclusions which may be drawn from them.

CHAPTER VII

RESULTS AND DISCUSSION

The results given in this chapter were obtained from seven experimental tubes. Except where otherwise stated, residual gas pressures of less than 10^{-9} mms.Hg. were obtained before the gas was introduced into the tube. Prior to any investigation of the spatial growth of ionization the stability of the initial photo-electric current, I_o, and of the cathode surface had to be estimated for each tube. Also, since at low values of inter-electrode gap distance, d, the anode cut off some of the ultra-violet radiation, the minimum usable value of d had to be determined by observing the variation of I_o with d.

7.1. Stability of the Initial Photo-Electric Current and the Cathode Surface

In order to estimate the stability of the photo-electric current the experimental tube was evacuated to a pressure of less than 10^{-9}mms.Hg. and a steady potential difference of 150 volts was applied between the electrodes. The cathode was irradiated by ultra-violet light from an air cooled, low pressure mercury glow discharge lamp. The lamp and the "Vibron" electrometer, which was used to measure the current, were allowed to warm up for 24 hours prior to the results being taken. Values of the current flowing were recorded every two minutes for one hour and then every ten minutes for a further two hours. As may be seen from Figure 51, the variation of the current

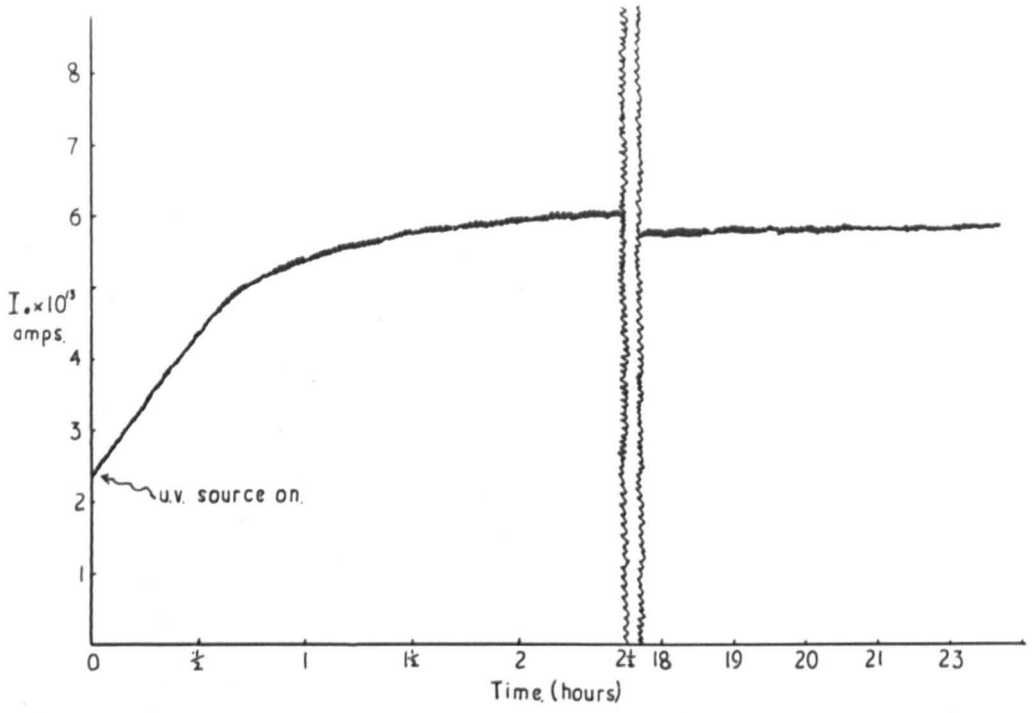

Figure 51. Stability of the U.V. Source.

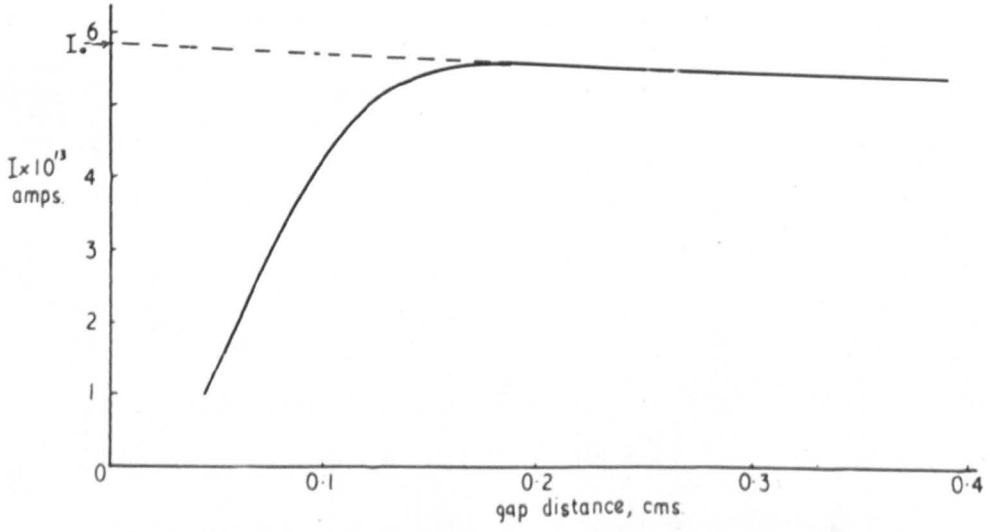

Figure 52. Variation of the Current with Gap Distance in Vacuum.

flowing over this time was less than 1%, and, since each set of current growth curves took about two hours, this would indicate considerable stability of the ultra-violet light source.

The variation in the sparking potential, V_s, with time is a measure of the stability of the cathode surface. Such measurements could not be made before the investigation of the pre-breakdown currents since the cathode surface may be damaged by a spark discharge. However, measurements of breakdown potentials carried out after α/p_o had been determined, were reproducible for $\pm$ 1 volt over one hour corresponding to a variation of only $\pm$ 0.3%. As each Paschen curve took only about half an hour it seems safe to assume that the condition of the cathode surface was constant during each set of measurements.

The effect of the variation of gap distance on the photo-electric current for each tube was observed by applying 150 volts across the electrode and measuring I_o as a function of d. The I_o.v.d. curves obtained were in all cases similar to those shown in Figure 52. At values of d below about 2 mms. the current was found to decrease rapidly due to part of the electron producing radiation being cut off from the cathode by the anode. The value of d at which this occured varied slightly from tube to tube and was dependent on the geometry of the tube. In the course of the subsequent current growth measurements in the gas, no values of d were used below this value.

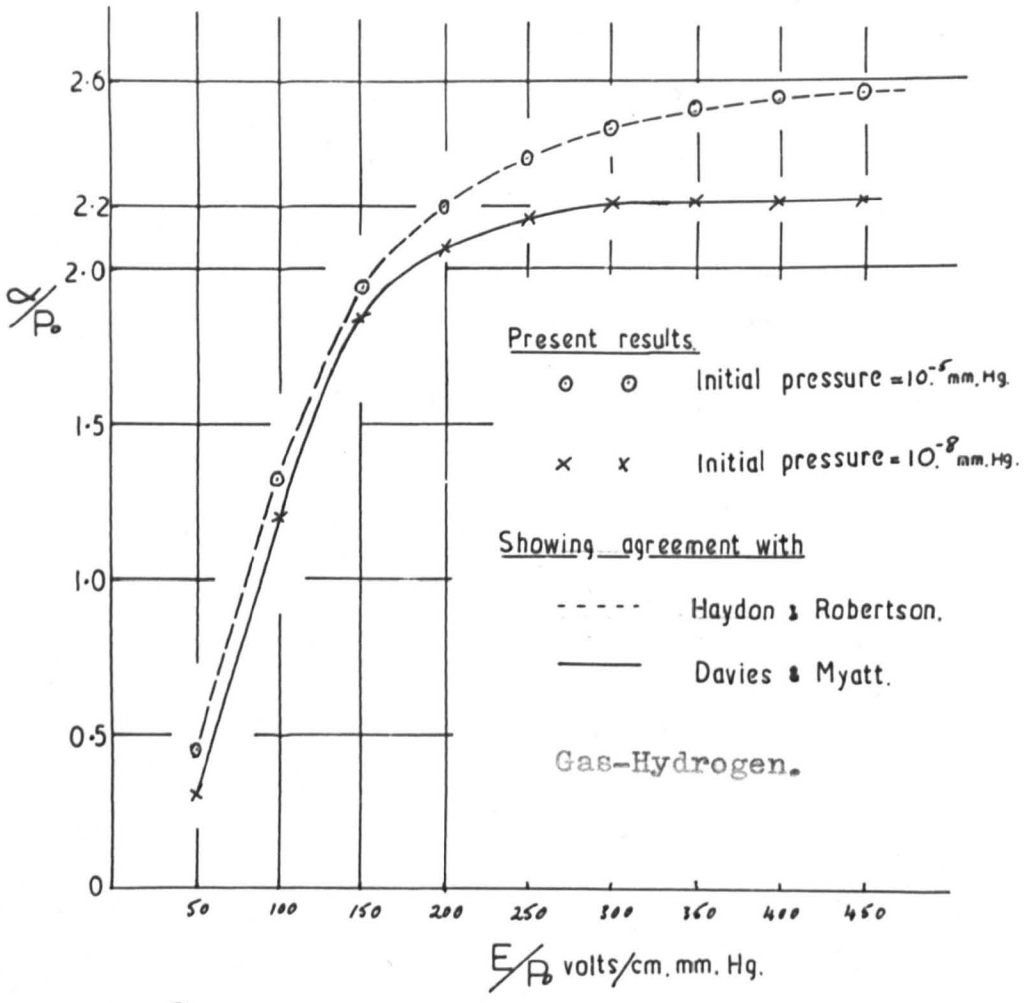

Present determinations of α/P_0 v. E/P_0.

Figure 53.

7.2. Preliminary Results in Hydrogen

The experiments carried out using the first two experimental tubes were essentially intended to determine the effect of using different analyses on the experimental data and not to determine absolute values of α/p_o. Because of this the residual gas pressure used with the first experimental tube was only of the order of 10^{-5} mms.Hg. and the hydrogen used was purified only by being passed through two hot palladium osmosis tubes. The values of the pre-breakdown current, I, as a function of inter-electrode gap distance, d, were observed, the increase in d between successive current measurements being fixed. The analyses used are given in the Appendices, the Davies and Milne analysis in Appendix 1 and the Haydon and Robertson analysis in Appendix 2. As may be seen from Appendix 2, this increase in d, Δd, is a necessary parameter of the Haydon-Robertson analysis and, although values of current at any given value of gap distance could be obtained from I.v.d. curves for which Δd had not been held constant, it was considered desirable to use the same experimental method as that of Haydon and Robertson, (92). In this way any discrepancy between the two sets of results could not be attributed to one set of results using experimental points and the other set using points from the smoothed I against d curves.

As may be seen from Figures 53 and 54, the values of α/p_o as a function of E/p_o from this determination agree well with all previous determinations at values of E/p_o below 100 volts/cm.mm.Hg. but at higher values of E/p_o the curve falls below all previous results

with the exception of that of Haydon and Robertson with which it agrees to within $\pm$ 3% over the full range of E/p_0 investigated and those of Jones and Llewellyn-Jones and of Myatt. The results obtained from the two analyses were observed to agree to within experimental error at all values of E/p_0. Hence it would appear that the use of these analyses gave consistent results.

The results of Myatt, (52, 53), fall appreciably lower than any other determination and, since Myatt's work was the only one to use ultra-high vacuum techniques, it seemed probable that the extra gas purity so obtained might be the cause of these low values of α/p_0. In order to check this hypothesis a new tube was constructed, Tube II. The system was evacuated to less than 10^{-8} mms.Hg. before any hydrogen was introduced into the tube and the hydrogen was purified by the formation of uranium hydride and its subsequent thermal decomposition. Once again both analyses were used on the experimental data and again no difference between the values of α/p_0 obtained from each analysis was observed. In this case, however, the α/p_0 against E/p_0 curve levelled off at a value of $\alpha/p_0 = 2.28 \pm 0.11$ as compared with $\alpha/p_0 = 2.56 \pm 0.12$ obtained from the first tube. Agreement was observed with Myatt's results over the full range of E/p investigated. This seemed to corroborate the hypothesis that the previously published results of α/p_0 in hydrogen are high because of impurities. The values of α/p_0 obtained are given in Appendix 6.

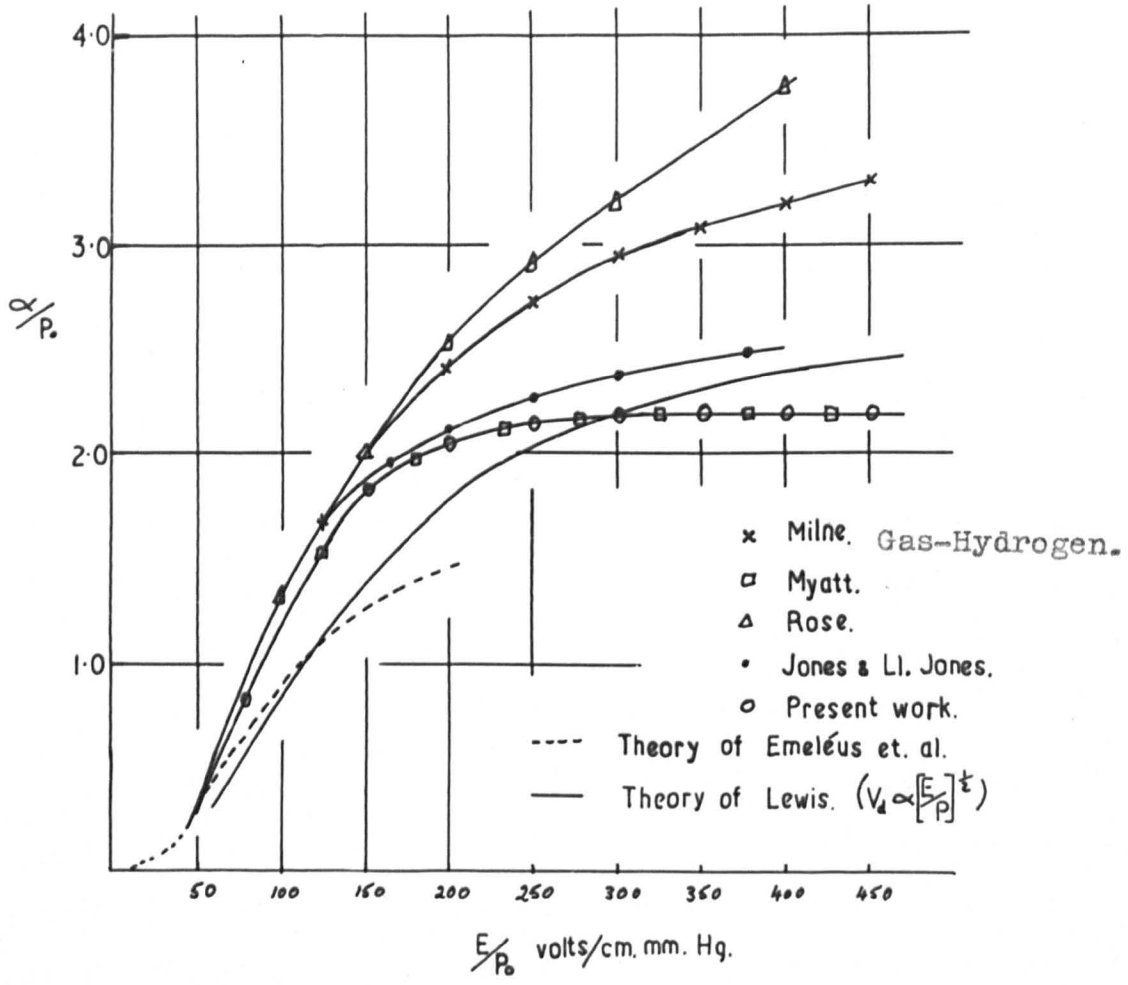

Comparison of present values of α/p_0. v. E/p_0:

with previous determinations.

Figure 54.

7.3. The First Ionization Coefficient in Hydrogen

The final values of α/p_o as a function of E/p_o obtained from the present determinations are given in Figure 54, and the numerical values in Appendix 6. Each point of the curve is the mean of twelve points, four from Tube II, four from Tube III and four from Tube IV. In these tubes residual gas pressures of less than 10^{-8} mms.Hg. were obtained, and uranium hydride purification of the hydrogen was used. The maximum scatter of these points was 3% which compared very favourably with the scatter of 8% observed when a residual gas pressure of 10^{-5} mms. Hg. was used with hydrogen purified only through hot palladium osmosis tubes. Tubes III and IV had electrodes of 3.8 cms. diameter compared with 2.2. cms. in tubes I and II. This enabled the maximum gap distance to be increased from 1.0 cms. to 1.8 cms. whilst maintaining a uniform field.

The ionization potential of hydrogen, 13.59 e.v. lies just below the ionization potential of the most likely contaminants, e.g. Nitrogen with an ionization potential of 15.60 e.v. and Oxygen, V_i = 13.9 e.v. Since at low values of E/p the mean electron energy is low, the probability of ionization of a hydrogen atom will be greater than the probability of ionization of an impurity atom with a higher ionization energy. At higher values of E/p, however, the mean electron energy increases and ionization of the impurity atoms will become more probable. Hence in hydrogen it should be expected that the effect of impurities should be noticed at high values of E/p. This is observed. At E/p_o < 100 volts/cm.mm.Hg., the present

results lie only 6% below the results of Jones and Llewellyn-Jones, whilst at E/p_o = 350 volts/cm.mm.Hg. they are 12% lower than Jones and Llewellyn-Jones and 35% lower than those of Davies and Milne, (51).

Agreement to an order of magnitude only is observed with the theoretical values of Emeleus, Lunt and Meek, (75), whereas agreement is noted with the theory of Lewis to within 5% from E/p_o = 50 volts/cm.mm.Hg. to E/p = 100 volts/cm.mm.Hg.. Above this value, however, Lewis' curve falls below the present experimental values and shows no indication of levelling off.

If the Townsend relation giving α/p as a function of E/p is considered, i.e.:

$$\alpha/p = A \exp. -\left[\frac{B}{(E/p)}\right]$$

then Lewis has shown that the shape of the α/p - E/p curve depends upon the manner in which A and B vary with E/p. Various shapes of curve have been computed for the cases in which A and B are independent of E/p over all ranges of E/p, A is independent of E/p but B becomes dependent of E/p above a certain value of E/p and for the case in which both A and B are dependent upon E/p. The present values of α/p_o as a function of E/p_o agree with the case in which A is constant but B varies with E/p above E/p_o = 150 volts/cm.mm.Hg.

If values of $\log_e \alpha/p_o$ are plotted against p_o/E, Figure 55, it may be seen that the curve is linear up to E/p_o = 150 volts/cm.mm.Hg. For this range of E/p, therefore, α/p_o may be written

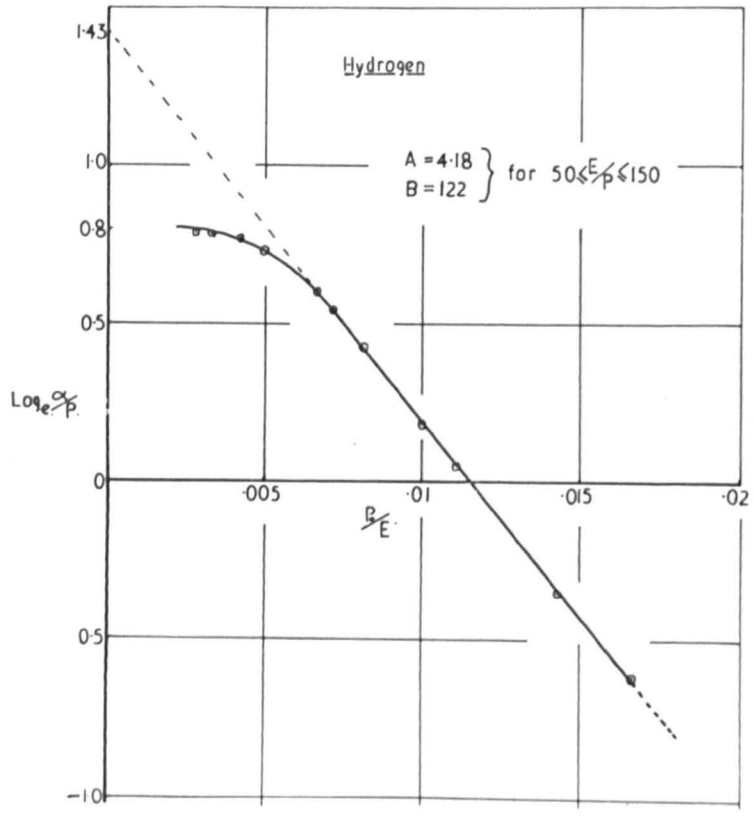

Figure 55. $\log_e \alpha/p$ as a Function of p/E.

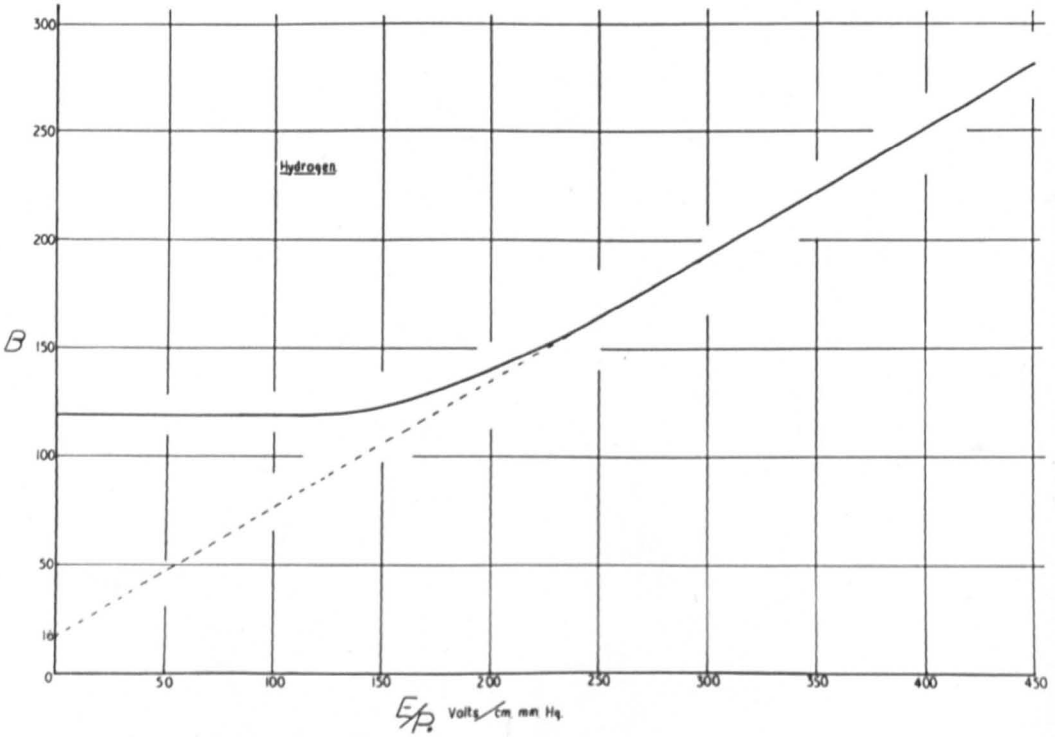

Figure 56. Townsend Factor, B as a Function of E/p.

$$\alpha/p_o = 4.18 \exp. -\frac{(122.5)}{E/p_o}$$

For the region of E/p_o over which α/p_o is only a very weak function of E/p_o, i.e. for $E/p_o > 200$ volts/cm.mm.Hg., B should approach a linear function of E/p_o. From a graph of B against E/p_o, Figure 56, this effect is clearly seen. In this range

$$B = 16 + 0.6(E/p_o)$$

therefore

$$\alpha/p_o = 4.18 \exp. -\frac{[16 + 0.6(E/p_o)]}{E/p_o}$$

so indicating the very weak dependency of α/p_o on E/p_o.

As stated above the finally accepted values of α/p_o were the mean of twelve values obtained from three different experimental tubes. For any one value of E/p_o several different pressures were used. No variation of α/p_o with pressure was observed so that the deviation from Paschen's law, which will be described later, could not have been caused by an α/p_o - pressure dependency. This result confirms the conclusions of Myatt, (53), who also noted the Paschen's law deviation.

7.4. The Generalised Secondary Coefficient in Hydrogen

Values of the generalised secondary coefficient, ω/α, in hydrogen were obtained from the current growth curves, taken prior to any breakdown being allowed, using the analysis given in Appendix I. The present values of α/p_o were used with this analysis. The ω/α - E/p_o variation so obtained indicated that ω/α is a monotonic

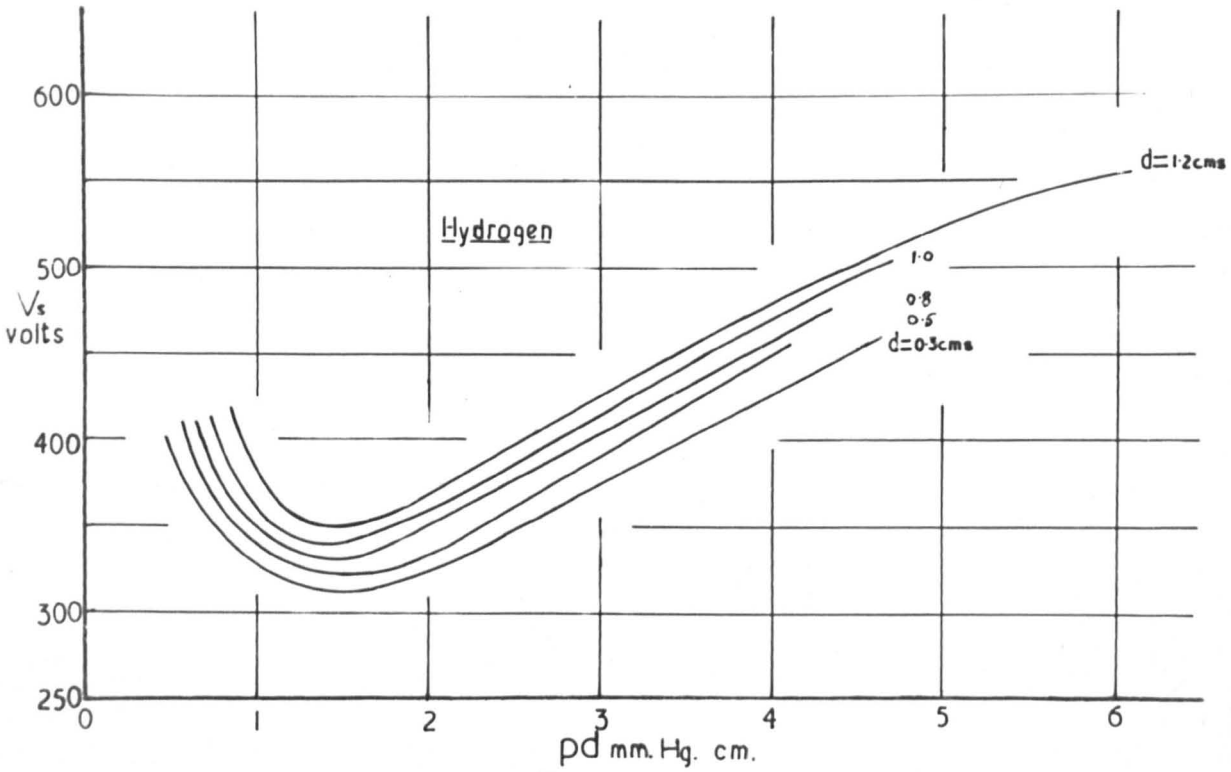

Family of Paschen curves obtained at various gap distances.

Figure 57.

function of E/p throughout the range of E/p_0 investigated, no peaks being evident as had been reported by Hale, (36, 37, 38). Because of the smooth curve obtained it was impossible to estimate the contribution to ω/α of the various individual secondary mechanisms. Since the metastable state of hydrogen is very weak and is easily destroyed in even a weak electric field, it is reasonable to assume that secondary electron liberation due to incident metastable atoms on the cathode plays no significant part in the discharge. This then leaves photon bombardment and positive ion bombardment of the cathode and since no peaks were observed the effect of these cannot be seperated by this approach.

When all pre-breakdown measurements had been taken, breakdown potentials were measured as a function of the product of the pressure and gap distance, pd. From this data Paschen curves of V_s against pd were plotted. Since Paschen's law states that the breakdown potential is a function of pd only, i.e. the number of molecules between the plates, and not of p or d seperately, values of the breakdown potential at different gap distances should coincide so long as the pressure is adjusted to keep pd constant. This was found not to be so in hydrogen. A family of Paschen curves was obtained, each at a constant gap distance, varying p so as to vary pd, Figure 57. The breakdown potential was found to increase with increasing d at constant pd. Since the values of V_s were reproducible to within 1 volt, it may be seen that the discrepancy is outside experimental error. These Paschen curves were obtained for values of

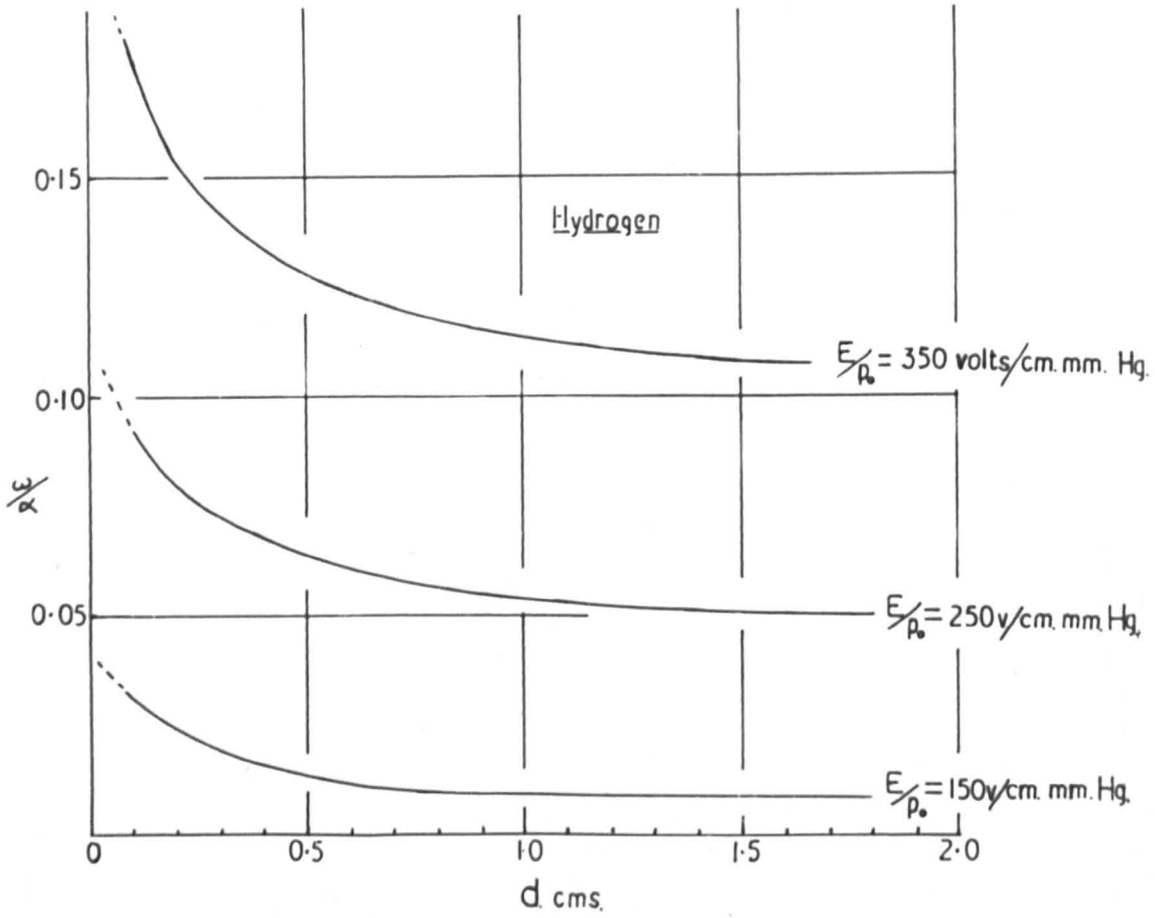

Variation of η/α with electrode separation, d.

Figure 58.

d ranging from 0.3 cms. to 1.8 cms. and the corresponding values of ω/α as a function of E/p were calculated from each by the Townsend expression

$$\omega/\alpha = \frac{1}{e^{\alpha d}-1}$$

From the resulting ω/α against E/p_o curves each at constant d the variation of ω/α with d could be obtained at constant E/p_o. These results are given in Figure 58, from which it may be seen that at low values of d, ω/α increases rapidly.

The cause of the dependence of ω/α on d in this region was originally explained as being due to the ommision of the distance an electron must travel in the electric field before it is in equilibrium with the field, d_o, from the above Townsend expression for ω/α. Since d_o cannot be calculated to within $\pm$ 50% from the preabreakdown data, an attempt was made to estimate the effect of including an arbitrary value of d_o in the ω/α calculation. d_o was assumed to be of the order of the electron mean free path in the gas at that pressure and, using this as d_o, the values of ω/α were re-calculated. It was found that inclusion of this value for d_o in the calculation did not reduce the values of ω/α at low values of d but served to further increase the upcurving. Hence it would appear that the observed effect is a real one.

A second explanation is that the effect may be geometric, in that as d increases the solid angle subtended by the cathode at the anode decreases and, therefore, since the majority of the photons

produced in the discharge are produced very close to the anode, the number of photons striking the cathode will decrease as d increases. However, this solid angle will only decrease by a factor of 2 or 3 in this range and the observed decrease in ω/α in hydrogen is a factor of ten and in mercury the decrease is a factor of one hundred, (54). The explanation which will account for this variation is that the photons are being absorbed in the gas as they cross the gap. This is supported by the variation of ω/α with pressure reported by Jones and Llewellyn-Jones, (47), and by the measurements of absorption coefficients at Liverpool reported by Meek at the VI International Conference on Ionization Phenomena in Gases at Paris, 1963. This explanation will also account for the variation of the minimum sparking potential, V_{sm}, with gap distance, d.

The existence of this deviation from Paschen's law indicates that photon bombardment of the cathode must play a considerable part towards secondary ionization in hydrogen over the whole range of E/p. The complete separation of this effect from the effect of positive ions, however, can only be done by temporal growth studies which are being carried out currently in these laboratories.

7.5. Note on the Purification of the Rare Gases

As has been indicated in Chapter IV, α/p is very sensitive to impurity. To obtain helium in as high a state of purity as possible, it was originally planned to use liquid helium and to allow it to evaporate into the experimental system via a capillary leak. The expense of this project, however, made such a system impossible and

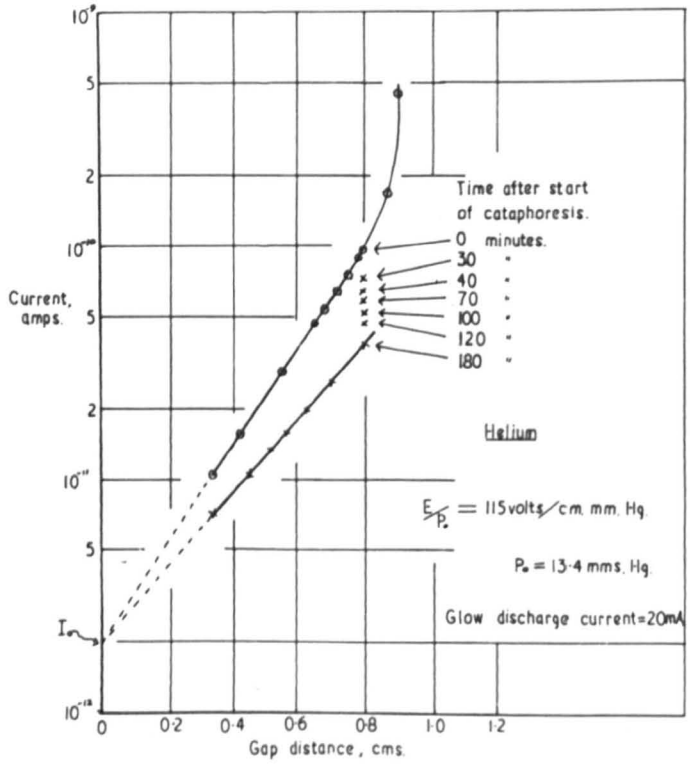

Figure 59. Effect of Purification on Current Growth Curves.

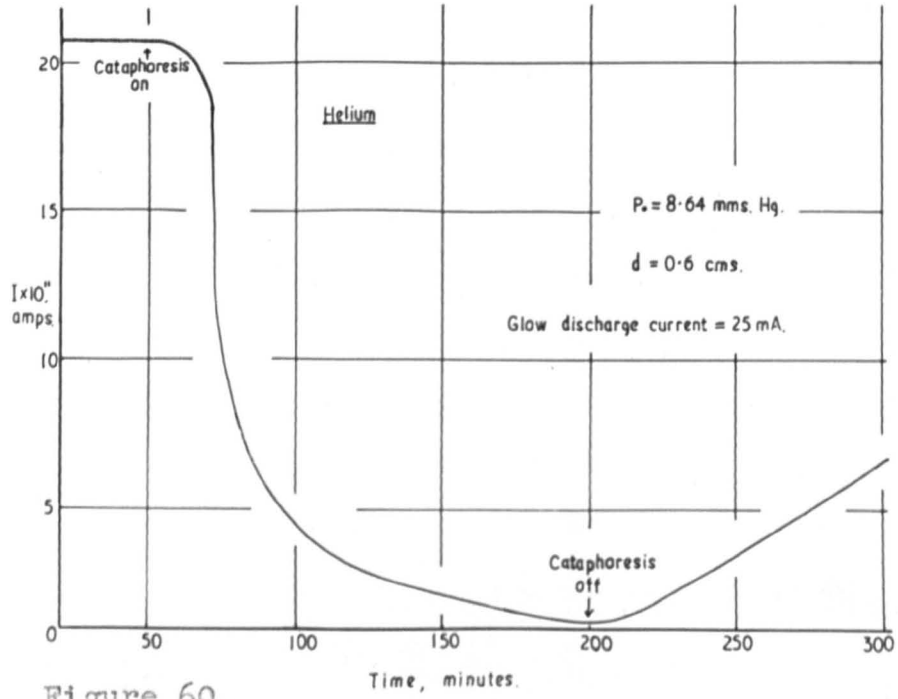

Figure 60. Variation of Current with Gas Purity.

cataphoretic cleaning of the rare gases was decided upon. This method, which has been previously discussed, has the advantage that it may be used for all the rare gases whilst the liquid helium method was restricted to helium. An attempt was made to estimate the purity of the helium used by spectroscopic analysis of the gas in the cataphoresis tube using a spectrometer to measure the relative intensity of the 5047Å line of helium and the 6402Å line of neon. It was hoped that the results would show a predominance of neon at the cathode and that some estimate could be made of the relative concentrations of each at various points in the glow discharge tube. Unfortunately no conclusive data was obtained from this arrangement.

Since α/p tends to decrease with increasing gas purity and α/p is given, to a first approximation, by the linear section of the current flow against gap distance curves, the value of the current at a fixed value of d and E/p should also decrease with increasing gas purity. This is illustrated in Figure 59. To obtain this curve the current was measured at various values of d until upcurving of the $\log_e$I.v.d. curve was noticed. The gap distance was then set at a value of d corresponding to the upper end of the linear section of this curve and the cataphoretic clean-up was started. The decrease of the current was noted until it showed no further change. The gap distance was then reduced and the new $\log_e$I.v.d. curve was followed to as low a value of d as possible. In this way the possibility of a variation of I_o over this period was eliminated. Several experiments were then performed keeping E/p_o and d constant and observing

the variation of I with time when the cataphoresis was started and then stopped, Figure 60. It was anticipated that the heating of the gas in the closed system by the glow discharge probably affected this curve but that the observed variation was far too great to be be due to this factor alone. Since the rise in temperature of the gas in the glow discharge was only in the order of 100°C this, with a ratio of glow discharge tube volume to experimental system volume of 5:1, would give an increase in pressure of 6% and hence a decrease in E/p of 6%. In this range of E/p this reduction corresponded to a reduction of 6% in α/p which would cause the current flow to be lowered by 26%. It may be seen from Figures 59 and 60 that the observed reduction is a factor of 10 in one case, and a factor of 6 in the other. Such a reduction is compatible with a reduction of 17% in α/p, at least 11% of which can be attributed to increased gas purity.

It must be stressed that the experiments described above can only be an approximate estimate of the purifying action of cataphoresis and that spectroscopic analysis of the glow discharge should be attempted using monochromators to determine more accurately the reduction in the neon content of the helium or the helium content of the neon at the anode of the cataphoresis tube.

7.6. The First Ionization Coefficient in Helium

The first ionization coefficient was determined in helium at three stages of gas purity from experimental tubes V and VI. Residual gas pressures of 10^{-10} mms.Hg. were achieved for

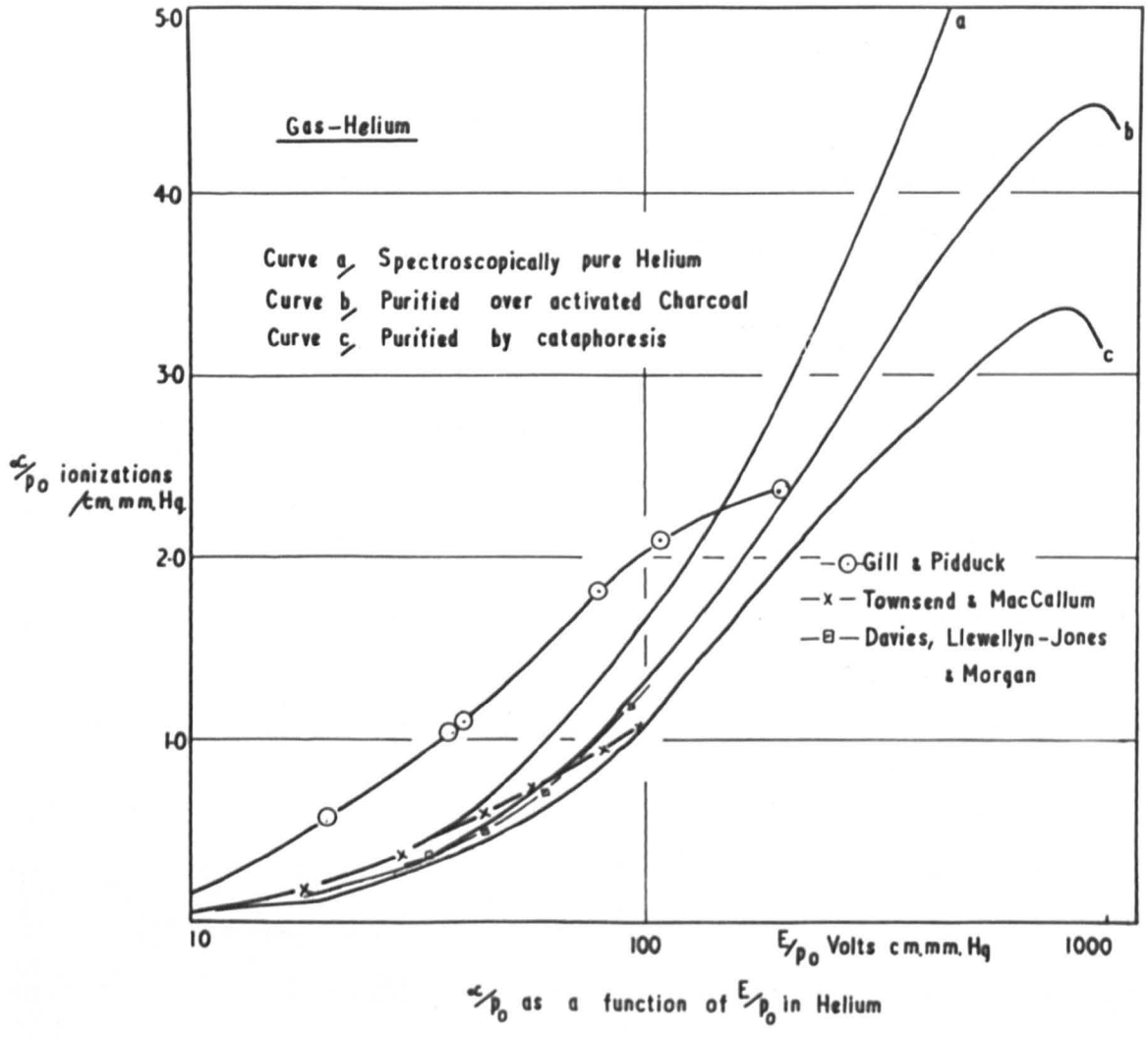
5·0
4·0
3·0
2·0
1·0
Gas – Helium
Curve a. Spectroscopically pure Helium
Curve b. Purified over activated Charcoal
Curve c. Purified by cataphoresis
a
b
c
α/p0 ionizations /cm. mm. Hg
Gill & Pidduck
Townsend & MacCallum
Davies, Llewellyn-Jones & Morgan
10
100
E/p0 Volts cm. mm. Hg
1000
α/p0 as a function of E/p0 in Helium

Figure 61.

these experiments. Commercial spectroscopically pure gas was first used which was later purified, firstly by standing over activated charcoal at liquid nitrogen temperatures and measurements taken at this purity and secondly by cataphoresis. The results obtained under each of these conditions are given in Figure 61 and Appendix 7. It may be seen that the present values of α/p_0 in cataphoretically clean helium, curve c, lie below all previously published experimental results, whilst the present determinations in helium purified over activated charcoal at -190°C, curve b, agree well with the recent results of Davies, Llewellyn-Jones and Morgan, (62). The results of Chanin, who also used cataphoresis purification, given at the International Conference on Ionization Phenomena in Gases at Paris, agree to within experimental error, with the present results given in curve c.

It was suggested at this conference that the increase of the discrepancy between the present results and those of Davies, Llewellyn-Jones and Morgan was of an unexpected nature since the present results fall increasingly lower as E/p increases. In helium, with an ionization potential above that of all possible contaminants, the largest discrepancy should be apparent at low values of E/p. However, it is not to be expected that the absolute discrepancy will increase with decreasing E/p but that the percentage discrepancy will. Calculation of the percentage discrepancy in the range of E/p over which the two determinations overlap confirms this, being 14.2% at $E/p_0 = 30$, 13.7% at $E/p_0 = 50$ and 7.6% at $E/p_0 = 100$.

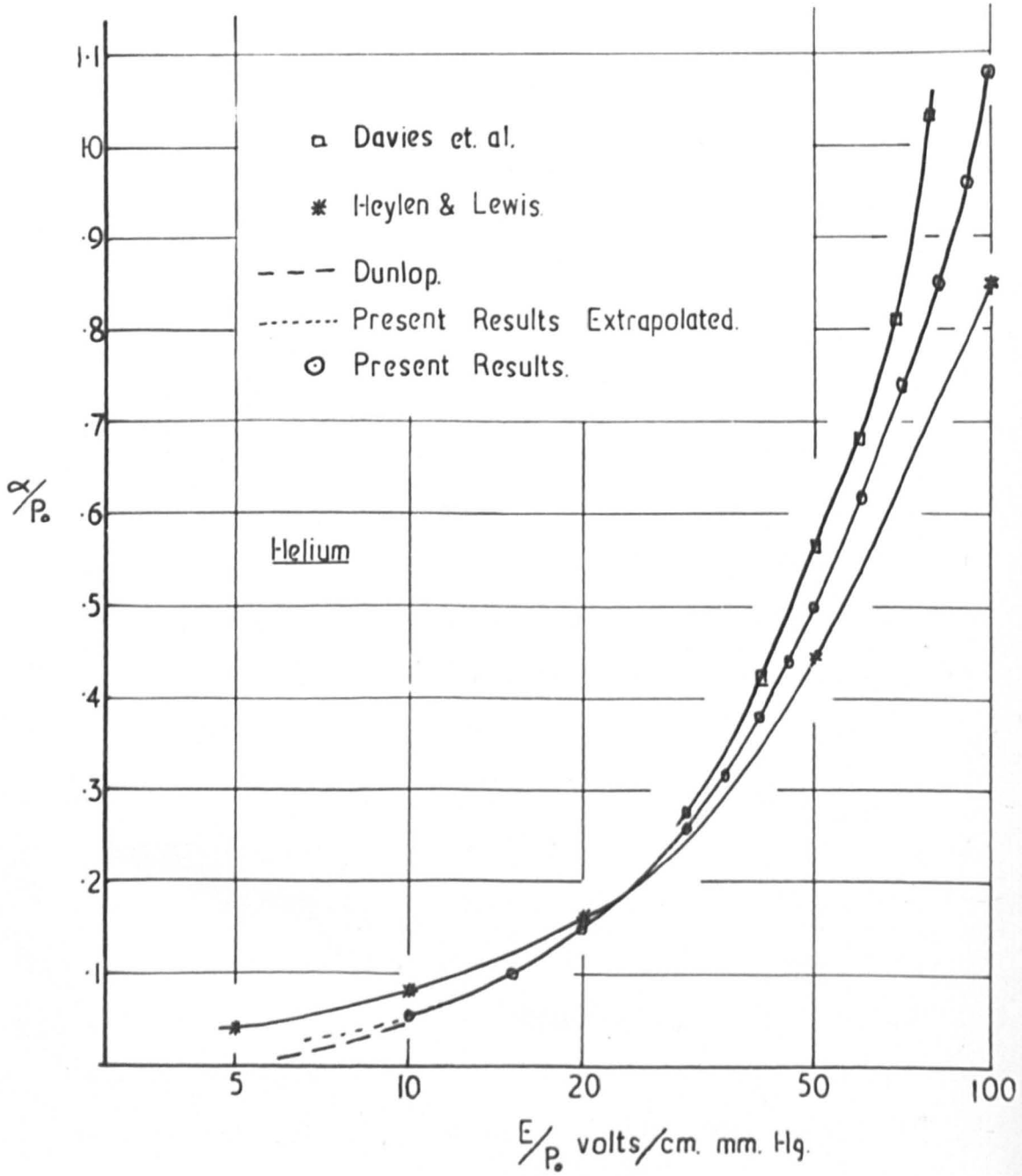

Figure 62.

α/p as a Function of E/p in Helium.

This trend is even more apparent when the results of Townsend and MaCallum and of Gill and Pidduck are compared with the present results.

Since it was probable that the present gas samples were the purest used to date for determinations of α/p, it was hoped that some measure of agreement could be reached with theoretical predictions. As may be seen from Figure 62, even with the most comprehensive theory yet published, that of Heylen and Lewis, (72), there is still a 20% discrepancy at $E/p_o = 100$ volts/cm.mm.Hg. although agreement is good for $E/p_o < 30$ volts/cm.mm.Hg.. Only at $E/p_o = 10$ volts/cm.mm.Hg. do the present results overlap the calculations of Dunlop, (77), and at this point the present values fall 16% higher.

The shape of the $\alpha/p_o - E/p_o$ curve in helium is unusual in that it has a maximum at $E/p_o = 850$ volts/cm.mm.Hg.. This may be due to one of two effects. Firstly, at these high values of E/p, double ionization of the helium atom may occur giving He^{++} ions in the gas. Since the analysis evolved to give α/p from the experimental data only allows for singly charged ions the value of α/p obtained from the linear section of the current growth curve will be overcorrected and hence the value of α/p obtained will be lower than the actual value. This hypothesis is supported by the extrapolation of published curves of mean electron energy as a function of E/p in helium, (94), which suggest that the second ionization potential, 54.6 e.v., corresponds to $E/p \approx 800$ volts/cm.mm.Hg.

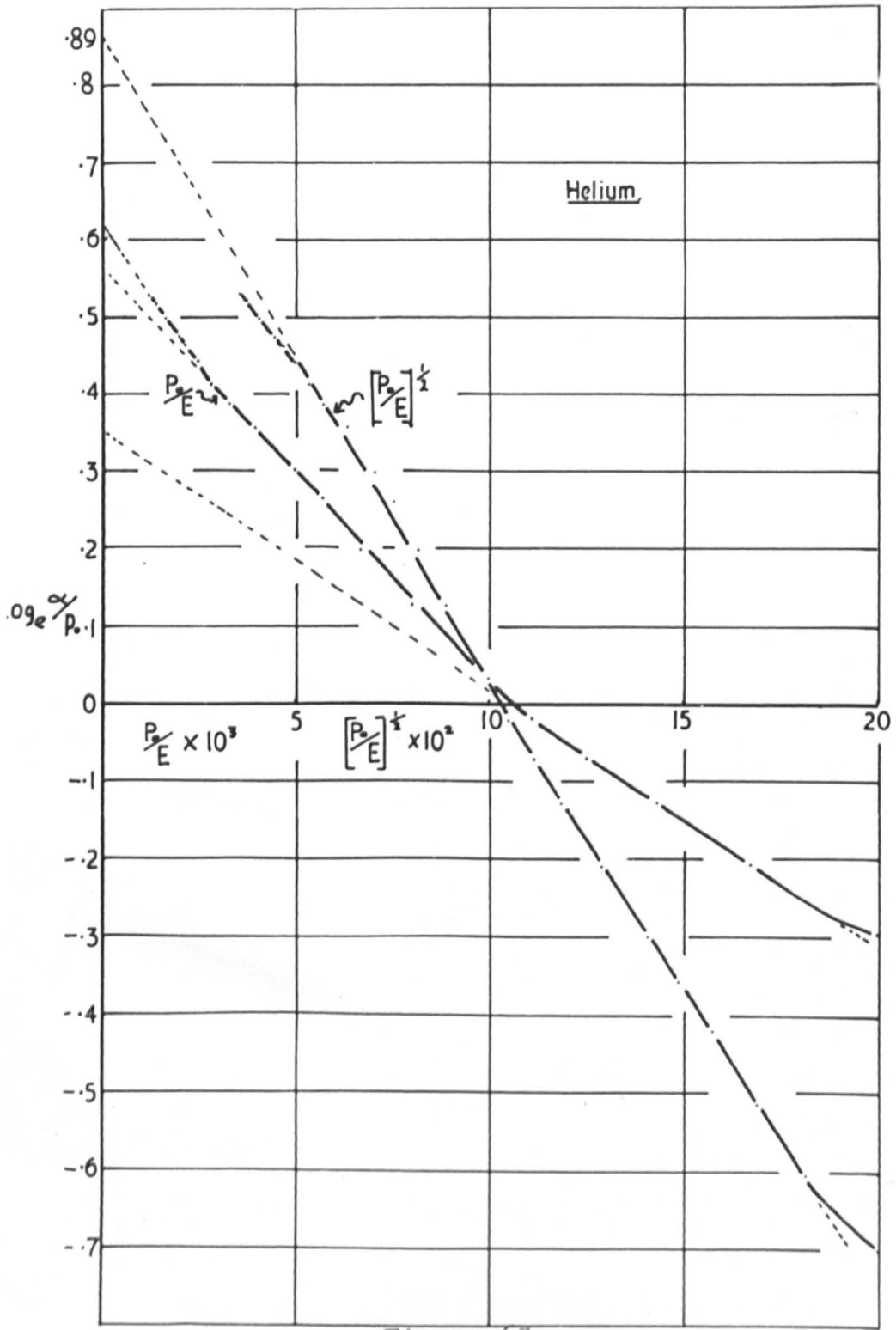

Figure 63.

$\text{Log}_e \alpha/p$. v. (p/E) and $\text{Log}_e \alpha/p$. v. $(p/E)^{\frac{1}{2}}$

Extrapolation of the mean electron energy - E/p curves obtained from the present work, (Section 7.7., Figure 66), also supports this. This reason would also explain why α/p from the linear section of the current growth curves shows no decrease although this may be explained by the effect on the current growth of the increase in ω/α being greater than the decrease in α/p in this range of E/p. The explanation which is perhaps most obvious is that at this value of E/p the probability of ionization decreases. However, when the probability of ionization as a function of incident electron energy is considered it is found that the maximum of this curve is at E/p_o of about 3600 volts/cm.mm.Hg., (96). Therefore, it would appear that the decrease in α/p with increasing E/p at $E/p_o > 850$ volts/cm. mm.Hg., is a property of the analysis and is not a real effect. It does, however, indicate the onset of double ionization in the gas.

Using the present values of α/p_o, a curve of $\log_e \alpha/p_o$ against p_o/E was plotted, Figure 63, in order to check the validity of the Townsend expression

$$\alpha/p = A \exp. -\left[\frac{B}{(E/p)}\right]$$

From the results three distinct sections were apparent within each of which the above expression is obeyed. The values of A, B and the apparent ionization potential V_i' given by B/A, are tabulated below.

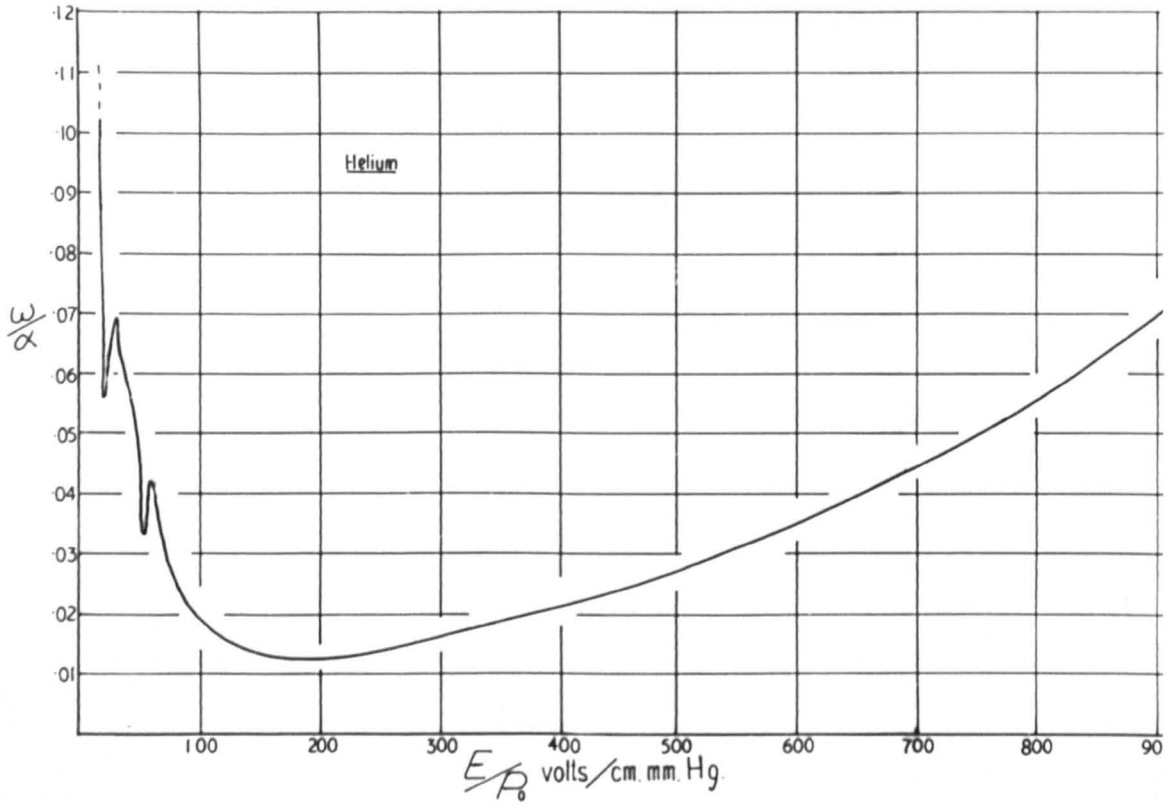

Figure 64.

Secondary Ionization Coefficients in Helium.

Range of E/p	A	B	V_i'
60 - 105	2.24	57.5	25.5
105 - 350	3.6	86	27.6
350 - 800	4.17	168	40

From this table it may be seen that for the first two ranges the Townsend equation gives values of V_i' close to the actual ionization potential of 24.4 e.v.. Above E/p_o = 350 volts/cm.mm.Hg., however, the theory is no longer valid.

The variation of $\log_e \alpha/p_o$ with $(p/E)^{\frac{1}{2}}$ gives a more widely applicable expression. This curve is also shown in Figure 63. A linear relationship is seen to hold for values of E/p_o from 30 - 350 volts/cm.mm.Hg. for which the constants are given by C = 6.5, D = 10.7. Therefore, in helium the Townsend empirical equation may be written

$$\alpha/p_o = 6.5 \exp. -\left[\frac{10.7}{(E/p)^{\frac{1}{2}}}\right] \text{ for } 30 < E/p_o < 350 \text{ volts/cm.mm.Hg.}$$

If the electron energy distribution in a gas is Maxwellian then α/p should be a function of p/E whereas for a Druyvesteyn distribution α/p is a function of $(p/E)^{\frac{1}{2}}$. It is, therefore, indicated that the electron energy distribution in helium is approximately Druyvesteyn and lies between a Druyvesteyn and a Maxwell distribution. This conclusion supports the theoretical results of Heylen and Lewis, (72).

7.7. The Secondary Ionization Coefficient in Helium

Values of the secondary ionization coefficient, ω/α, were calculated from the pre-breakdown current growth measurements and

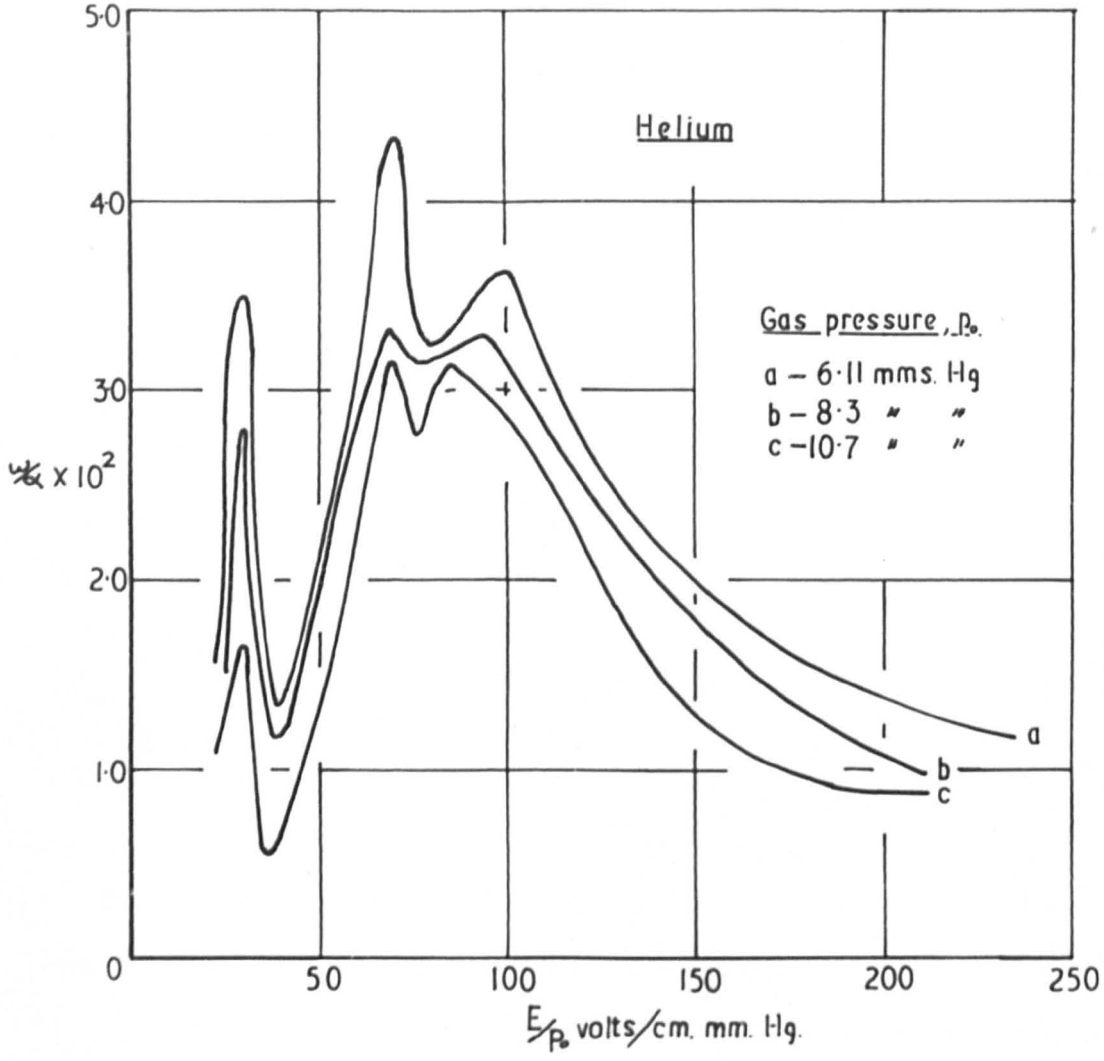

Figure 65.

w/α v. E/p for Helium showing peaks.

these are given in Figures 64 and 65. Peaks were noted in this curve at E/p_o = 35, 55 and 105 volts/cm.mm.Hg.. De Groot and Penning, (93), have observed that there are four possible excitation states of helium which the atom may be raised to by electron collision and from which the atom may either decay to the ground state with the emission of an ultra-violet quanta, or which are metastable and can cause secondary electron emission at the cathode. These are the 2^3S state at 19.75 e.v., the 2^1S state at 20.6 e.v., the 2^1P state at 21.2 e.v. and the 3^1P state at 22.9 e.v.. At the value of E/p at which the maximum of a peak is observed it is reasonable to conclude that the mean electron energy is equivalent to that value of E/p. The peak at E/p_o = 35 volts/cm.mm.Hg. was then attributed to the 19.75 e.v. excitation state, the E/p_o = 55 volts/cm.mm.Hg. peak to the 20.6 e.v. or the 21.2 e.v. state the the E/p_o = 105 volts/cm.mm.Hg. peak to the 22.9 e.v. state. This led to some uncertainty as to the state causing the peak at E/p_o = 55 volts/cm.mm.Hg.. When breakdown potential measurements were made and the secondary coefficient calculated from these, however, this broad peak was found to be two peaks, one at E/p_o = 50 volts/cm.mm.Hg. and one at E/p_o = 60 volts/cm. mm.Hg., Figure 65. When the mean electron energy is equal to the ionization potential excitation of the helium atoms will be a minimum and hence the photo-electric contribution to the generalised secondary coefficient will be a minimum. The ionization potential, 24.6 e.v., would then be expected to correspond with the minimum of the ω/α - E/p curve since at these values of E/p the positive

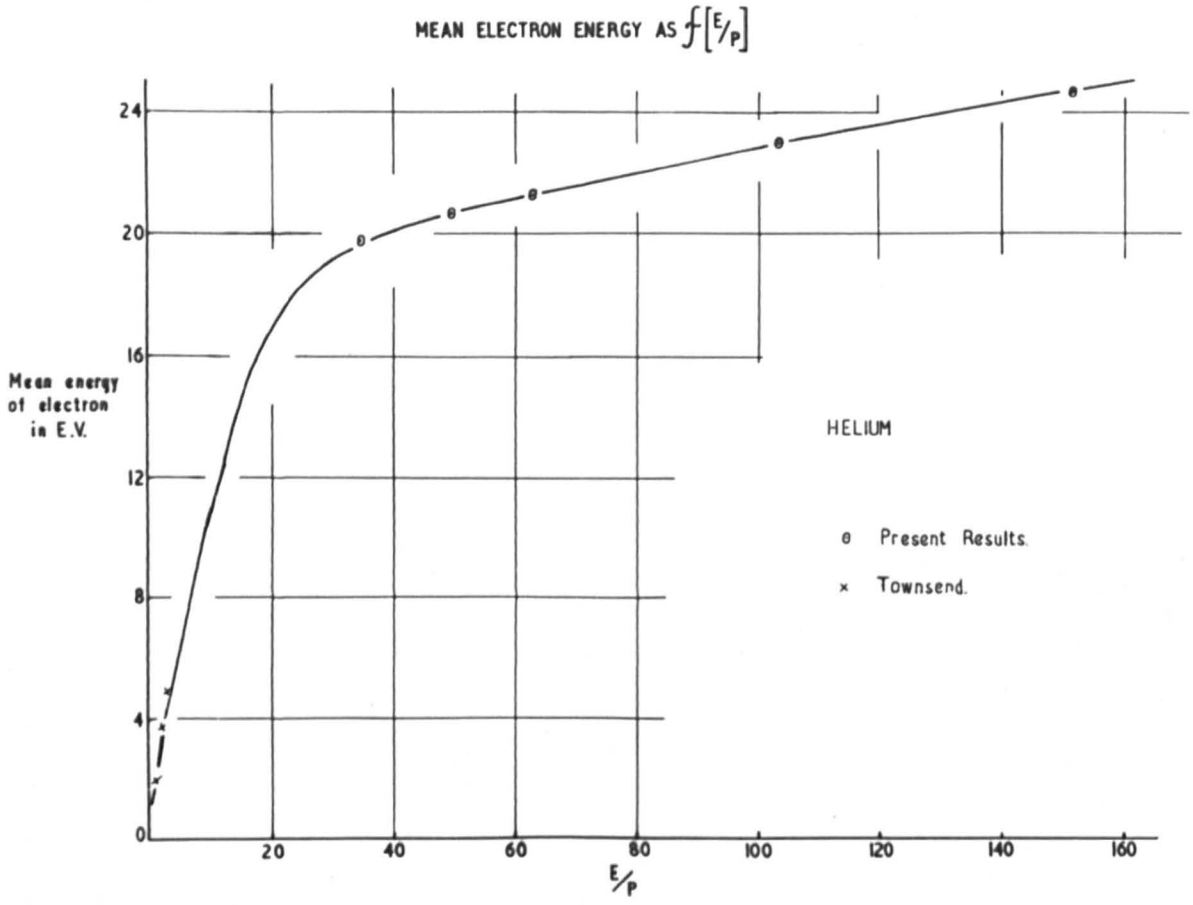
MEAN ELECTRON ENERGY AS $f\left[\frac{E}{P}\right]$
Mean energy of electron in E.V.
0
4
8
12
16
20
24
20
40
60
80
100
120
140
160
E/P
HELIUM
θ Present Results.
× Townsend.

Figure 66.

ion contribution is approximately constant.

The final conclusions can then be tabulated

E/p	e.v.
35	19.75
50	20.6
60	21.2
105	22.9
155	24.6

From these points a graph of mean electron energy, , as a function of E/p may be drawn, Figure 66. This curve has been extrapolated to low values of E/p to include the results of Townsend and Bailey, (95). It may be seen that in the range of E/p above 50 volts/cm.mm.Hg., $\bar{\varepsilon}$ is approximately a linear function E/p, a result previously arrived at by Reder and Brown, (90).

No good comparison can be made between the present values of ω/α and those of previous determinations since the value of the secondary coefficient is so critical to surface conditions. However, peaks were found by Davies, Llewellyn-Jones and Morgan, (62), at the same values of E/p as observed in the present work, so supporting the belief that in helium these are real effects. To further investigate the secondary mechanisms in helium temporal growth of ionization measurements will have to be taken and this work is at present being carried out in these laboratories.

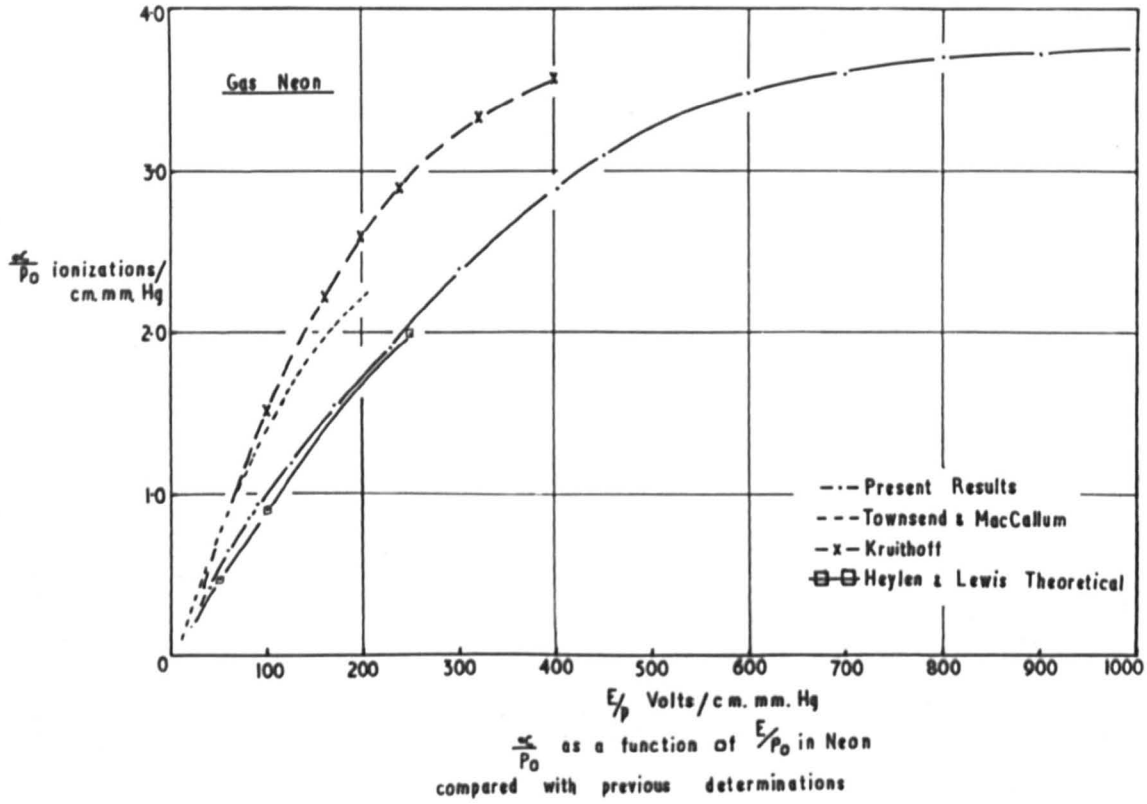

α/P0 as a function of E/P0 in Neon
compared with previous determinations

Figure 67.

7.8. The First Ionization Coefficient in Neon

Unlike the case of hydrogen and helium the values of α/p as a function of E/p in neon were all obtained from one experimental tube. A residual gas pressure of 10^{-10} mms.Hg. was obtained before any gas was admitted. The gas was purified initially over activated charcoal at liquid nitrogen temperatures and was then subjected to cataphoretic clean-up in a 25mA glow discharge for about a week before any measurements were taken. Pre-breakdown currents were measured as a function of inter-electrode separation for each value of E/p. To enable values of α/p_o to be determined from E/p_o = 30 volts/cm.mm.Hg. to E/p_o = 1000 volts/cm.mm.Hg. a pressure range of 8 mms.Hg. to 0.7 mms.Hg. was used. This experimental data was then analysed by the Davies and Milne analysis given in Appendix I.

The results obtained are summarised in Figure 67 and all the numerical values are given in Appendix 8. Once more the present results fall below previous determinations because of the higher gas purity, due to improved vacuum techniques and better purification processes. A notable feature of this determination in neon is the very good agreement with the theoretical values of Heylen and Lewis, (72), having a maximum discrepancy of 6% at E/p_o = 30 volts/cm.mm.Hg.. It has been shown by Heylen and Lewis and by Salmon, (97), that the electron energy distribution in neon is almost Maxwellian, as it is in hydrogen, and this is reflected in the similarity of the shape of the α/p - E/p curves in the two gases.

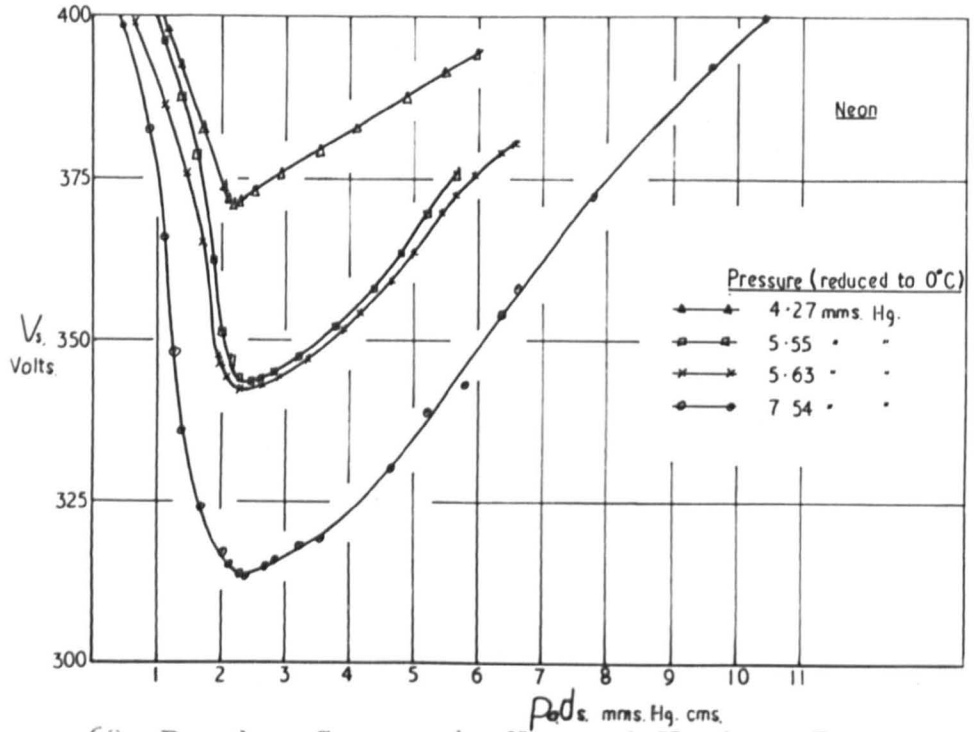

Figure 68. Paschen Curves in Neon at Various Pressures

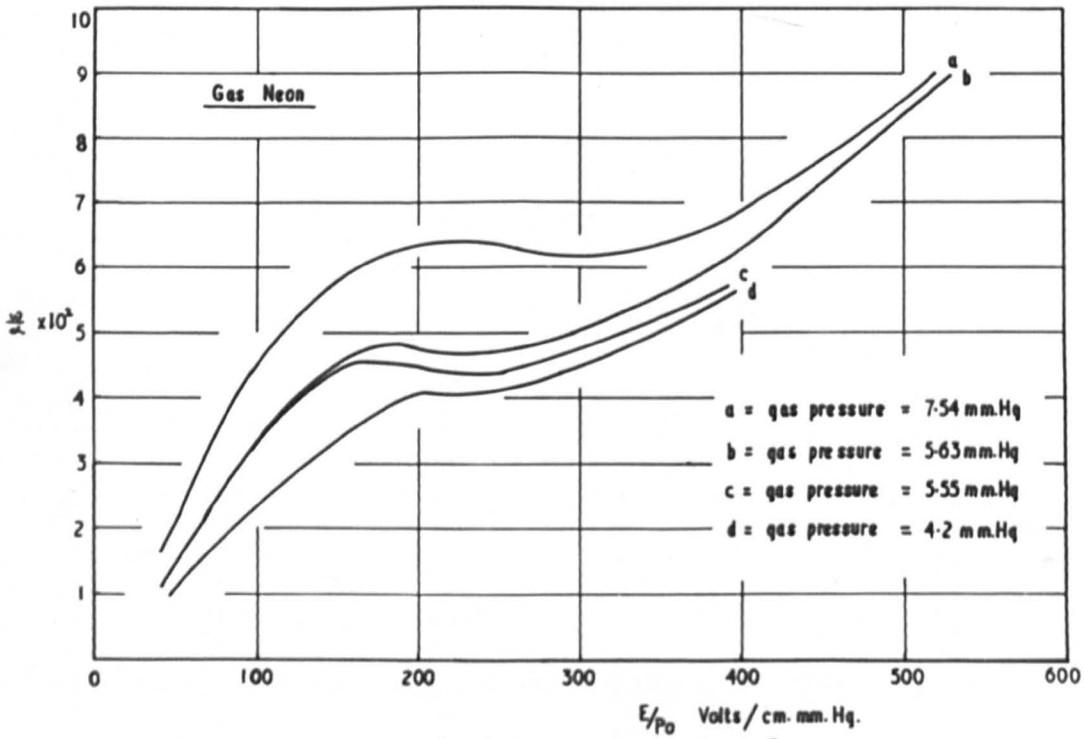

Fig 69. [$\frac{\alpha}{P}$ as a function of E/P_0 in Neon]

The curve shows no maximum as does the helium curve, probably due to the mean electron energy at a given E/p in neon being lower than that in helium and subsequently the second ionization potential is not reached below $E/p_o = 1000$ volts/cm.mm.Hg..

At $E/p_o > 800$ volts/cm.mm.Hg., α/p_o becomes only a weak function of E/p_o, tending to a saturation value of 3.8 ionizations/cm.mm.Hg.. A graph of $\log_e \alpha/p_o$ against p_o/E gives the values of the constants A and B in the Townsend relationship

$A = 2.2 \quad B = 78 \quad$ for $65 < E/p_o < 160$

$A = 4.8 \quad B = 204 \quad$ for $160 < E/p_o < 800$

Above $E/p_o = 800$ volts/cm.mm.Hg., B becomes dependent on E/p_o but since only a few values of α/p_o have been determined above this value of E/p_o, the variation of B with E/p_o could not be investigated.

7.9. The Second Ionization Coefficient in Neon

Breakdown potentials as a function of the product $p_o d_s$ were measured in neon by keeping the pressure constant and varying d. This was done for several values of pressure and a series of Paschen curves was then obtained, Figure 68. It was observed that the curves fell higher up on the V_s axis the lower the pressure. Errors in either p or d may have affected the placement of the curve along the pd axis but since the breakdown potential was measurable to an accuracy of 0.5% and was reproducible to $\pm$ 0.5 volts, the observed variation in the minimum sparking potential, V_{sm}, is well outside experimental error. Since the electron mean free path increases as the pressure decreases, the electrons will undergo fewer collisions in the gas at lower pressures. Because of this less excitation will occur and fewer

positive ions will be formed and hence a higher potential will be required for breakdown at lower pressure than at higher. This effect has also been noticed by Myatt in hydrogen, (53), and by Smith and Overton in mercury vapour, (54, 94).

Hence it would appear that deviations from Paschen's law are evident for two reasons, the above mean free path variation and the absorption effect described in section 7.4.

The values of ω/α obtained from these breakdown potential measurements reflect the reduction in secondary electron liberation as pressure decreases, Figure 69. A peak is observed at E/p_o = 180 volts/cm.mm.Hg. due to the excitation states at 16.6 e.v. Values of ω/α obtained from current growth measurements also exhibit this peak.

Comparison of the positive ion contribution to ω/α as a function of E/p in hydrogen, helium and neon, show that for a given value of E/p, ω/α increases as the ionization potential increases. This is to be expected since the energy required to extract an electron from a metal surface is taken predominantly from the potential energy of the incident ion and hence the higher the potential energy of the ion the deeper from within the metal energy band can the electron be extracted.

7.10. Comparison of First Ionization Coefficient in Hydrogen, Helium and Neon

Previously in this thesis, the first ionization coefficient has been considered as α/p, the number of ion pairs produced by an

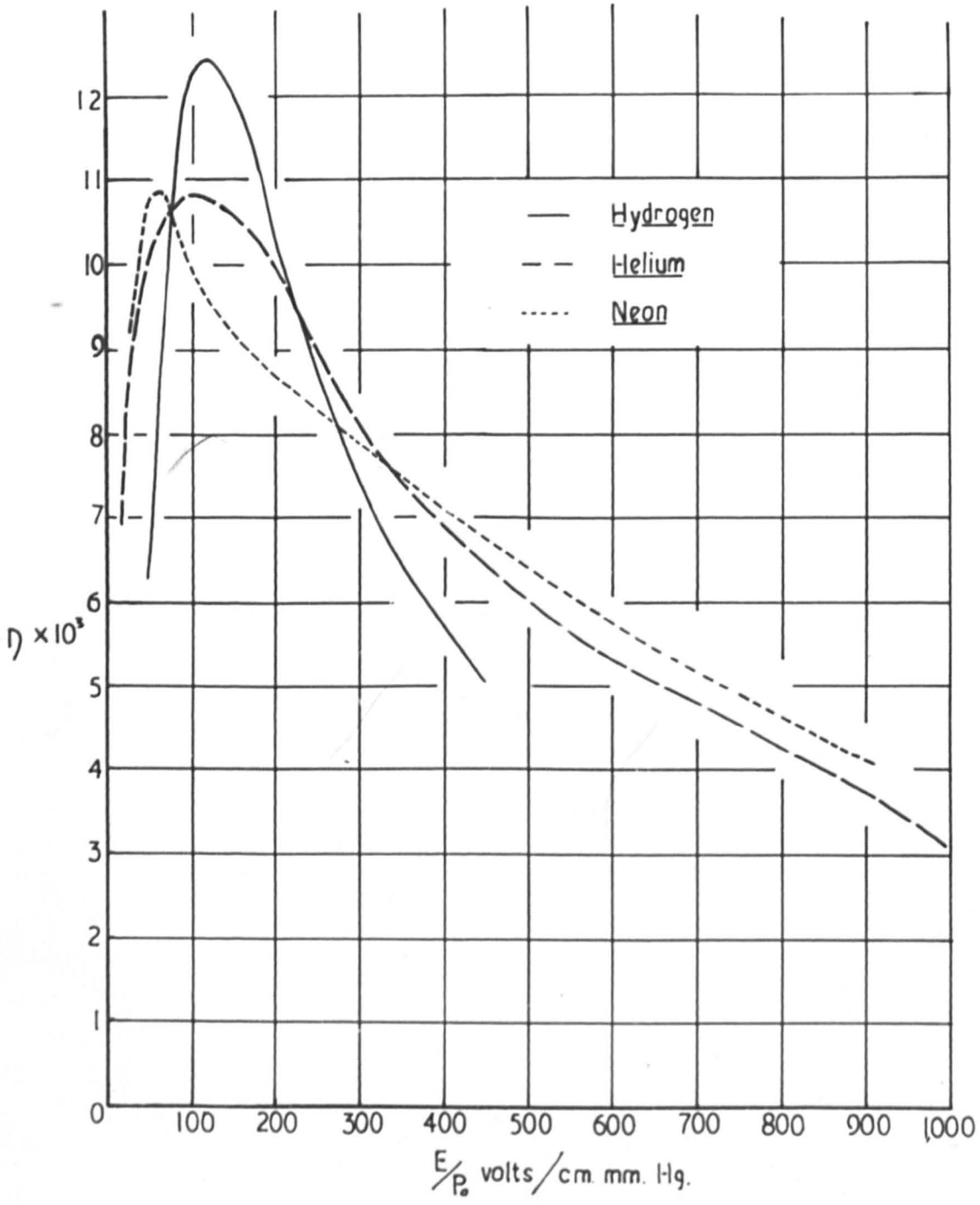

Figure 70.

η as a Function of E/p for Hydrogen, Helium and Neon.

electron moving 1 cm. in the direction of the electric field divided by the pressure. The first coefficient may also be defined as the number of new electrons formed by an electron falling through unit potential different whilst moving in the field, η. In this case $\eta = \alpha/E$ which is the gradient of the $\alpha/p - E/p$ curve. η is a measure of the efficiency of ionization and from Figure 70 it may be seen that there is a value of E/p for which the ionization efficiency is a maximum. The magnitude of η_{max} and the optimum value of E/p at which this occurs, $E/p_{opt.}$ are tabulated below.

Gas	η max. x10^2	$E/p_{opt.}$ volts/cm.mm.Hg.
Hydrogen	1.24	125
Helium	1.08	100
Neon	1.09	60

At values of E/p above $E/p_{opt.}$ the electrons are no longer in equilibrium with the field since they are gaining energy from the field faster than they can dissipate it by ionization. In this range the mean electron energy will tend to increase as d increases so giving a value of η dependent upon both E/p and d. This effect is not observed in the present determinations but it is possible that it may be detected if measurements of current as a function of applied potential, at a fixed value of d, are made, changing the pressure to keep E/p constant, and η determined from this data. η may be then found to be a function of d at constant E/p.

The values of η max. given above are lower than results

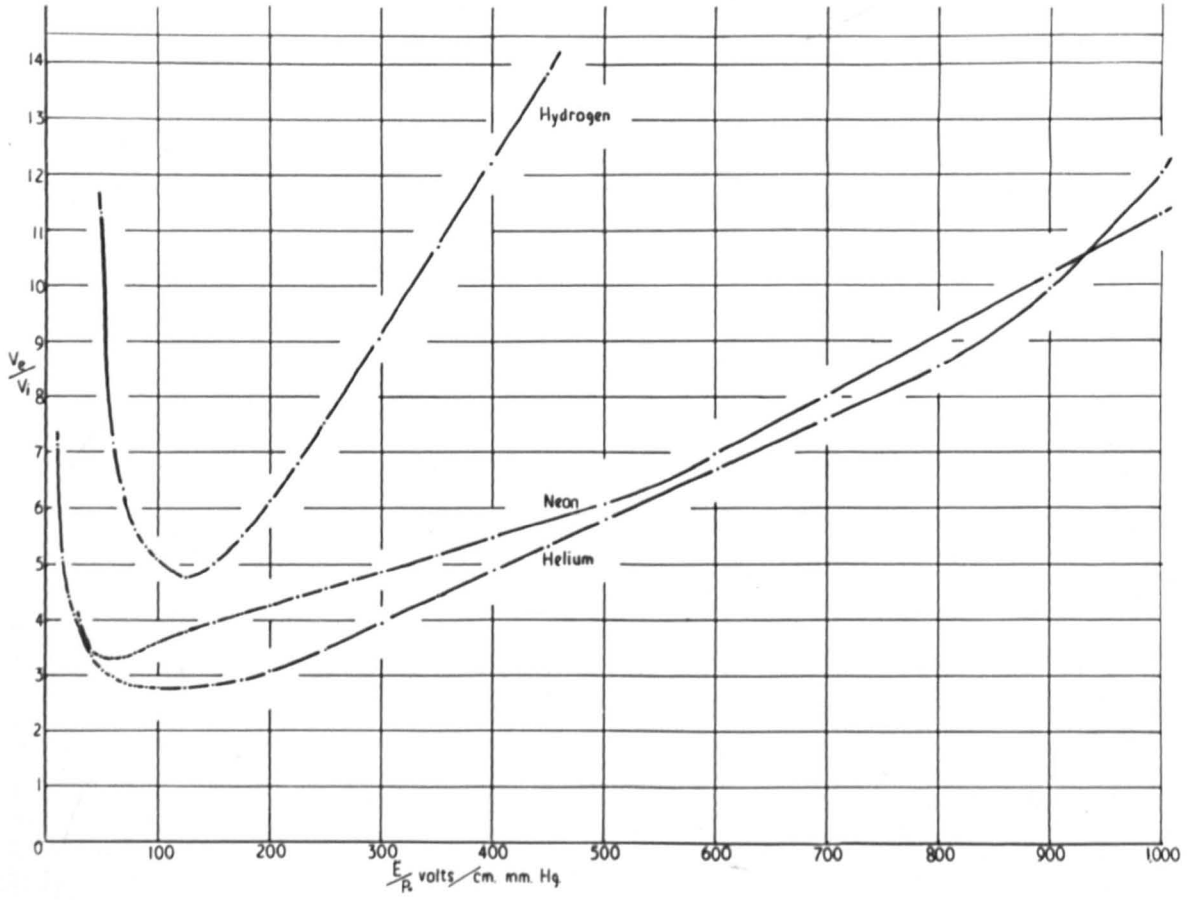

Figure 71.

Ratio Exitation Energy to Ionization Energy as a Function of E/p.

previously published but agreement is observed for values of $E/p_{opt.}$ (66, 61, 58, 39). It would appear, therefore, that $E/p_{opt.}$ is not a critical function of gas purity as is η or α/p.

Since the units of η are ionizations per volt, $\frac{1}{\eta}$ will give the energy in volts required to cause one ionization in the gas. Since the actual process of one ionization only needs the ionization energy, V_i, the excess energy, i.e. $(\frac{1}{\eta} - V_i)$ volts, must go towards excitation of the gas atoms. Therefore the ratio of excitation energy to ionization energy, V_e/V_i, at any value of E/p will be given by

$$V_e/V_i = \frac{\frac{1}{\eta} - V_i}{V_i}$$

Curves of V_e/V_i for hydrogen, helium and neon obtained in this way from the present determinations of η are given in Figure 71. It is immediately obvious that for all values of E/p there is a higher ratio of excitation to ionization in hydrogen than in the other gases. Since hydrogen has the lowest ionization potential, 13.6 e.v. as opposed to 21.6 and 24.6 e.v., this would not be expected and is due to the occurence in hydrogen of low energy excitation states. Conversly in neon and helium the excitation states are high and lie close to the ionization potential. This is reflected in the fact that for the range $50 < E/p < 200$ volts/cm.mm.Hg., excitation to all states is only about four times more probable than is ionization.

A further feature of this curve is the linear relationship

of V_e/V_i to E/p for a large range of E/p. In helium the function is linear for E/p_o from 200 - 800 volts/cm.mm.Hg. and in hydrogen from 200 volts/cm.mm.Hg. to the limit of the investigated range at E/p_o = 450 volts/cm.mm.Hg.. For neon the relationship exhibits a discontinuity at E/p_o = 500 volts/cm.mm.Hg. From this graph it can be seen that in hydrogen

$$V_e/V_i = 0.03\ E/p_o;\ \text{for } 200 < E/p_o < 450$$

In helium

$$V_e/V_i = 0.0125\ E/p_o + 1.2;\ 200 < E/p_o < 800$$

In neon

$$V_e/V_i = 0.0055\ E/p_o + 3.25;\ 125 < E/p_o < 450$$

and

$$V_e/V_i = 0.01\ E/p_o + 0.5;\ 600 < E/p_o < 1000$$

7.11. Conclusion and Suggestions for Further Work

The determinations of α/p_o in hydrogen are in very good agreement with those of Myatt, lying within $\pm$ 2% over the full range of E/p_o investigated. Such an agreement was to be expected since a very similar experimental tube was used along with similar gas purification techniques. Good agreement was also observed between the present results for which a residual gas pressure of 10^{-5}mm.Hg. was used, and those of Haydon and Robertson. Both determinations involved extensive outgassing techniques, liquid air trapping and rigorous hydrogen purification, and hence it seems probable that the chief contaminant would be the residual air in the experimental tube. Since the residual gas pressure was approximately the same in both

cases, both the nature and the amount of the impurity content were similar. Hence it would appear that the agreement observed is not fortuitous but is the result of similar gas purity. If these results are compared with those obtained using ultra high vacuum techniques, it may be seen that at high E/p ($E/p_o > 250$ volts/cm.mm.Hg.), α/p_o is lowered by as much as 12% due to the extra purity so achieved when residual gas pressures of the order of 10^{-9} mm.Hg. are used. It must, therefore, be concluded that the use of ultra high vacuum techniques is a necessity when gas discharge parameters are being measured.

The present results in helium fall below those of Davies, Llewellyn-Jones and Morgan, it is believed, due to increased gas purity. The current growth measurements in each case were subjected to a very similar type of analysis. Theoretical determinations of α/p in helium indicate that if the gas could be obtained in an even higher state of purity than has been used in the present work, the $\alpha/p_o - E/p_o$ curve would be further lowered. It is suggested that this may be done by using liquid helium both as a gas source, admitted to the system via a capillary leak, and as a freezing trap to condense out all contaminants. Dewars for this purpose have been designed by the author and are now available. Such work would also give an indication as to whether the glow discharge used for cataphoretic clean-up in the present work affected the values of α/p obtained, for example, by the introduction of extra metastable atoms of helium into the experimental tube which would tend to increase α

at low values of E/p. This effect is not the same as the "Penning effect" which is the result of metastable atoms of a gas other than the bulk gas and causes a stepped current growth curve at low values of d. No indication of the "Penning effect" was observed in the present work.

Since the first ionization coefficient has been found to be so critically dependent upon the impurity content of the gas in both hydrogen and helium, further work is required to investigate the purity of the gases obtained by the techniques described in Chapter VI. This may be done by either mass spectrometer measurements or by running a glow discharge and comparing the intensity of a spectral line of the bulk gas with one of the impurity gas during the purification procedure.

A surprising feature of the present determinations of the first ionization coefficient in neon is the good agreement with the theoretical values obtained by Heylen and Lewis. This may be due to the theoretical results being more accurate than those in helium, perhaps due to the Ramsauer effect being very small in neon, or because the effect of any helium impurity in neon will be less than that of neon impurity in helium. This could be determined by the analysis of the gases suggested above and by the determination of α/p_o in argon in which the Ramsauer effect is not marked and in which Heylen and Lewis have also predicted α/p_o.

The gases used for the present determinations of the primary ionization coefficients were almost certainly the purest to

be used to date with the possible exception of the helium used by Chanin, (98), who also used cataphoretic purification and whose results are to be published in the near future.

A deviation from Paschen's law has been observed in all the three gases presently investigated with V_s being dependent not only on $p_o d_s$ but also on p_o and d_s separately. As the pressure was increased, at constant $p_o d_s$, the breakdown potential was found to decrease. This may be explained as being due to less atoms being present between the plates at lower pressure and hence less ionization and excitation occuring to maintain the discharge and subsequently a higher breakdown potential is necessary. V_s was found also to increase as the gap distance increased and this has been attributed to a geometric loss of photons from the discharge and to photon absorption in the gas, each loss increasing as d increases. Photon absorption would lead to excited molecules which would quickly decay, re-emitting the photon and the only net effect would be a randomisation of the photon. This would have little effect on the discharge. During its life time, however, such an excited molecule may collide with a neutral molecule and its potential energy may go to the dissociation of the neutral molecule. In this way the photons will be lost to the discharge and ω/α will be subsequently reduced. Since the destruction of excited molecules is gap distance dependent, being a function of the number of neutral molecules present between the plates, ω/α will decrease as the gap distance increases so causing the observed increase in V_s. The relative importance of the

geometric loss of photons and the absorption of photons needs to be investigated further. By using electrodes of different diameter the anode can be made to subtend the same solid angle at the cathode with different values of d. Since the geometric loss is dependent only upon this solid angle, it may be expected to be constant under these conditions and hence any change in ω/α with d will be a measure of the absorption effect only.

It has been shown recently at Swansea, (62), by formative time lag techniques, that the predominant secondary process in helium is too slow for direct photon emission at the cathode and too fast for either positive ion or metastable atom emission. A delayed radiation mechanism has been suggested. Time lag measurements are currently required in the rare gases to elucidate the processes by which a current flows through them and the predominant mechanisms involved in their breakdown.

APPENDIX 1.

DAVIES AND MILNE ANALYSIS.

APPENDIX 1

THE DAVIES AND MILNE ANALYSIS

To find α

Using the Townsend equation involving both primary and secondary ionization

$$I = \frac{I_o \exp.\alpha(d-d_o)}{1-\omega/\alpha[\exp.\alpha(d-d_o)-1]}$$

and taking three values of current, I_1, I_2, and I_3, for the corresponding values of inter-electrode gap distance, d_1, d_2, and d_3, by using I_2, I_3, and d_2 d_3, the expression

$$\frac{I_3}{I_2} = \exp.\alpha(d_3-d_2)\ \frac{[1-\omega/\alpha[\exp.\alpha(d_2-d_o)-1]]}{[1-\omega/\alpha[\exp.\alpha(d_3-d_o)-1]]} \qquad (1)$$

may be obtained.

Hence rearranging

$$1 - {}^{1}/\omega/\alpha = \exp.[\alpha(d_3-d_o)]\frac{[I_3 - I_2]}{[I_3-I_2\exp.[\alpha(d_3-d_2)]]} \qquad (2)$$

Similarly using I_3, I_1 and d_3, d_1

$$1 - {}^{1}/\omega/\alpha = \exp.[\alpha(d_3-d_o)]\frac{[I_3 - I_1]}{[I_3-I_1\exp.[\alpha(d_3-d_1)]]} \qquad (3)$$

Equating (2) and (3)

$$I_1(I_3-I_2)\exp.[\alpha(d_3-d_1)]-I_2(I_3-I_1)\exp.[\alpha(d_3-d_2)] + I_3(I_2-I_1) = 0 \qquad (4)$$

Since α is the only unknown it can be determined from this expression. As this equation is algebraically insoluble, Newton's method of successive approximations must be used.

If α' is an approximate value of α, then

$$\alpha = \alpha' - \frac{f(\alpha')}{f'(\alpha')}$$

where $f(\alpha')$ is equation (4) and $f'(\alpha')$ is the first differential of equation (4). In this way α may be found without knowing I_o or d_o.

To find $^{\omega}/\alpha$

From Townsend's equation, by rearranging

$$\exp.(-\alpha d_o) = \frac{I + I(^{\omega}/\alpha)}{I_o \exp.(\alpha d) + I(^{\omega}/\alpha)\exp.(\alpha d)} \qquad (5)$$

taking two values of current I_1, I_2 at the corresponding values of gap distance, d_1, d_2 and substituting these in equation (5) and equating the two equations d_o is eliminated

$$\frac{I_1 + I_1\,(^{\omega}/\alpha)}{I_o \exp.(\alpha d_1) + I_1(^{\omega}/\alpha)\exp.(\alpha d_1)} = \frac{I_2 + I_2\,(^{\omega}/\alpha)}{I_o \exp.(\alpha d_2) + I2(^{\omega}/\alpha)\exp.(\alpha d_2)}$$

Hence

$$^{\omega}/\alpha = \frac{I_o(I_2 - I_1 \exp.[\alpha(d_2 - d_1)])}{I_1 I_2(\exp.\alpha(d_2 - d_1) - 1)} \qquad (6)$$

From equation (6) $^{\omega}/\alpha$ may be obtained, knowing α, without involving d_o. I_o must be known however.

To find d_o

From equation (5)

$$d_o = {}^{1}/\alpha \left[\log_e\left[\frac{I + I(^{\omega}/\alpha)}{\exp.(\alpha d)[I_o + I(^{\omega}/\alpha)]}\right]\right]$$

Since errors in α, $^{\omega}/\alpha$ and I_o are all involved in this expression d_o cannot be calculated to better than 50%.

APPENDIX 2.

HAYDON AND ROBERTSON ANALYSIS.

APPENDIX 2

The Haydon and Robertson Analysis

For a steady state ionization current, I, between electrodes d cms. apart

$$I = \frac{I_o \exp.\ \alpha(d-d_o)}{1-{}^{\omega}/_{\alpha}[\exp.\alpha(d-d_o)-1]} \qquad (1)$$

If $P = \frac{[1+{}^{\omega}/_{\alpha}][\exp.\alpha d_o]}{I_o}$

and $Q = \frac{({}^{\omega}/_{\alpha})}{I_o}$

Then

$${}^{I}/_{I} = P \exp.(-\alpha d) - Q = Y_d \qquad (2)$$

If the current at gap distance d is I_d and current at gap distance $(d + \Delta d)$ is $I_{d+\Delta d}$ then

$$Y_{(d+\Delta d)} = P \exp.\ -[\alpha(d+\Delta d)] - Q$$

By substituting for $P \exp.(-\alpha d)$ in (2)

$$Y_{(d)} = Y_{(d+\Delta d)} \exp.\ \alpha\Delta d + Q\ [\exp.(\alpha\Delta d)-1]$$

Therefore a graph of $Y_{(d)}$ against $Y_{(d+\Delta d)}$ at one value of ${}^{E}/_{p_o}$ gives both α and Q.

Since $Q = \frac{({}^{\omega}/_{\alpha})}{I_o}$, ${}^{\omega}/_{\alpha}$ may be calculated.

Since at breakdown I tends to ∞, $Y_{(d)}$ tends to zero.

From equation (1), therefore, under these conditions

$$d_s = \frac{\log_e({}^{P}/_{Q})}{\alpha}$$

APPENDIX 3.

PENNING GAUGE CALIBRATION CURVE.

PENNING GAUGE CALIBRATION IN AIR AND HYDROGEN

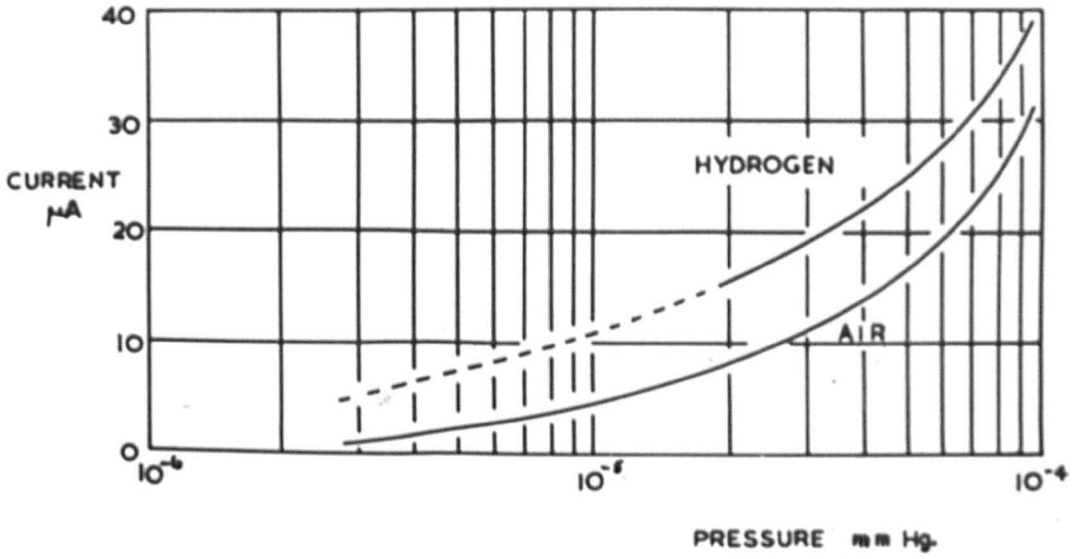

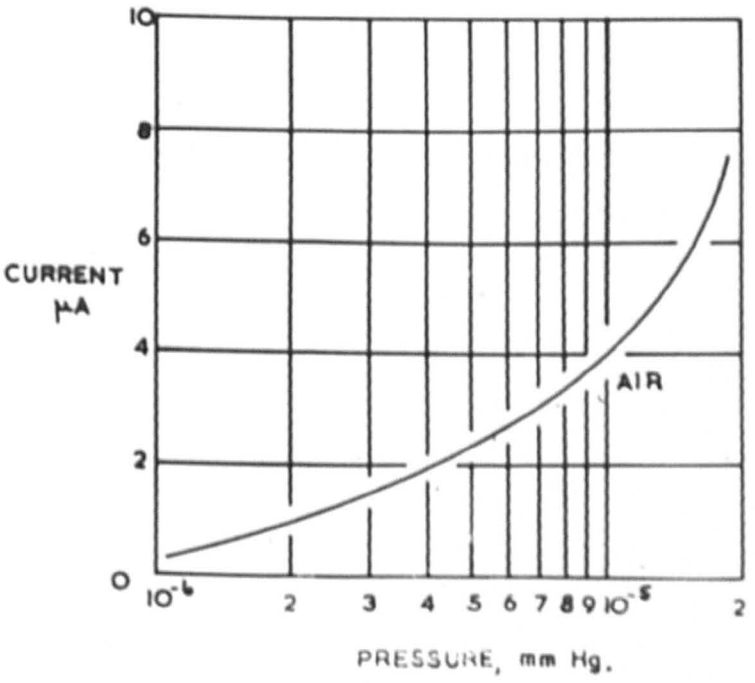

APPENDIX 4.

OIL MANOMETER CALIBRATION CURVE.

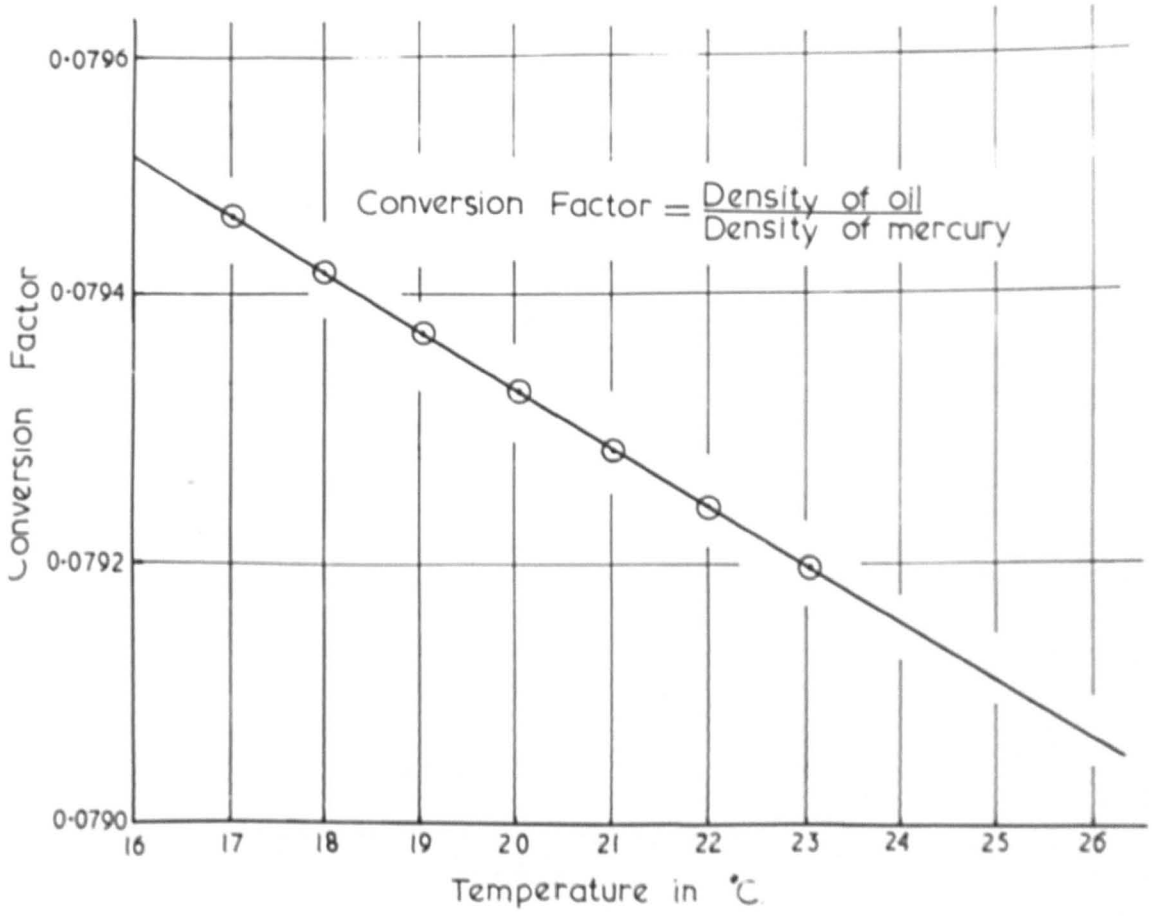

Variation of Conversion Factor with Temperature for the oil manometer.

APPENDIX 5.

CALIBRATION OF RESISTANCE CHAIN.

APPENDIX 5

Calibration of Resistance Chain

Ten resistors, each of approximately 1 MΩ, were accurately calibrated against a standard 1 MΩ resistor after they had been connected in series. The values were

Resistor Number	Nominal Value	Calibrated Value
31	2MΩ	2.05 MΩ
32	1MΩ	1.032 MΩ
33	2MΩ	2.016 MΩ
17	2MΩ	2.05 MΩ
35	2MΩ	2.023 MΩ
36	2MΩ	2.054 MΩ
37	1MΩ	1.022 MΩ
38	0.5MΩ	0.505 MΩ
19	1MΩ	1.005 MΩ
	13.5MΩ	13.757 MΩ

A nominal 30 KΩ resistor was connected in series with this chain and calibrated against the standard 1 MΩ. This was found to be 29.74 KΩ.

Therefore $\frac{\text{potential drop across nominal 13.5 MΩ + 30KΩ}}{\text{potential drop across nominal 30KΩ}}$

$$= \frac{13786.74}{29.74} = 463.6$$

Hence voltages across experimental tube were 463.6 times the measured voltage across the potentiometer.

APPENDIX 6.

FIRST IONIZATION COEFFICIENT IN HYDROGEN

APPENDIX 6

E/p_o	α/p_o			
	Residual Gas Pressure 10^{-8} mm.Hg.		Residual Gas Pressure 10^{-5} mm.Hg.	
	Davies-Milne Analysis	Haydon-Robertson Analysis	Davies-Milne Analysis	Haydon-Robertson Analysis
50	0.3	0.31	0.38	0.36
100	1.2	1.22	1.32	1.31
150	1.83	1.81	1.93	1.94
175	1.98	1.99	2.08	2.10
200	2.06	2.08	2.16	2.15
225	2.12	2.14	2.26	2.25
250	2.16	2.19	2.33	2.35
300	2.20	2.24	2.43	2.41
350	2.20	2.25	2.50	2.48
400	2.22	2.28	2.55	2.55
450	2.22	2.28	2.56	2.55

APPENDIX 7

FIRST IONIZATION COEFFICIENT IN HELIUM.

APPENDIX 7

E/p	α/p_o		
	Spectroscopically pure	Purified over activated charcoal	Cataphoresis pure
10			0.052
15			0.10
20	0.20	0.16	0.15
25			0.20
30	0.38	0.26	0.25
35			0.30
40	0.58	0.46	0.38
45			0.44
50	0.73	0.59	0.50
60		0.72	0.615
70		0.83	0.74
80		1.05	0.85
90		1.20	0.96
100	1.70	1.32	1.08
125	1.92	1.64	1.34
150	2.25	1.90	1.58
175	2.56	2.16	1.83
200	2.85	2.36	2.00
250	3.36	2.70	2.27
300	3.8	3.00	2.43

Continued . . . . .

350	4.2	3.26	2.58
400	4.54	3.48	2.76
500	5.35	3.80	2.98
600	5.85	4.05	3.15
700	6.32	4.24	3.32
800	6.7	4.38	3.4
900	6.85	4.46	3.34
1000	6.9	4.42	3.10
1250	6.84	4.18	
1500	6.54		

APPENDIX 8

FIRST IONIZATION COEFFICIENT IN NEON.

APPENDIX 8

E/p_o	α/p_o
30	0.28
40	0.43
50	0.54
60	0.65
70	0.76
80	0.84
90	0.95
100	0.98
125	1.19
150	1.37
175	1.55
200	1.73
225	1.90
250	2.07
300	2.4
350	2.65
400	2.82
450	3.1
500	3.26
600	3.48
700	3.6
800	3.7
900	3.72
1000	3.75

LIST OF SYMBOLS

α	Townsend primary ionization coefficient.
ω/α	Townsend generalised secondary ionization coefficient.
p	Gas pressure.
p_o	Gas pressure reduced to 0^oC.
E	Field Strength.
η	α/E.
λ_e	Electron mean free path.
ϕ	Work function.
ν	Frequency of radiation.
d	Inter electrode distance.
d_s	Sparking distance.
ν_i	Frequency of ionization.
V_s	Sparking potential.
V_{sm}	Minimum sparking potential.
d_o	Distance an electron must travel in the field before being in equilibrium with it.
h	Planck's constant.
I	Current flow.
I_o	Current flow when d is zero.
V	Voltage.
V_i	Ionization potential
E_i	Ionization energy.
e	Electronic charge.
$\bar{\varepsilon}$	Mean electron energy.

LIST OF FIGURES

REFERENCES

1.	Thomson, J.J.	Conduction of Electricity through gases Cambridge University Press			1928
2.	Townsend, J.S.	Nature	62	340	1900
3.	Townsend, J.S.	Phil.Mag.	1	198	1901
4.	Townsend, J.S.	Electricity in Gases Oxford: Clarendon Press			1915
5.	Townsend, J.S.	Phil.Mag.	3	557	1902
6.	Townsend, J.S.	Phil.Mag.	6	389 598	1903
7.	Holst, G.; Oosterhuis, E.	Phil.Mag.	46	1117	1923
8.	Druyvesteyn, M.J.; Penning, F.M.	Rev.Mod.Phys.	12	87 119	1940
9.	Massey, H.S.W.; Burhop, E.H.S.	Electronic and Ionic Impact Phenomena Oxford: Clarendon Press			1952
10.	Ecker, G.; Emeleus, K.G.	Proc.Phys.Soc.	B 67	546	1954
11.	Bowles, W.E.	Phys.Rev.	53	293	1938
12.	Kapitza, L.	Phil.Mag.	45	989	1923
13.	Oliphant, M.L.E.; Moon, P.B.	Proc.Roy.Soc.	A127	388	1930
14.	Morgan, C.G.	Phys.Rev.	104	566	1956
15.	Hagstrum, H.D.	Phys.Rev.	89	244	1953
16.	Hagstrum, H.D.	Phys.Rev.	91	543	1953
17.	Hagstrum, H.D.	Phys.Rev.	96	325 336	1954
18.	Hagstrum, H.D.	Phys.Rev.	104	309	1956

19.	Hagstrum, H.D.	Phys.Rev.	104	317	1956
20.	Hagstrum, H.D.	Phys.Rev.	106		1957
21.	Von Engel, A.	Ionized Gases Oxford University Press			1955
22.	Soskin, S.	Phys.Rev.	43	788	1933
23.	Dorrestein, R.	Physica	9	447	1942
24.	Bowles, W.E.	Phys.Rev.	53	293	1938
25.	Sutton, R.M.; Mouzon, J.C.	Phys.Rev.	37	379	1931
26.	Varney, R.N.	Phys.Rev.	47	483	1935
27.	Beeck, O.	Ann.Phys.	6	1001	1930
28.	Penning, F.M.	Phil.Mag.	11	961	1931
29.	Penning, F.M.; Addink, C.G.J.	Physica	1	1007	1934
30.	Boyd, K.	Proc.Phys.Soc.	A 63	543	1950
31.	Biondi, R.; Brown, S.C.	Phys.Rev.	76	1647 1697	1949
32.	De la Rue, W.; Muller, H.W.	Phil.Trans.Roy.Soc.	171	109	1880
33.	Paschen, F.	Weid.Ann.	37	69	1889
34.	Ayres, J.L.R.	Phil.Mag.	45	353	1923
35.	Penning, F.M.	Proc.Roy.Akad. Amsterdam	31	14	1928
36.	Hale, D.H.	Phys.Rev.	55	1199	1939
37.	Hale, D.H.	Phys.Rev.	54	241	1938
38.	Hale, D.H.	Phys.Rev.	55	815	1939
39.	Rose, D.J.	Phys.Rev.	104	273	1956
40.	Sanders, F.H.	Phys.Rev.	44	1020	1933

41.	Loeb, L.B.; Meek, J.M.	Mechanism of the Electric Spark California: Stanford University Press.				1941
42.	Crompton, R.; Dutton, J.; Haydon, S.C.	Proc.Roy.Soc.	B	69	2	1956
43.	Hopwood, W.; Peacock, N.J.; Wilkes, A.	Proc.Roy.Soc.	A	235	334	1956
44.	Llewellyn-Jones, F.; Davies, D.E.	Proc.Roy.Soc.	B	64	519	1951
45.	Rogowski, W.	Arch. Elektrotech.		12	1	1923
46.	Milne, J.G.C.	Ph.D. Thesis University of Birmingham				1958
47.	Jones, E.; Llewellyn-Jones, F.	Proc.Phys.Soc.		72	363	1958
48.	Davies, D.K.; Dutton, J. Llewellyn-Jones, F.	Proc.Phys.Soc.		79	1061	1958
49.	Bradbury, W.E.	Phys.Rev.		40	980	1932
50.	Theobald, J.K.	J.Appl.Phys.		24	123	1953
51.	Davies, D.E.; Milne, J.G.C.	Brit.Appl.Phys.		10	301	1959
52.	Davies, D.E.; Myatt, J.; Smith, D.	Proc. 5th Int.Conf. Ion.Phenom.Gases. Munich.				1961
53.	Myatt, J.	Ph.D. Thesis University of Birmingham.				1960
54.	Smith, D.	Ph.D. Thesis University of Birmingham.				1962
55.	Gill, E.W.B.; Pidduck, F.B.	Phil.Mag.		16	280	1908
56	Gill, E.W.B.; Pidduck, F.B.	Phil.Mag.		23	837	1912

57.	Townsend, J.S.; MacCallum, S.P.	Phil.Mag.	5	695	1928
58.	Townsend, J.S.; MacCallum, S.P.	Phil.Mag.	6	857	1934
59.	Kruithoff, A.A.; Penning, F.M.	Physica	3	515	1936
60.	Kruithoff, A.A.; Penning, F.M.	Physica	4	430 450 464	1937
61.	Kruithoff, A.A.;	Physica	7	519	1940
62.	Davies, D.K.; Llewellyn-Jones, F.; Morgan, C.G.	Proc.Phys.Soc.	80	898	1962
63.	Riesz, R.; Dieke, G.H,	J.Appl.Phys.	25	196	1954
64.	Herlin, R.; Brown, S.C.	Phys.Rev.	74	291	1948
65.	MacDonald, T.; Brown, S.C.	Phys.Rev.	75 76	411 1634	1949
66.	Varnerin, L.J.; Brown, S.C.	Phys.Rev.	79	946	1950
67.	Pidduck, F.B.	Proc.Lond.Math.Soc.	15	89	1915
68.	Morse, P.M.; Allis, W.P.; Lamar, E.S.	Phys.Rev.	48	412	1935
69.	Druyvesteyn, M.J.	Physica	3	65	1936
70.	Smit, J.A.	Physica	3	543	1936
71.	Lewis, T.J.	Proc.Roy.Soc.	A 244	166	1953
72.	Heylen, A.E.D.; Lewis, T.J.	Proc.Phys.Soc.	A 271	531	1963
73.	Margenau, H.	Phys.Rev.	69	508	1946
74.	Von Engel, A.; Steenbeck, M.	Elekrische Gasentladungen (Julius Springer, Berlin)			1932

75.	Emeleus, K.G.; Lunt, R.W.; Meek, C.A.	Proc.Roy.Soc.	A 156	394	1936
76.	Deas, H.D.; Emeleus, K.G.	Phil.Mag.	40	460	1949
77.	Dunlop, S.H,	Nature	164	452	1949
78.	Bradbury, N.E.; Nielson, R.A.	Phys.Rev.	49	388	1936
79.	Llewellyn-Jones, F.	Phil.Mag.	11	163	1931
80.	Reder, F.H. Brown, S.C.	Phys.Rev.	95	885	1954
81.	Darling, A.S.	Plat.Metals Review	2	16	1958
82.	Crompton, R.W.; Elford, M.T.	J.Sci.Instrum.	39	480	1962
83.	Baly, E.C.	Phil.Mag.	35	200	1893
84.	Oskam, H.J.	Bull.Am.Phys.Soc. II	3	85	1958
85.	Druyvesteyn, M.J.	Physica	2	255	1935
86.	Bayard, R.T.; Alpert, D.	Rev.Sci.Inst.	21	571	1950
87.	Haydon, S.C.	Unpublished Communication.			
88.	Holstein, T.R.	Phys.Rev.	70	367	1946
89.	Townsend, J.S.; Bailey, V.A.	Phil.Mag.	46	657	1923
90.	Reder, F.H.; Brown, S.C.	Phys.Rev.	95	885	1954
91.	Llewellyn-Jones.	Phil.Mag.	11	163	1931
92.	Haydon, S.C.; Robertson, A.G.	Proc. V Int.Conf. Ion.Phenom.Gases Munich.			1961
93.	De Groot, W.; Penning, F.M.	Handb.der.Phys.	23	23	1933

94.	Overton, G.D.N.	M.Sc. Thesis University of Birmingham			1963
95.	Townsend, J.S. Bailey, V.A.	Phil.Mag.	42	873	1921
96.	Compton. K.T. Van Voorhis, C.C.	Phys.Rev.	27	724	1926
97.	Salmon, J.	VI Inter.Conf.Ion. Phenom.Gases, Paris.			1963
98.	Chanin, L.M.; Rork, G.D.	VI Inter.Conf.Ion. Phenom.Gases, Paris,			1963